Fast X-ray Imaging and Diffraction

Lianyi Chen

Charles Ringrose Associate Professor

Department of Mechanical Engineering

Department of Materials Science and Engineering
University of Wisconsin-Madison
Email: lianyi.chen@wisc.edu
Phone: 608-890-0664

25th National School on Neutron and X-ray Scattering, ANL, August 15, 2023

32-ID:
Dr. Tao Sun (UVA)
Dr. Kamel Fezzaa
Dr. Samuel Clarke

1-ID:
Dr. Andrew Chuang

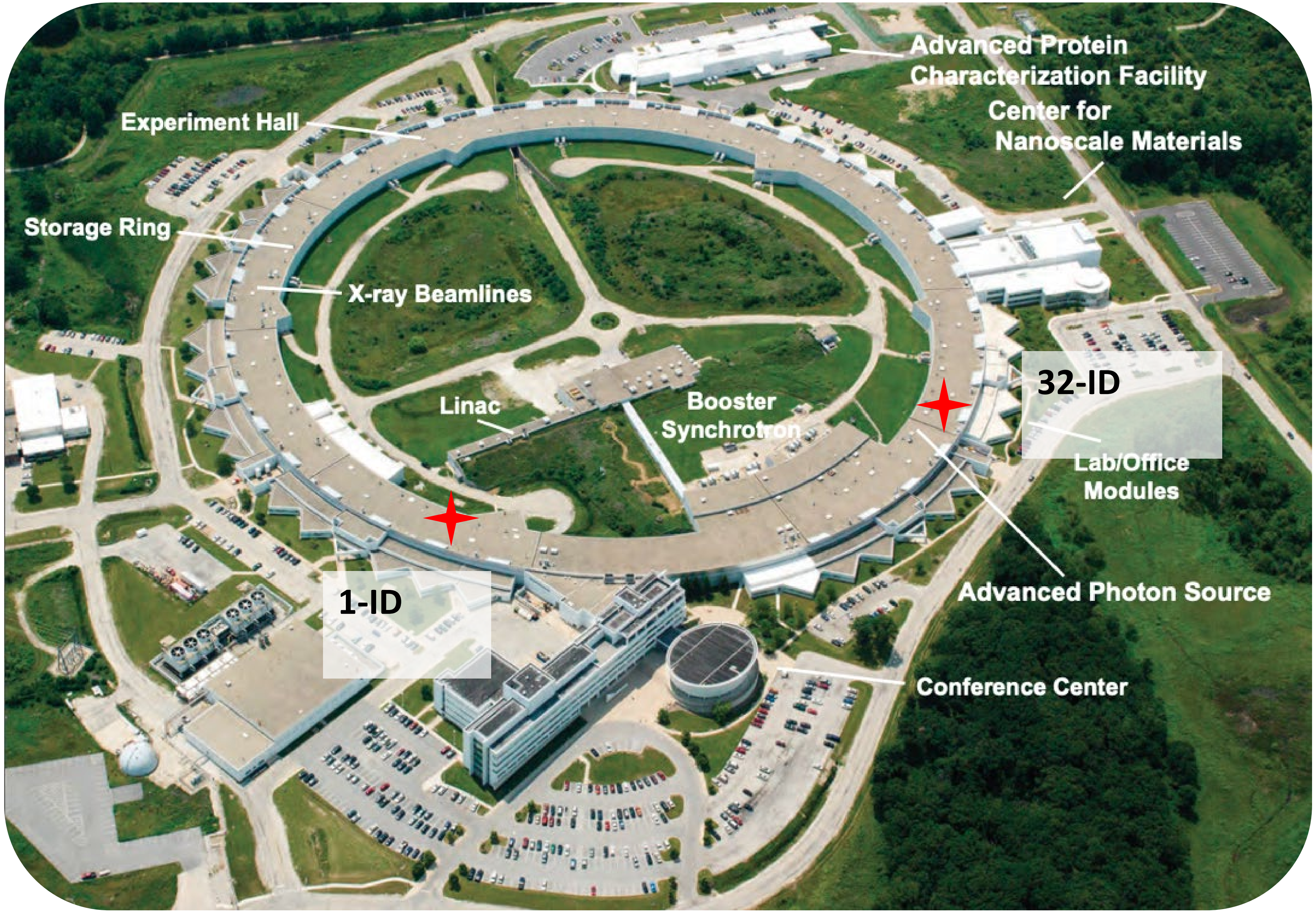

Outline

- Introduction to fast X-ray imaging and diffraction
- Fast X-ray imaging system
- Fast X-ray diffraction system
- Revealing dynamics of additive manufacturing processes by fast X-ray imaging and diffraction
- Approaches to mitigate/eliminate defects in additive manufacturing

What is fast X-ray imaging and diffraction?

Why do we need fast X-ray imaging and diffraction?

- Fluid dynamics
- Energetic materials and rapid reactions
- Dynamic loading
- Materials machining and processing
- Additive manufacturing

Dynamic irreversible and non-repeatable materials and engineering processes





What are the major technical challenges?

- Signal to noise ratio
- Exposure time and frame rate
- Timing
- Data processing and management

High flux X-ray beam

32-ID beamline undulator sources

Tandem undulators

❑ U33 (white beam)

- Length: 2.4 m
- Period: 3.3 cm
- Min Gap: 11 mm
- E1 range: 5~14 keV
- $\Delta E_1/E_1$: 1~2%

❑ U18 (pseudo pink beam)

- Length: 2.4 m
- Period: 1.8 cm
- Min Gap: 11 mm
- E_1 range: 23.7~25.7 keV
- $\Delta E_1/E_1$: 5~10%

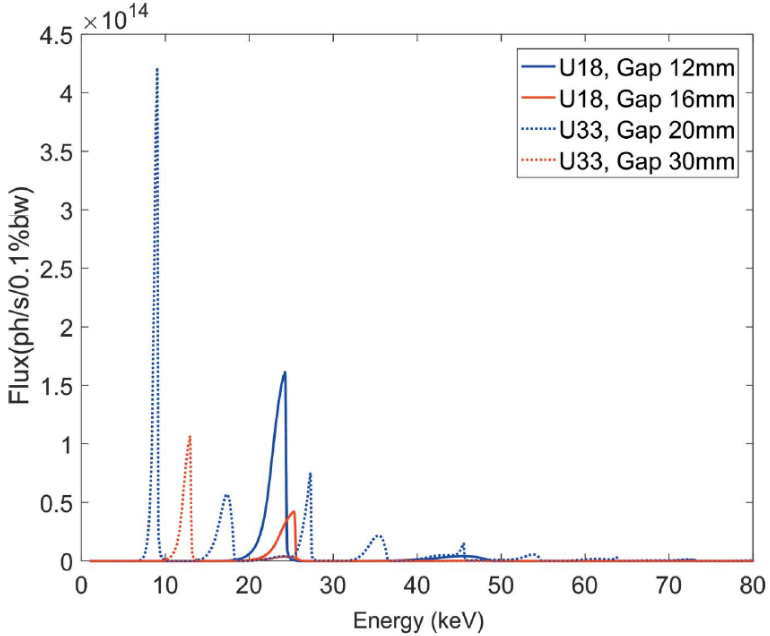

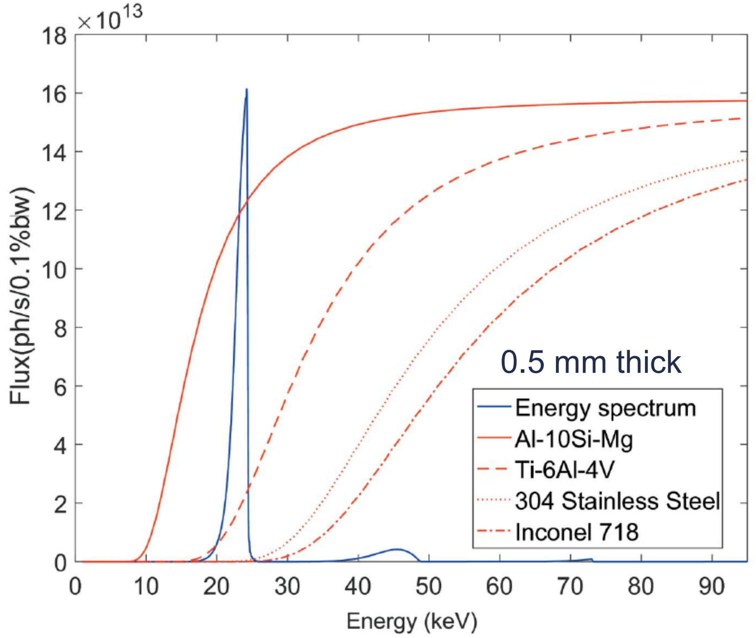

Undulator		Integrated over 1-65 keV		1st harmonic	
Period (cm)	Gap(mm)	Flux*	Singlet	Flux	Singlet
3.3	20	1.8×10^{16}	2.8×10^{9}	1.3×10^{16}	2.0×10^{9} (71%)
	30	4.7×10^{15}	7.3×10^{8}	4.5×10^{15}	6.9×10^{8} (95%)
1.8	11	4.5×10^{16}	6.9×10^{9}	4.1×10^{16}	6.3×10^{9} (92%)

* Unit: ph/s/0.1%BW, 1.5x1.5 mm^2 beam size

Temporal resolution

- **Exposure time**:
  - Camera specs (CMOS: 100s' ns; Hybrid-CMOS: 50 ns)
  - Scintillator decay time
- **Frame rate**:
  - Camera specs (CMOS: 1 MHz; Hybrid-CMOS: 10 MHz)
  - Needed field-of-view for experiment
  - X-ray pulse structures

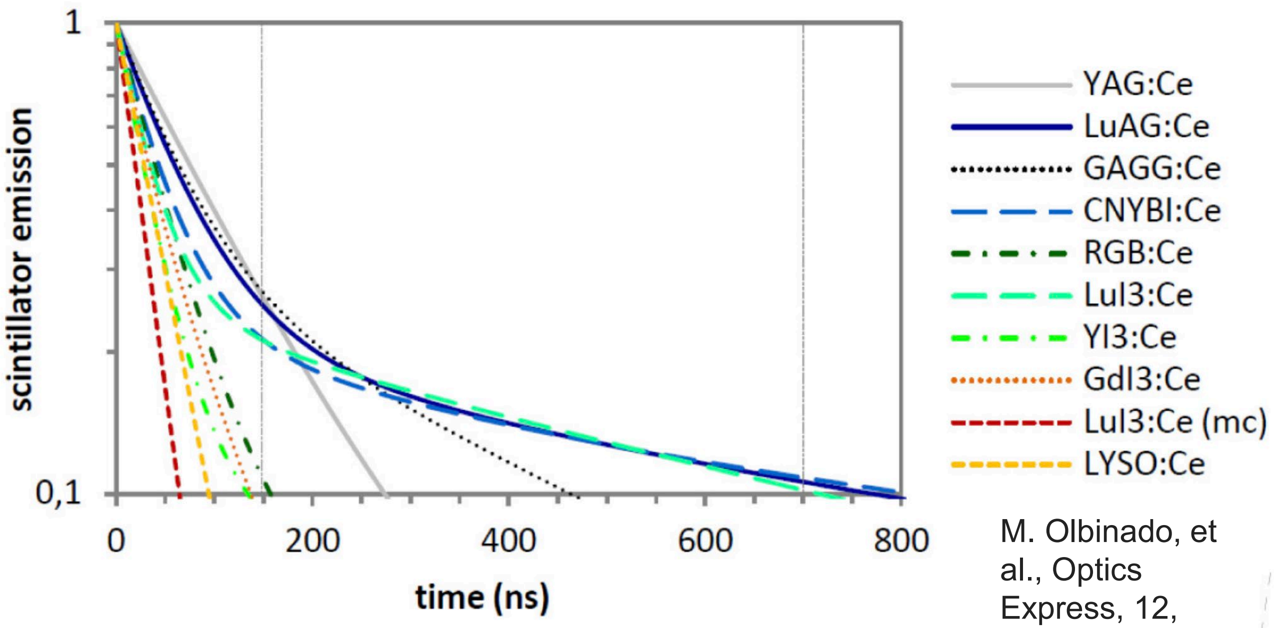

M. Olbinado, et al., Optics Express, 12, (2017) 13857

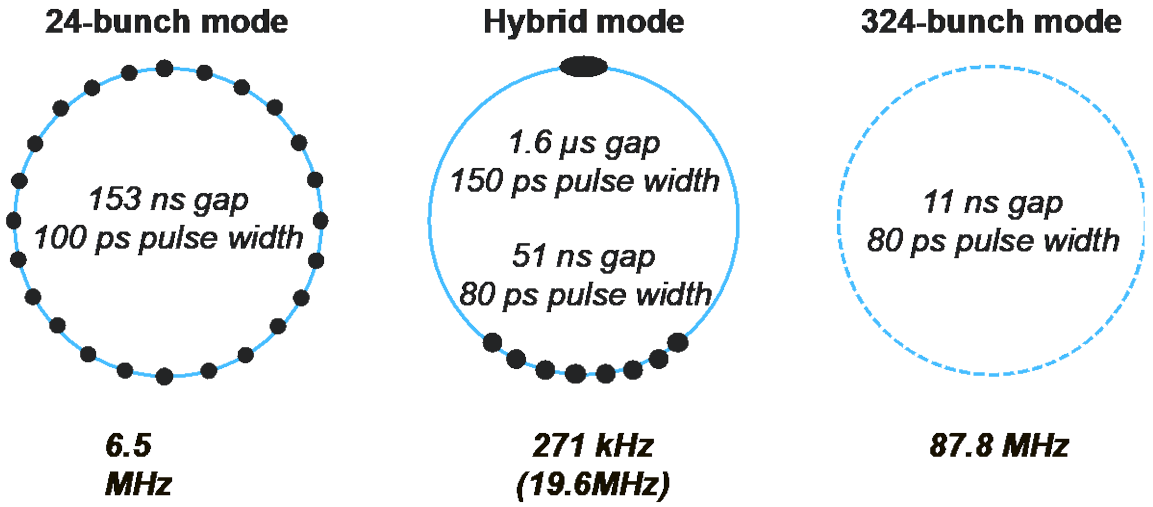

24-bunch mode: MHz imaging with single pulse exposure

Hybrid mode: Fixed frame rates, but stronger single pulse

324-bunch mode: Experiments with > µs exposure, no intensity fluctuation in each image

Timing

A laser beam moves at a speed of 1 m/s along the horizontal direction of the field of view. The field of view is 2 mm along the horizontal direction. How many milliseconds does it take for the laser beam to pass the field of view?

Timing scheme and beamline control

Slow shutters

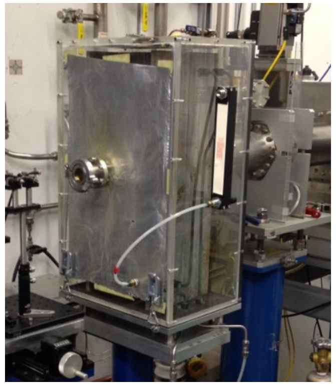

Opening — **50 ms** — *Closing*

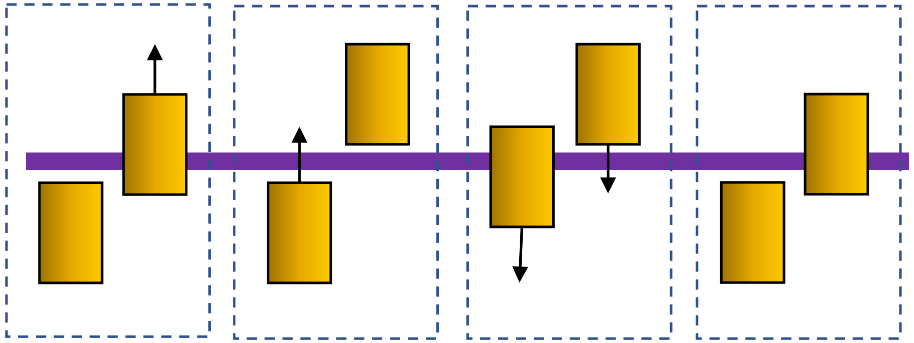

Fast shutters

Close — **700 µs** — *Open*

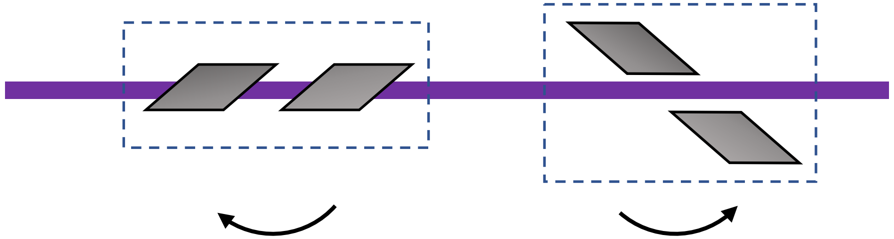

Delay generators

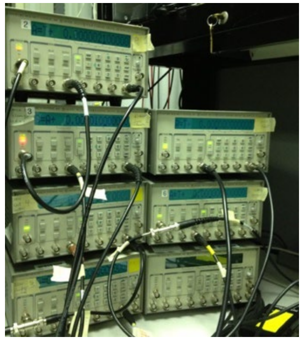

SRS535

SRS645

Timing scheme

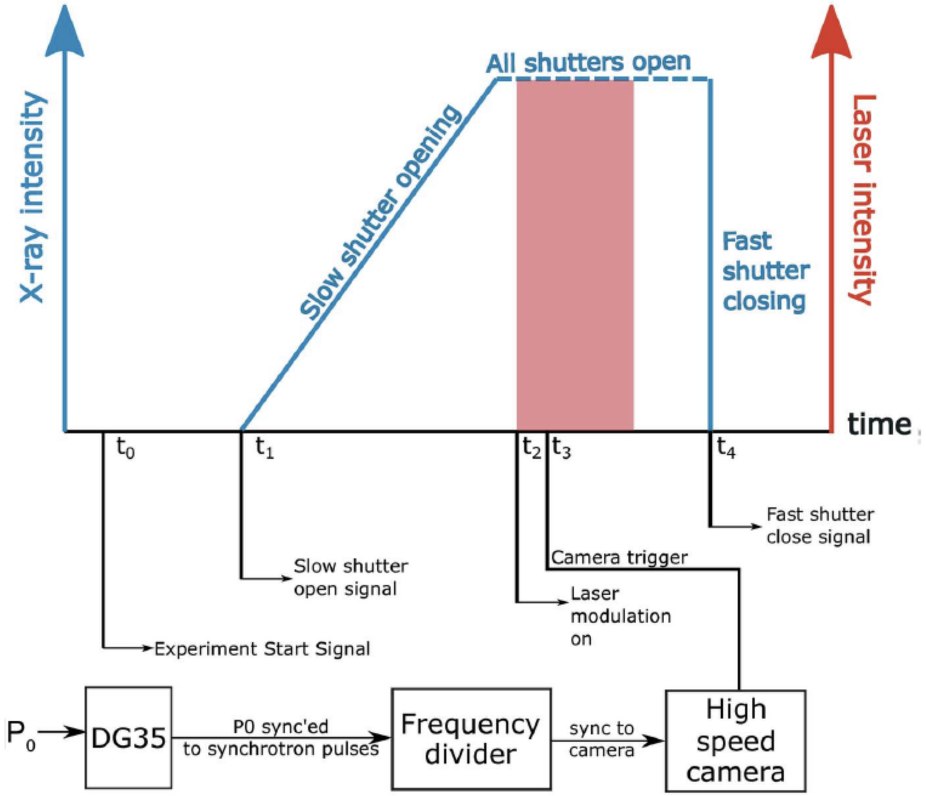

Data processing and management

- The amount of data is big
- Fast storage
- Fast transfer
- Fast processing

Outline

- Introduction to fast X-ray imaging and diffraction
- **Fast X-ray imaging system**
- Fast X-ray diffraction system
- Revealing dynamics of additive manufacturing process by fast X-ray imaging and diffraction
- Approaches to mitigate/eliminate defects in additive manufacturing

X-ray imaging techniques

❑ Scanning probe microscopy

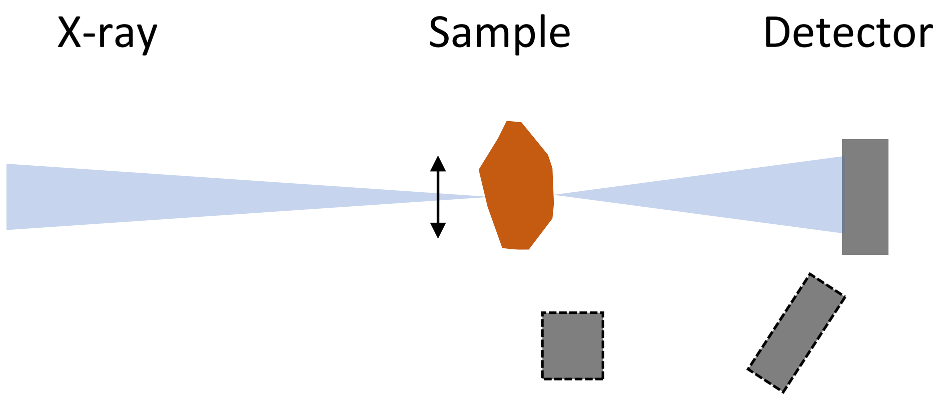

- Fluorescence contrast
- Absorption contrast
- Absorption fine structure contrast
- Scattering contrast
- Diffraction contrast
- Computed tomography (3D)

Spatial resolution: probe size

❑ Coherent imaging

- Ptychography
- Coherent diffractive imaging

Spatial resolution: q range

❑ Propagation-based full-field imaging

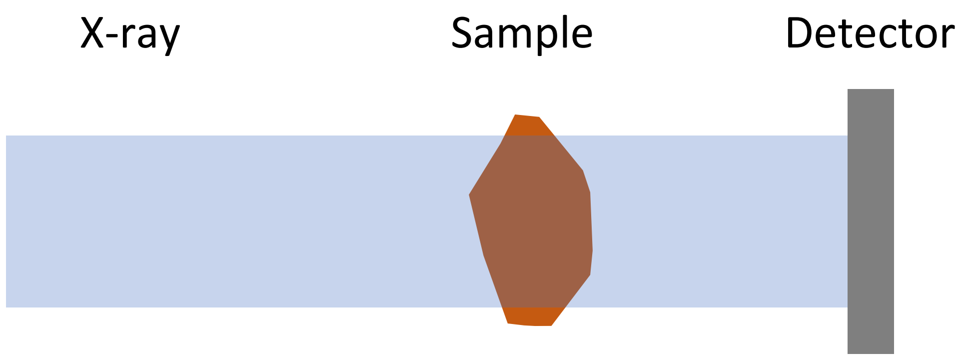

- Absorption contrast
- Phase contrast imaging
- Projection microscopy
- Transmission x-ray microscopy
- Diffraction contrast
- Computed tomography (3D)

Spatial resolution: detection pixel size

High-speed X-ray image detection system

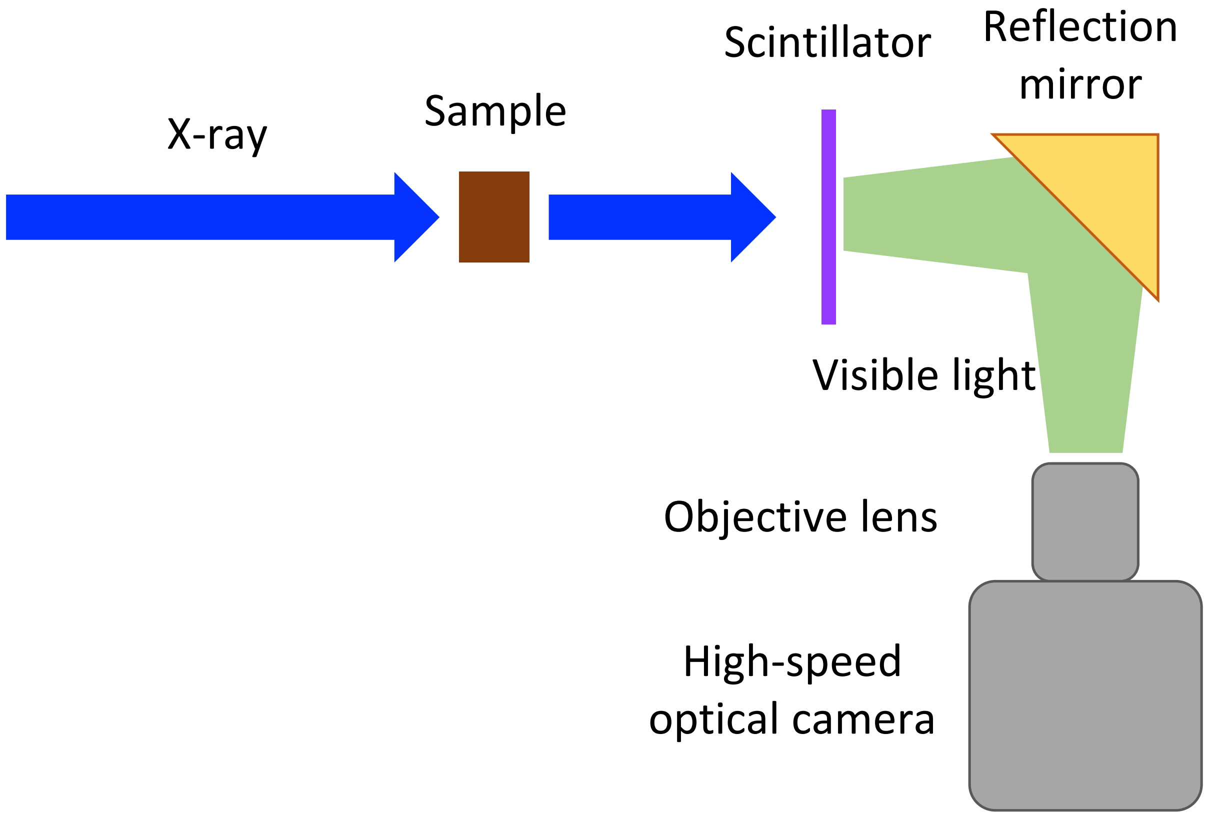

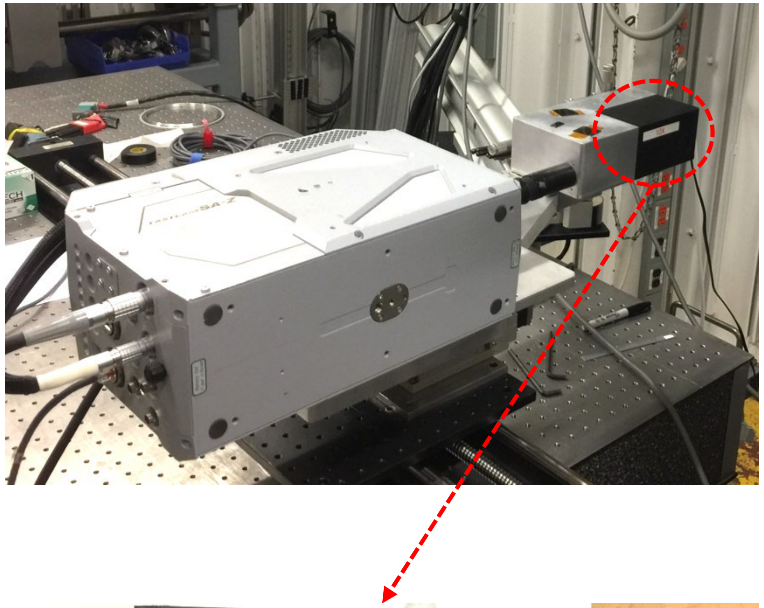

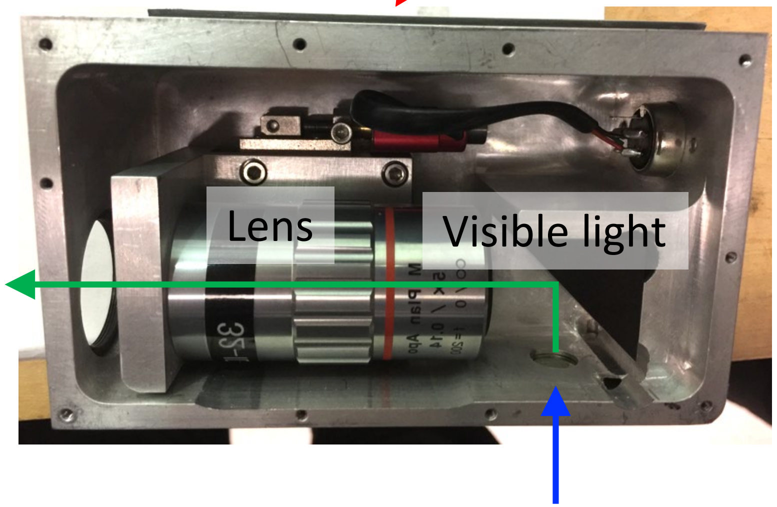

Scintillator-couple optical detection

- High spatial resolution: imaging sensor pixel size, magnification by the lens
- High temporal resolution: delay time of scintillator, frame rate and exposure time of camera, x-ray pulse structure

High-speed X-ray image detection system

- X-ray beam size: 2 mm x 2 mm
- Camera sensor:
  - CMOS: 20 µm/pixel, 1024 x 1024, image size reduces as frame rate increases
  - Hybrid CMOS (with on-pixel storage): 30 µm/pixel, 400 x 250, image size remains the same
- Objective lens: 2x, 5x, 10x, 20x
- Scintillator light emission: visible light (wavelength: 400~700 nm)

Photron FastCam SA-Z

Shimadzu HPV-X2

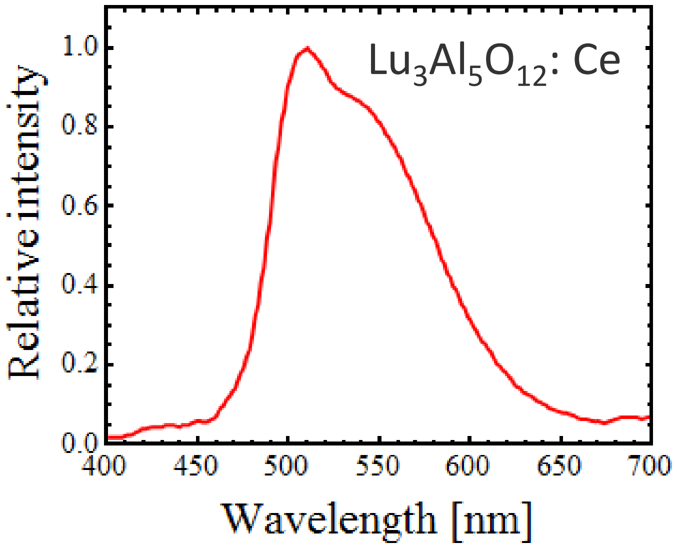

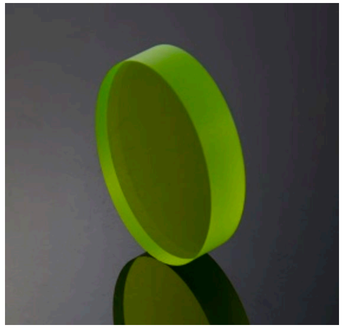

32-ID-B experimental hutch

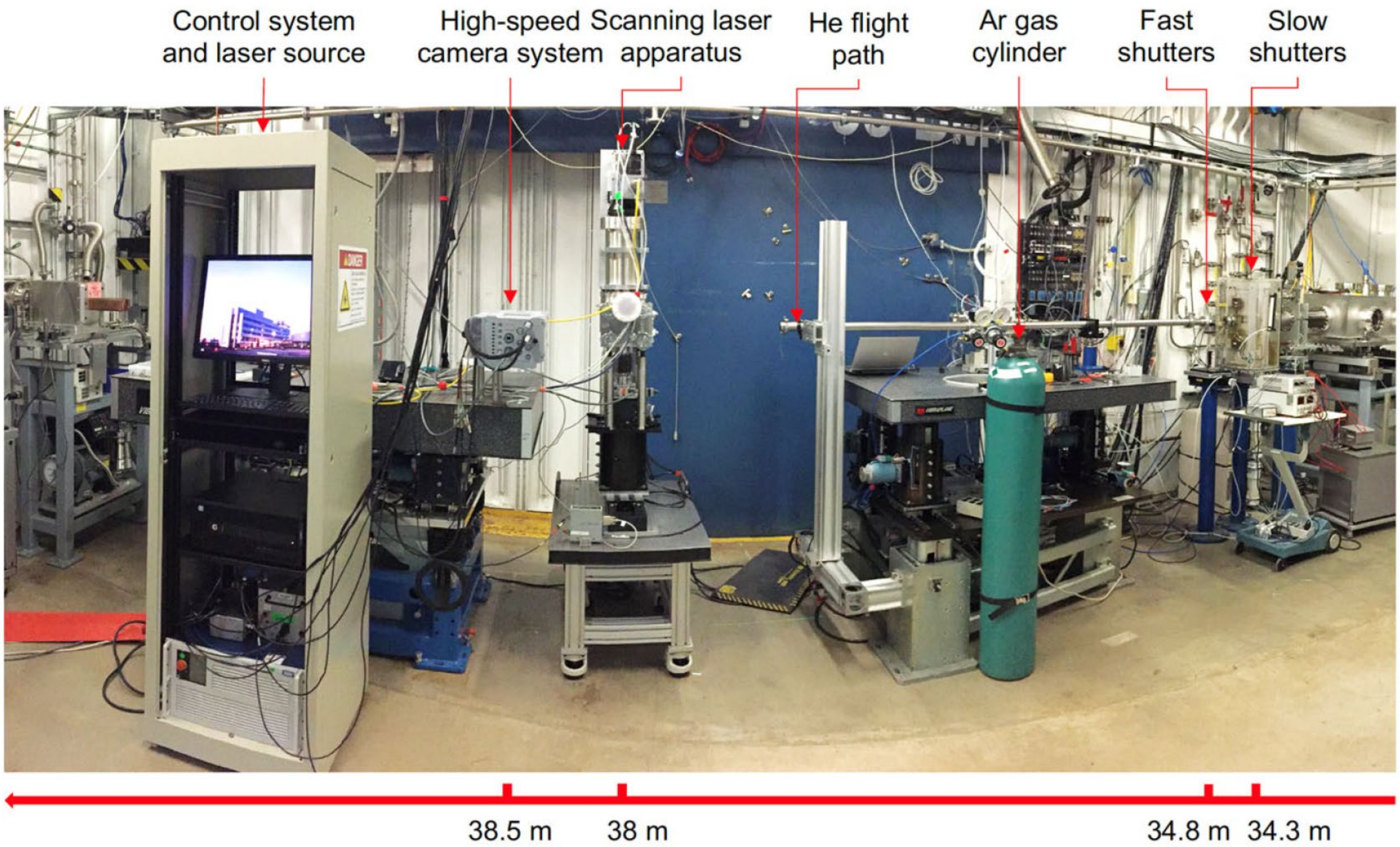

Outline

- Introduction to fast X-ray imaging and diffraction
- Fast X-ray imaging system
- **Fast X-ray diffraction system**
- Revealing dynamics of additive manufacturing process by fast X-ray imaging and diffraction
- Approaches to mitigate/eliminate defects in additive manufacturing

Fast X-ray diffraction at 32-ID

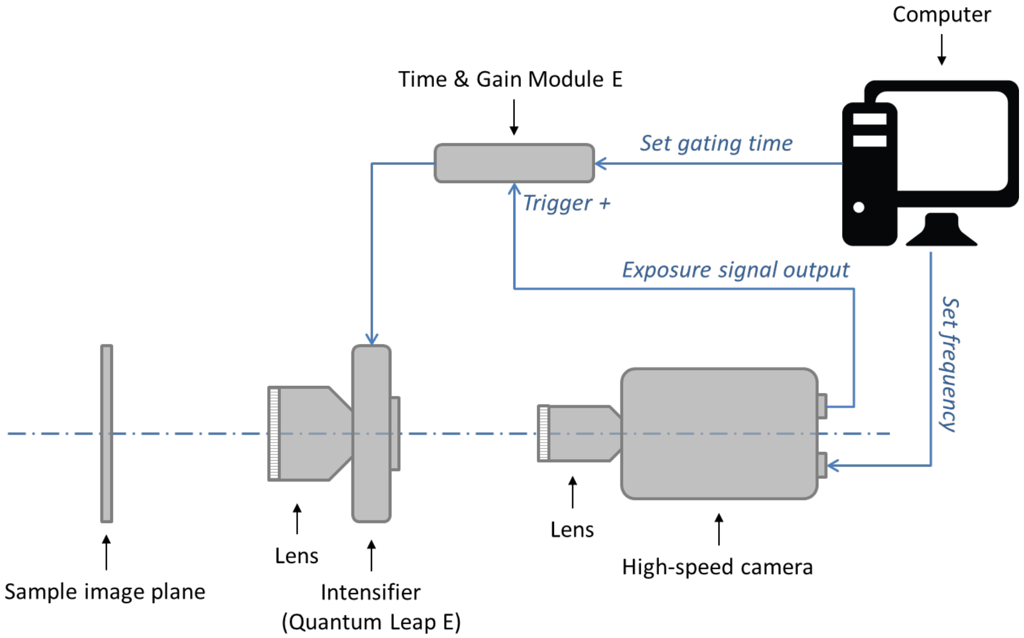

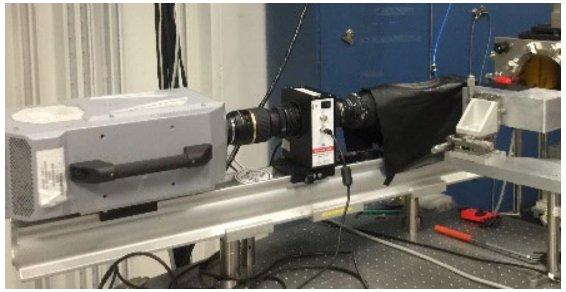

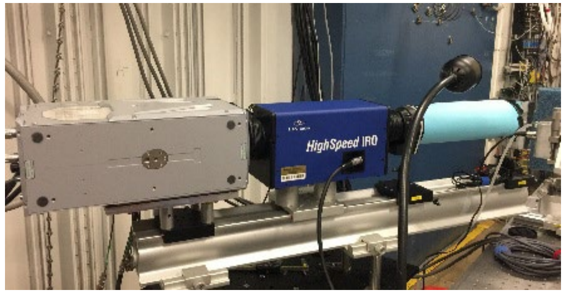

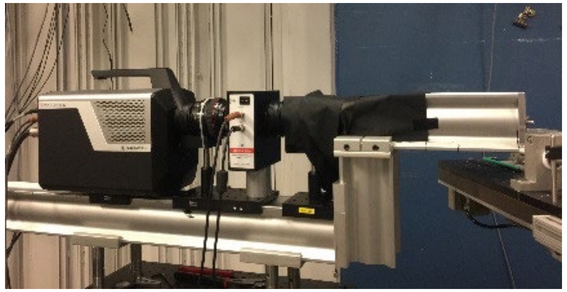

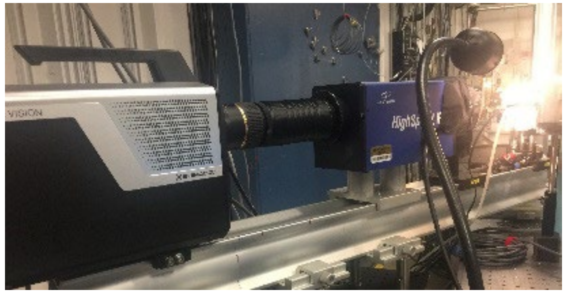

- ❑ **Intensifier**: LaVision IRO, Quantum Leap
- ❑ Camera: Photron SA-Z, Shimadzu HPV-X2
- ❑ Scintillator: $Lu_{1.8}Y_{0.2}SiO_5$:Ce (LYSO)
  - Thickness: 300 µm
  - Diameter: 65 mm
  - Al front coating

- Camera: Photron SA-Z
- Intensifier trigger: multiple
- Pixels: 1024 x 1024 (60~70 µm/pixel)
- Min exposure: 100 ps
- Max frame rate: 200 kHz
- Fast dynamics spanning 10s' ms

- Camera: Shimadzu HPV-X2
- Intensifier trigger: single
- Pixels: 400 x 250 (60~70 µm/pixel)
- Min exposure: 100 ps
- Max frame rate: 10 MHz
- Ultrafast dynamics spanning 10s' µs

Pink beam diffraction at 32-ID

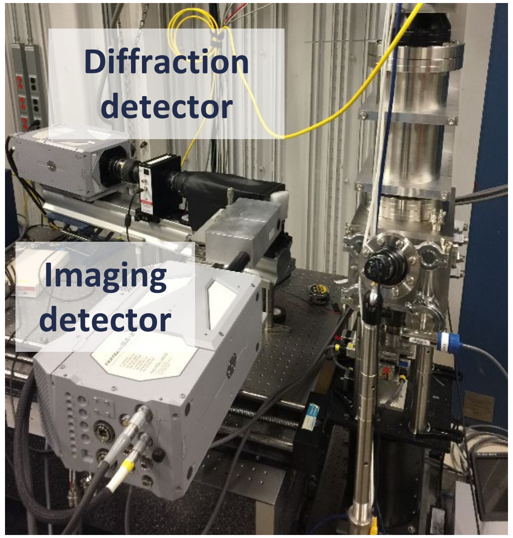

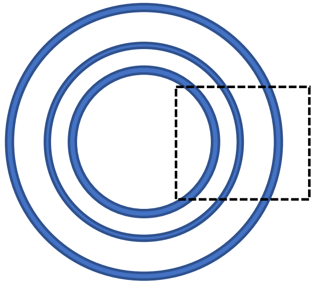

- **Phase transformation of Ti-6Al-4V**
  α-Ti → melting → β-Ti with coarse grains → α-Ti with fine grains
- **32-ID source**
  - U18 pink: ~24 keV (1st)
  - Bandwidth: ~5%
- **Detector**
  - Scintillator + intensifier + optical CMOS camera

Scanning laser mode

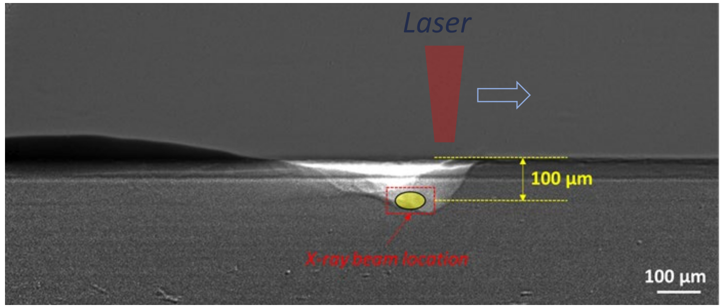

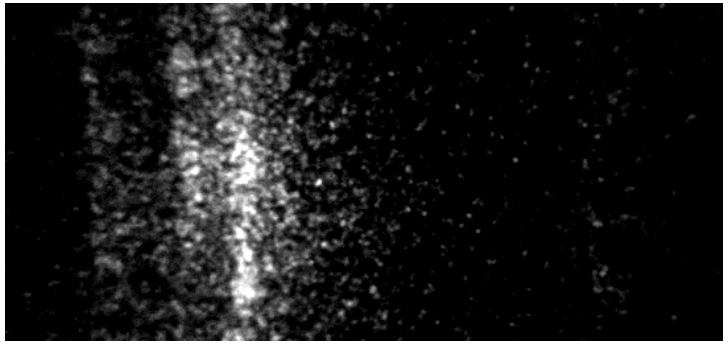

Frame rate: 100,000 fps
Exposure: 5 μs
X-ray beam size: H100 x V60 μm^2

Spot welding mode

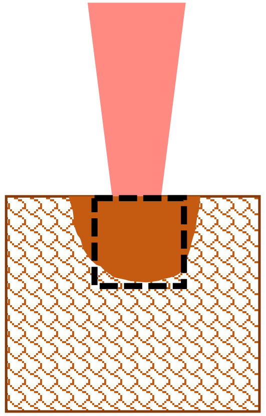

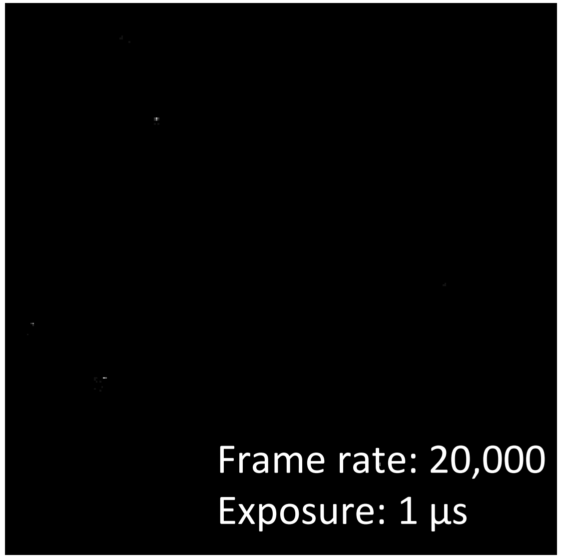

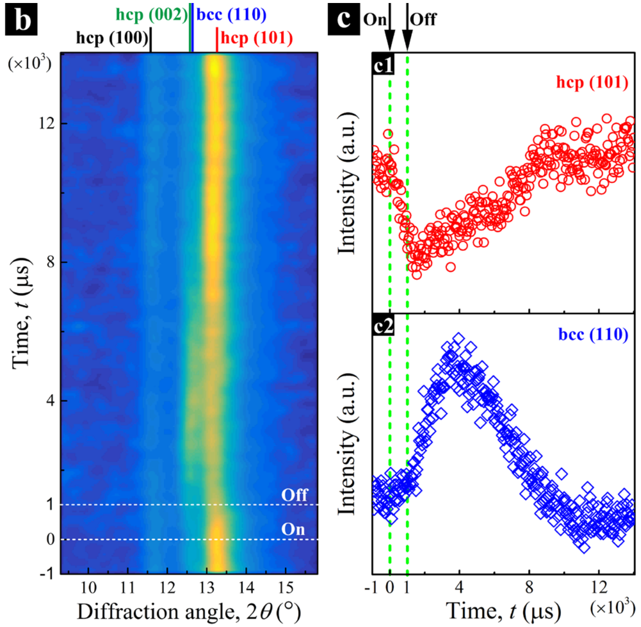

C. Zhao, et al., Scientific Reports, 7, (2017) 3602

Mono beam diffraction at 1-ID

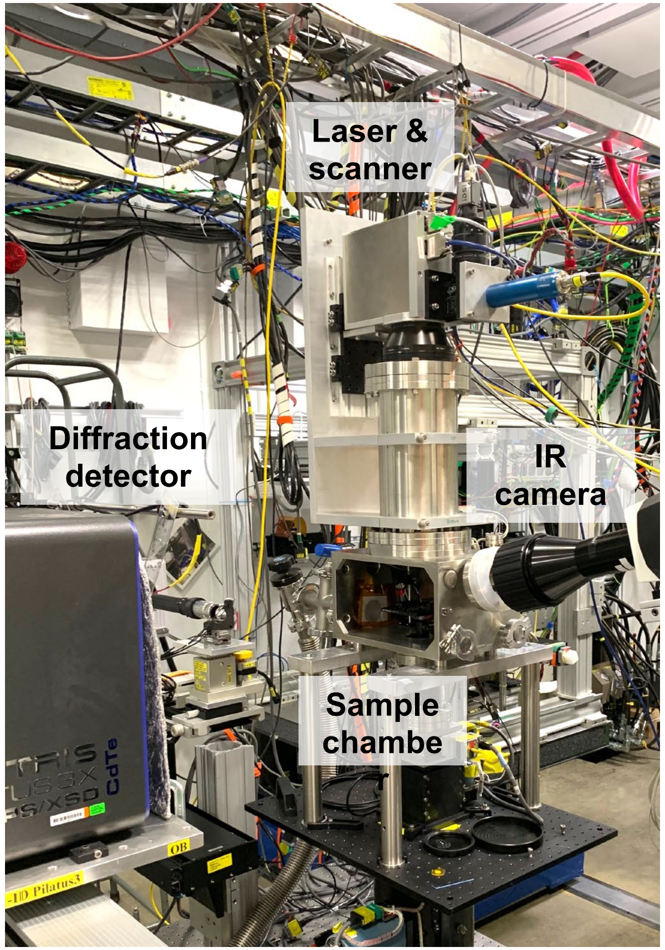

(with Andrew Chuang, APS)

- **1-ID source**
  - Superconducting undulator
  - Mono: E = 55.6 keV
- **Detector**
  - PILATUS3X 2M CdTe

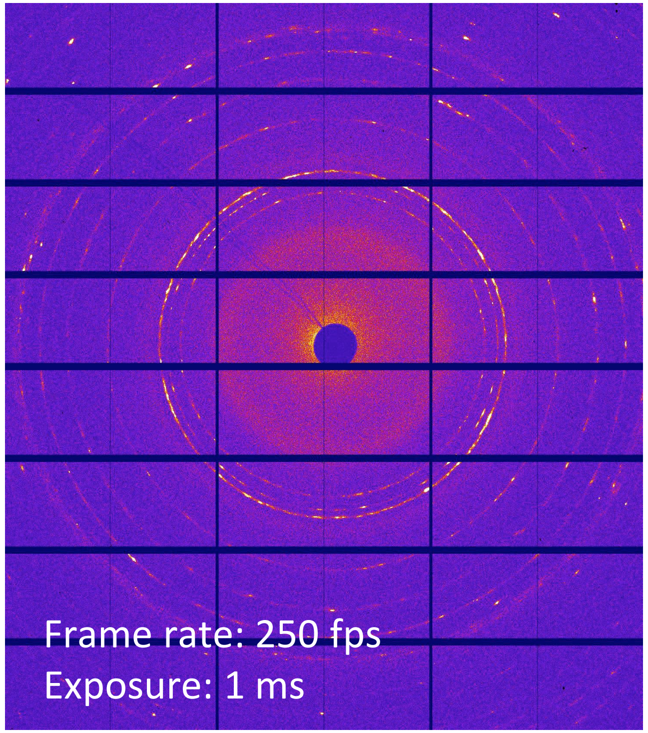

S. Oh, et al., Materials Research Letters, 9, (2021) 429

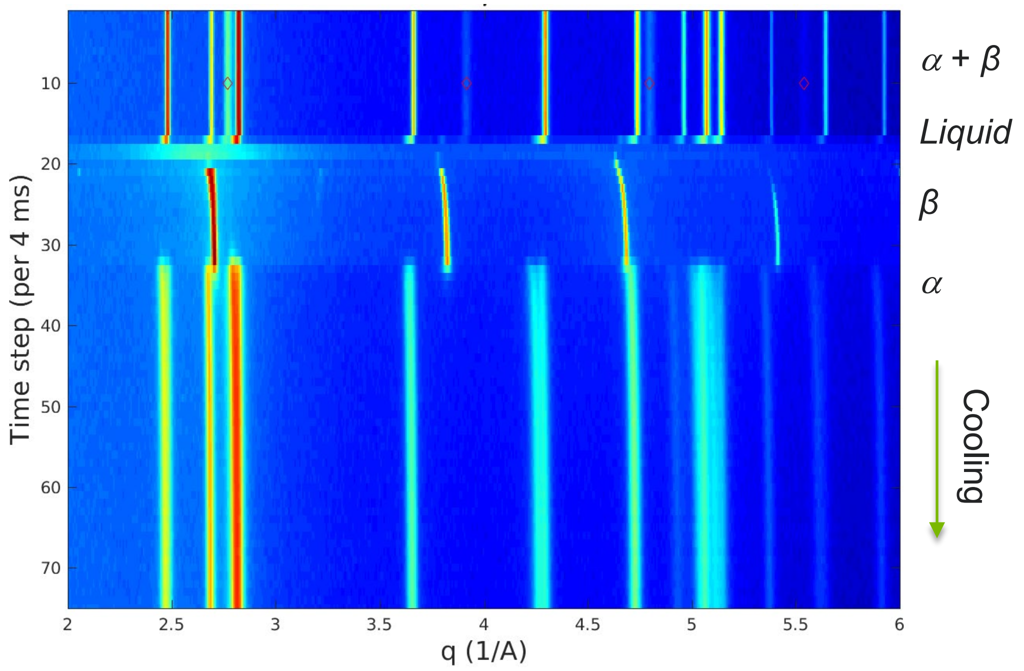

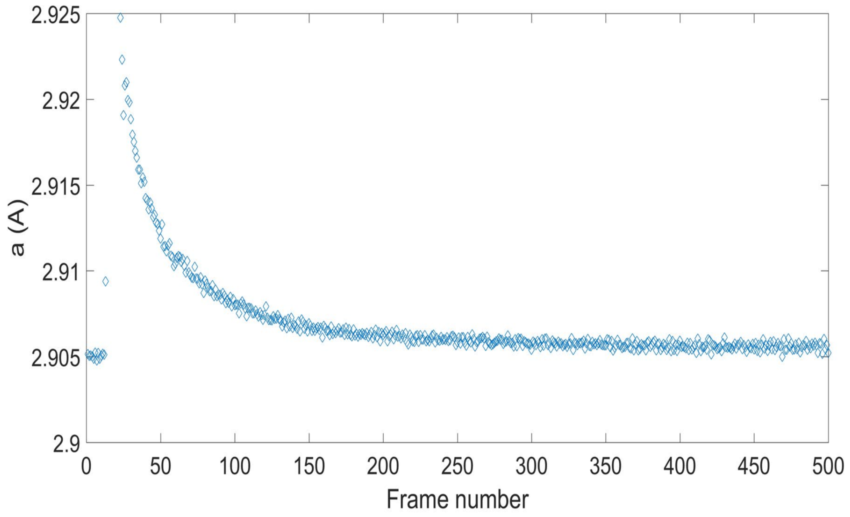

Comparison of diffraction data

32-ID
pink beam

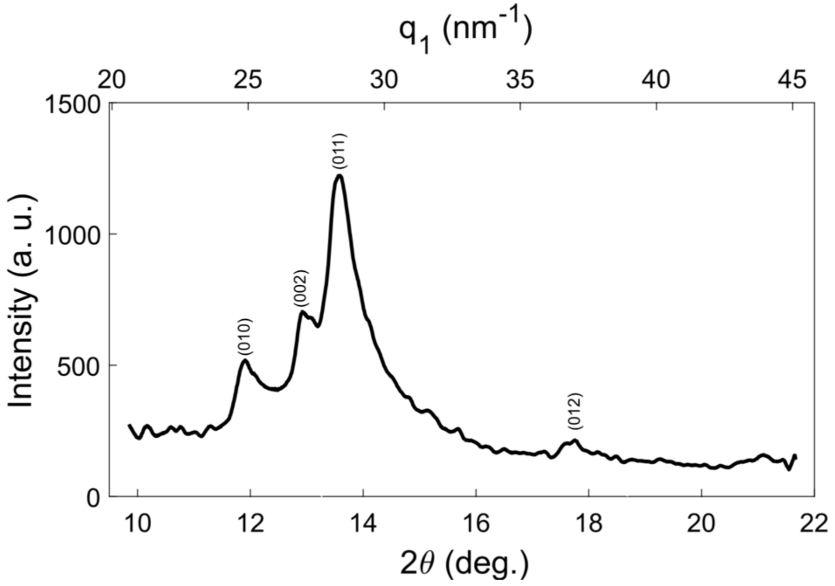

- X-ray energy: mid-energy pink beam
- Detector: small indirect detection
- Frame rate: 100s' kHz
- Exposure time: microsecond
- Detector dynamic range: low
- S/N: low

Fast, but limited detection

1-ID
mono beam

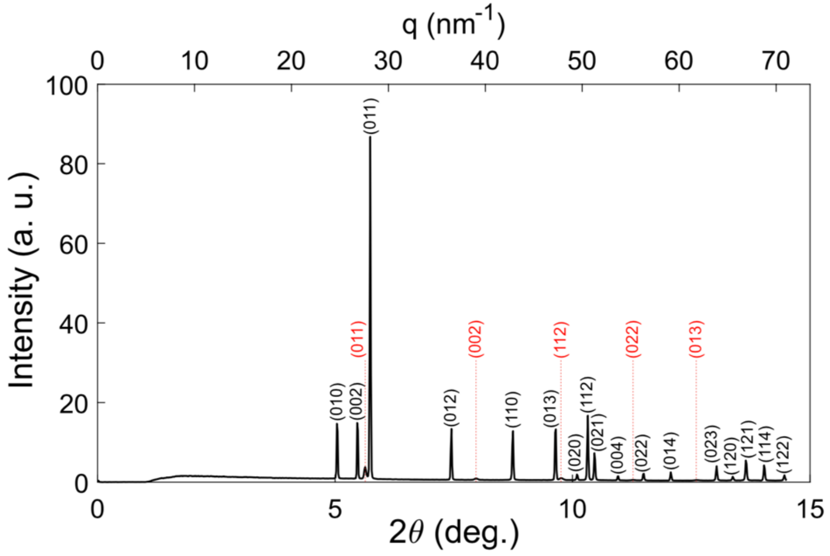

- X-ray energy: high-energy mono beam
- Detector: large direct detection
- Frame rate: 100s Hz
- Exposure time: millisecond
- Detector dynamic range: high
- S/N: high

Slow, but high resolution

Outline

- Introduction to fast X-ray imaging and diffraction
- Fast X-ray imaging system
- Fast X-ray diffraction system
- **Revealing dynamics of additive manufacturing process by fast X-ray imaging and diffraction**
- Approaches to mitigate/eliminate defects in additive manufacturing

What is additive manufacturing

ASTM F2792 − 12a: Additive manufacturing (AM), n—**a process of joining materials to make objects from 3D model data**, usually layer upon layer, as opposed to subtractive manufacturing methodologies. Synonyms: additive fabrication, additive processes, additive techniques, additive layer manufacturing, layer manufacturing, and freeform fabrication.

GE Additive

Laser powder bed fusion (LPBF) additive manufacturing (AM) process

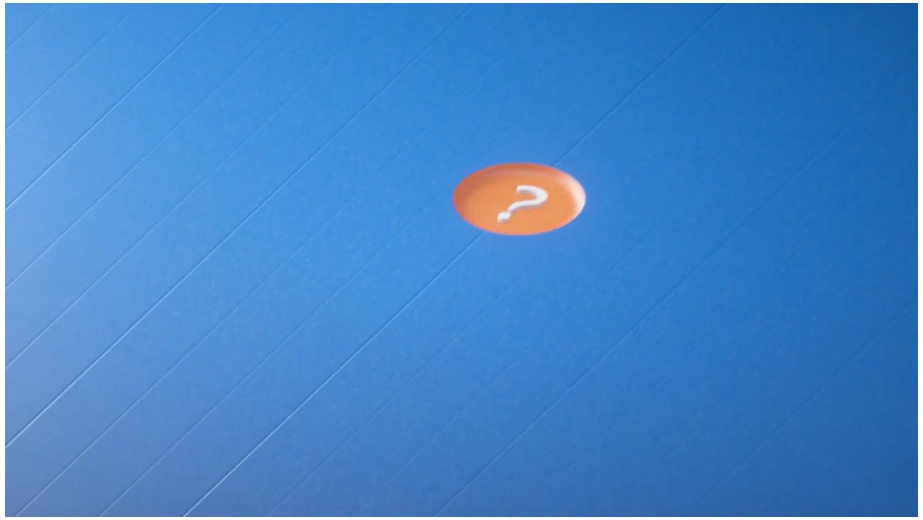

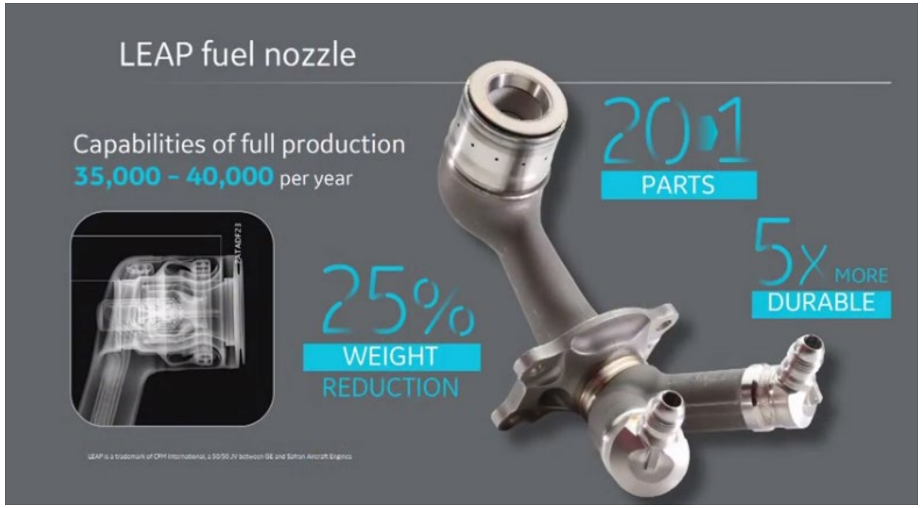

GE Additive

Advantages

- ✓ Complex geometry and functionality
- ✓ Design freedom
- ✓ Faster time to market
- ✓ Part count and interfaces reduction

Challenges

- ✓ Hard to predict
- ✓ Containing many uncertainties
- ✓ Low fatigue life in AM parts
- ✓ Lack of qualification and certification

Laser powder bed fusion (LPBF) AM process

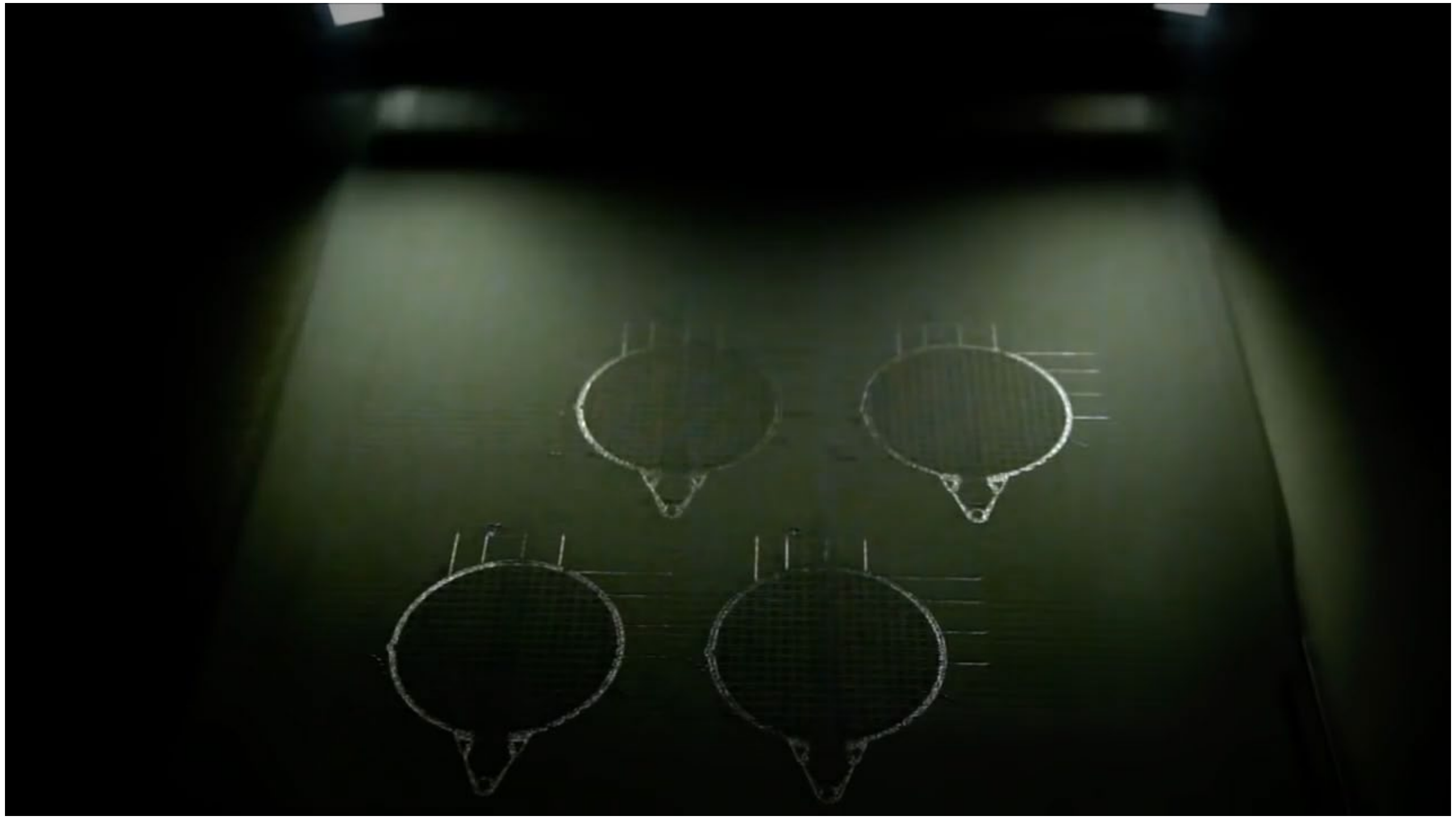

- Very fast (microseconds)
- Highly localized (100s of μm)
- Opacity of metals to visible light
- Harsh environments (high temperature, spatter)

Questions:

- What happens during laser-material interaction?
- What is the underlying mechanism?

Quantitatively reveal the dynamics and mechanisms of LPBF process

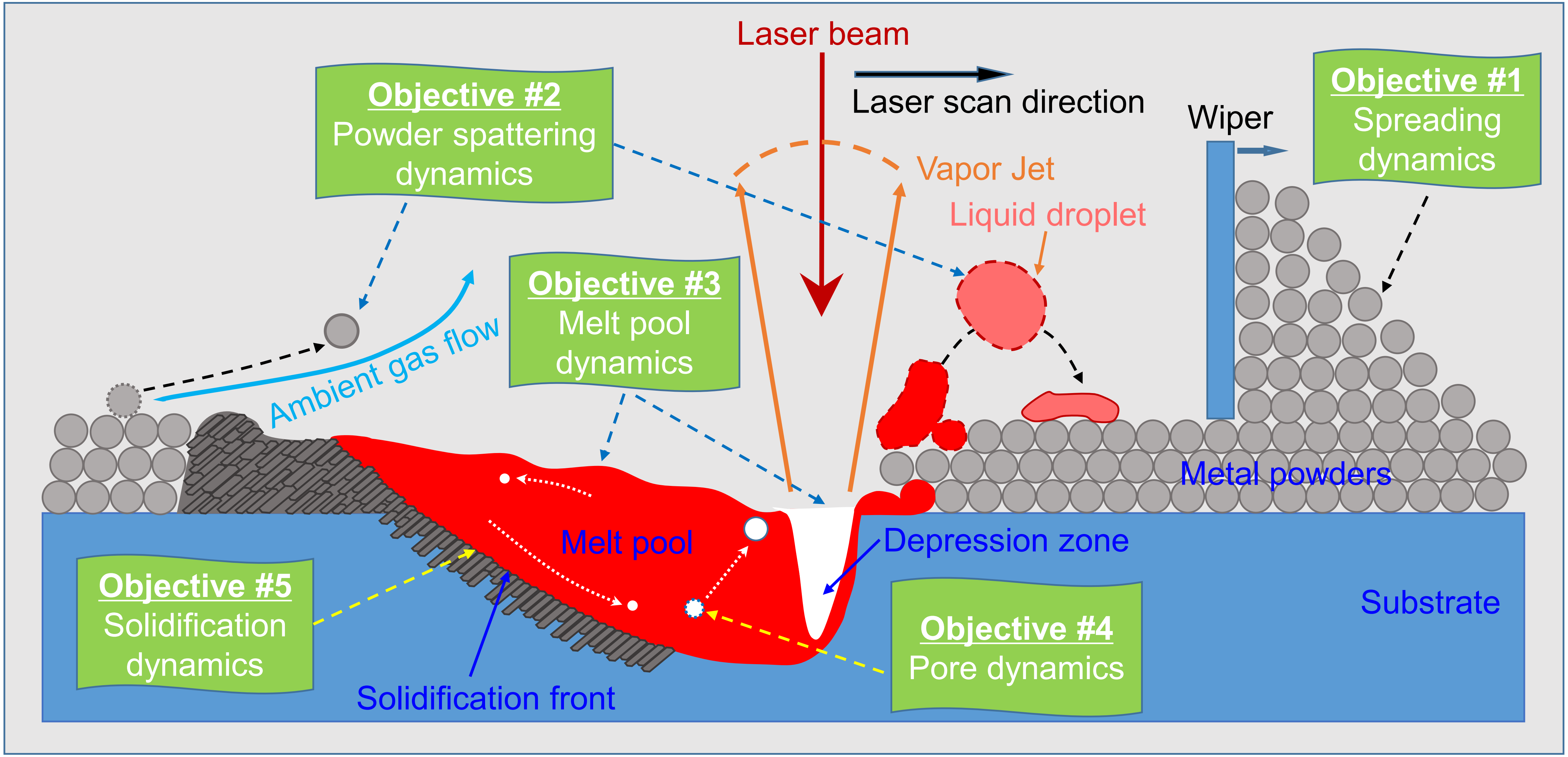

Laser scan speed: about m/s, wiper speed: 100s mm/s

High-speed high-energy synchrotron x-ray imaging and diffraction

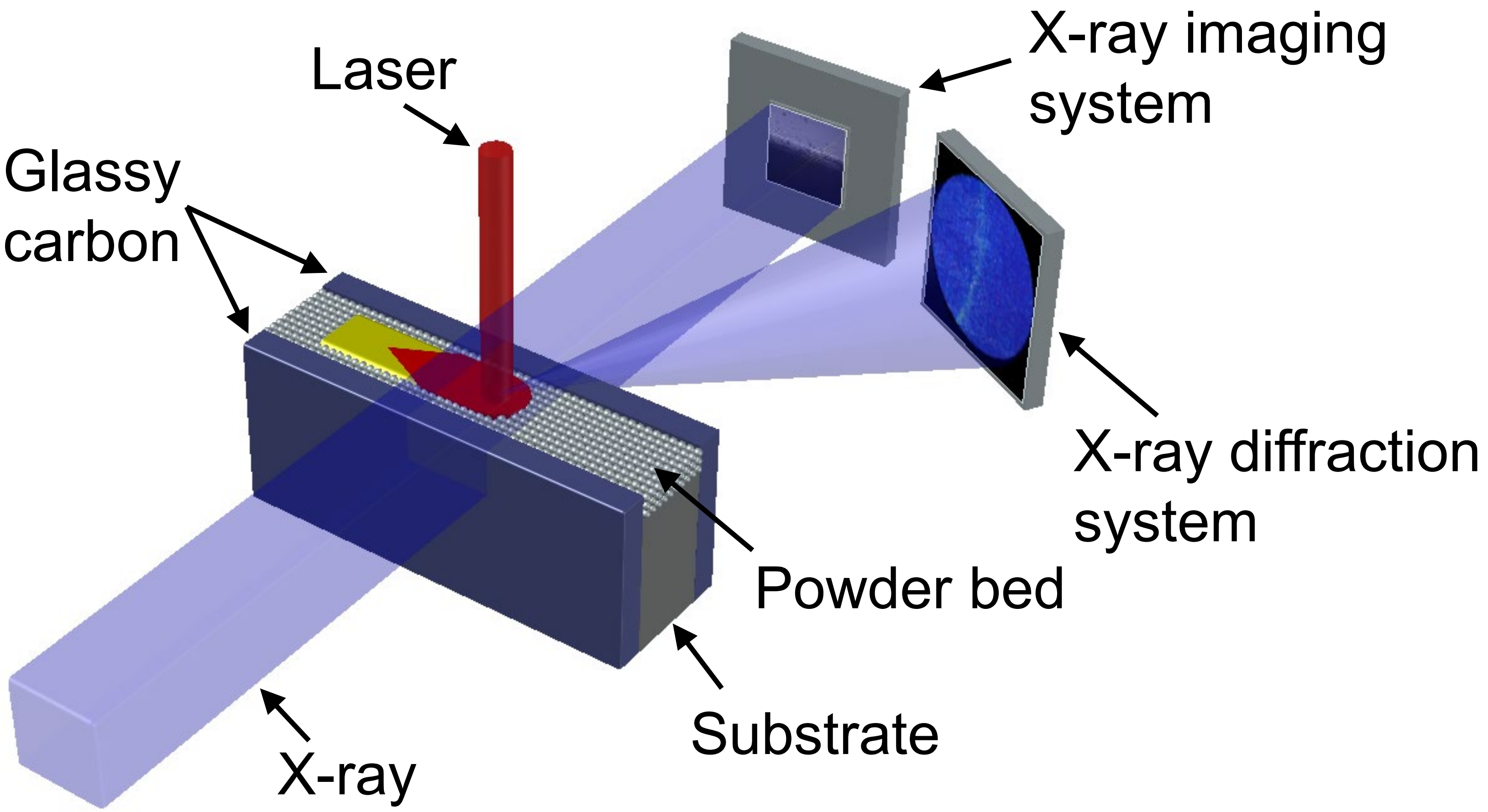

APS 32-ID-B, X-ray energy: 24 keV, resolution: up to 1 μm, frame rate: up to 6.5 MHz, exposure time: down to100 ps

In-situ x-ray imaging/diffraction system

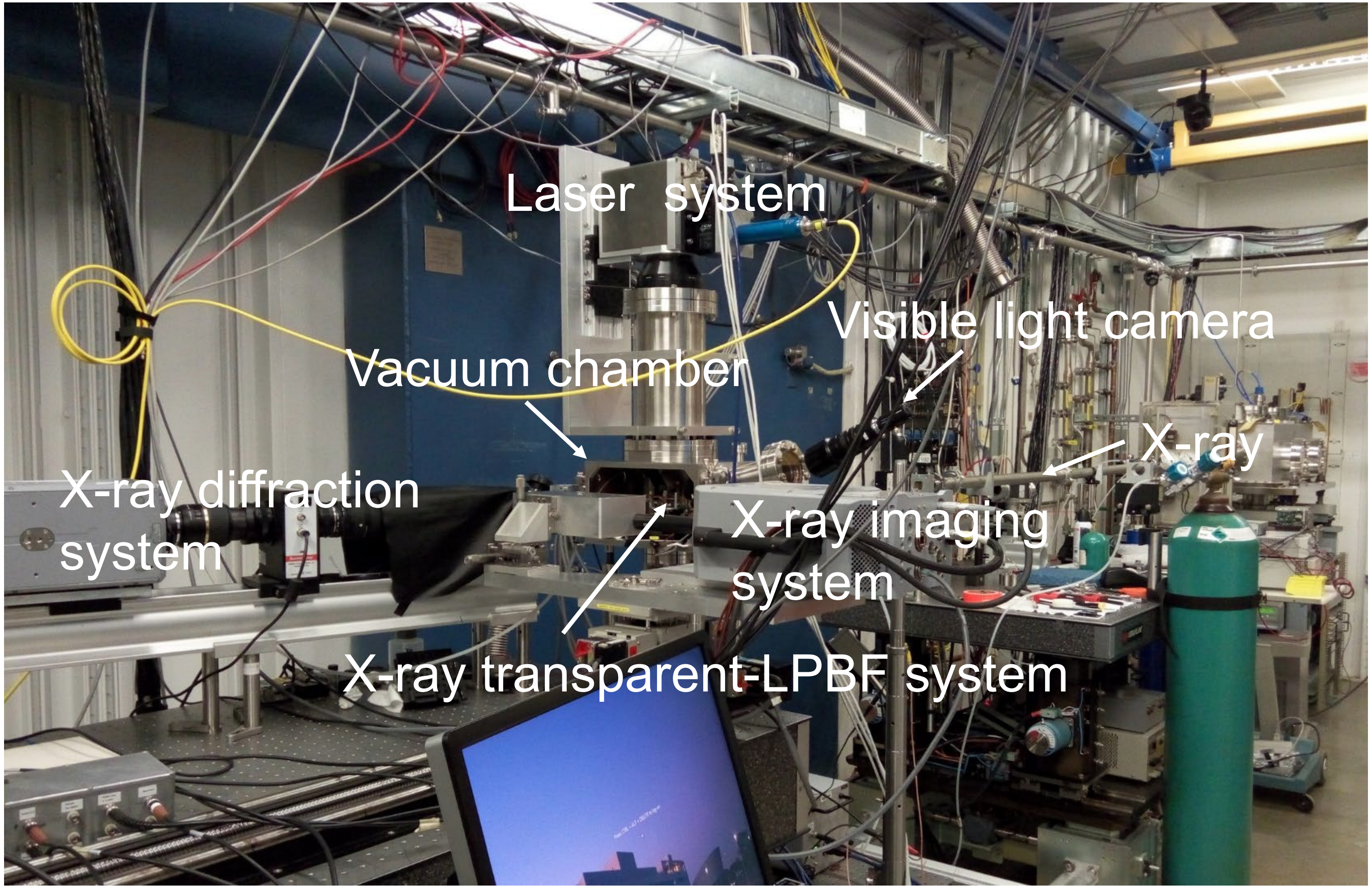

Cang. Zhao et al., Real-time monitoring of laser powder bed fusion process using high-speed X-ray imaging and diffraction, Scientific Reports, 7, 3602 (2017).

Quantitatively reveal the dynamics and mechanisms of LPBF process

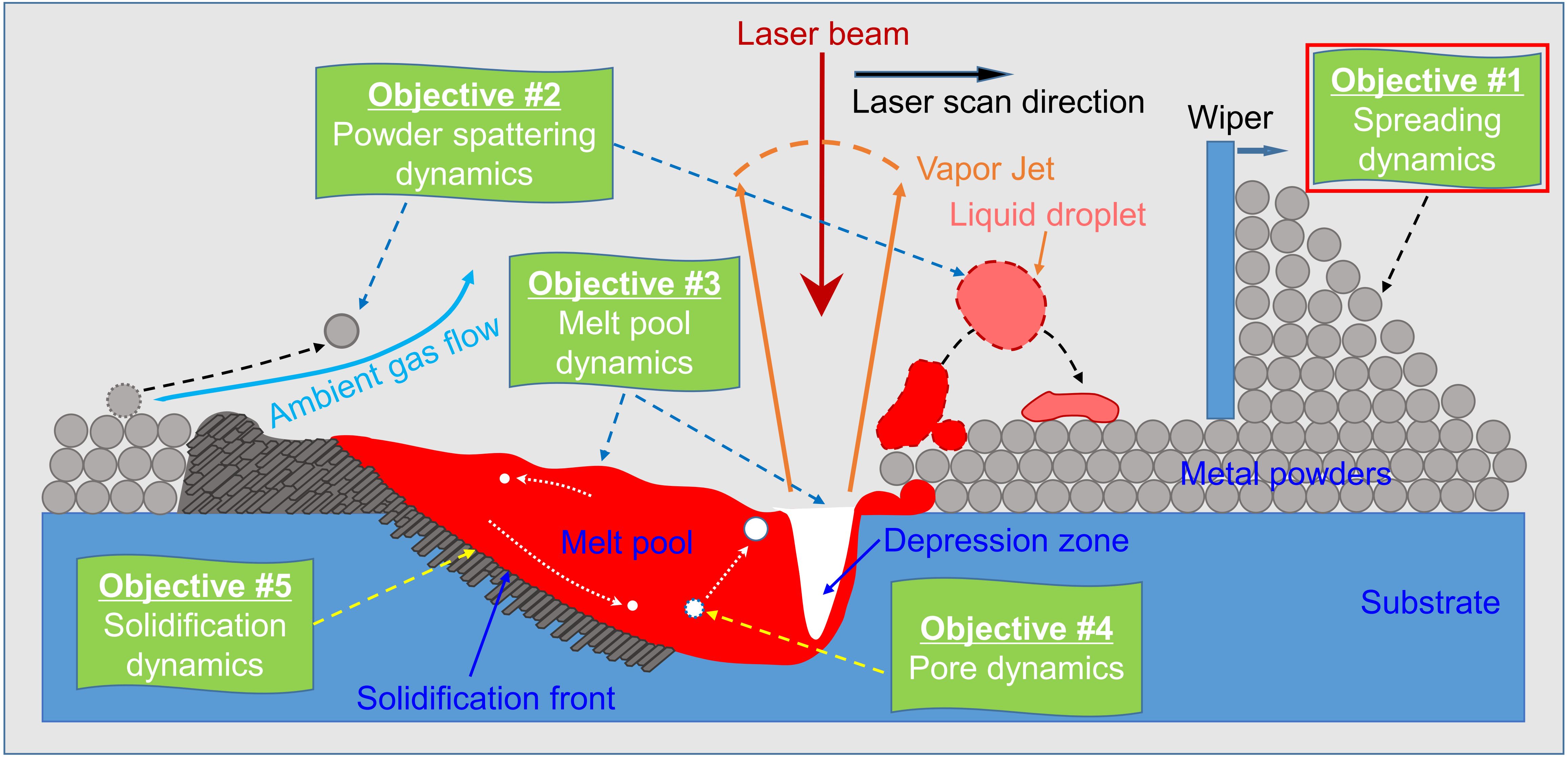

Laser scan speed: about m/s, wiper speed: 100s mm/s

Powder spreading

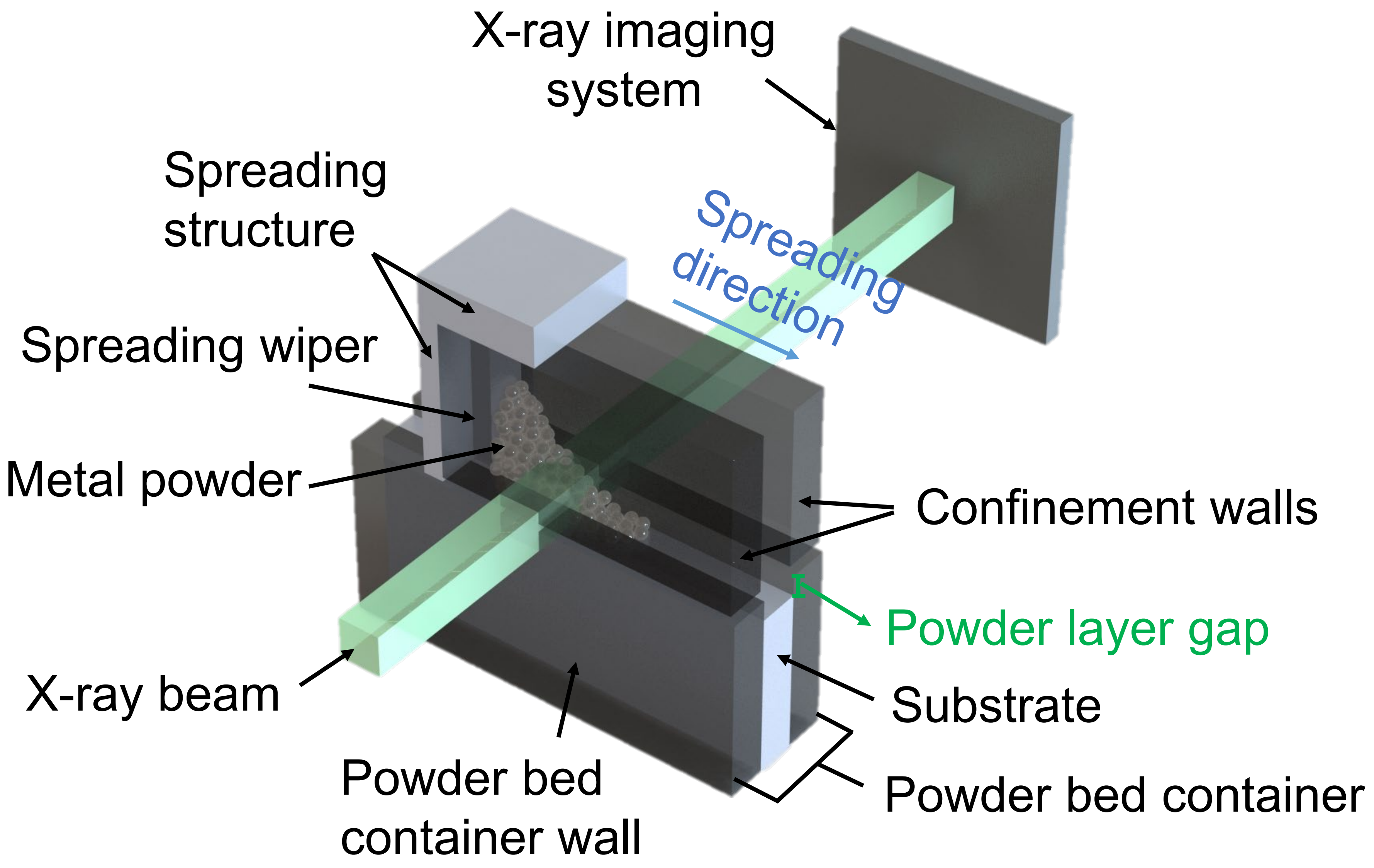

Dynamics of powder spreading

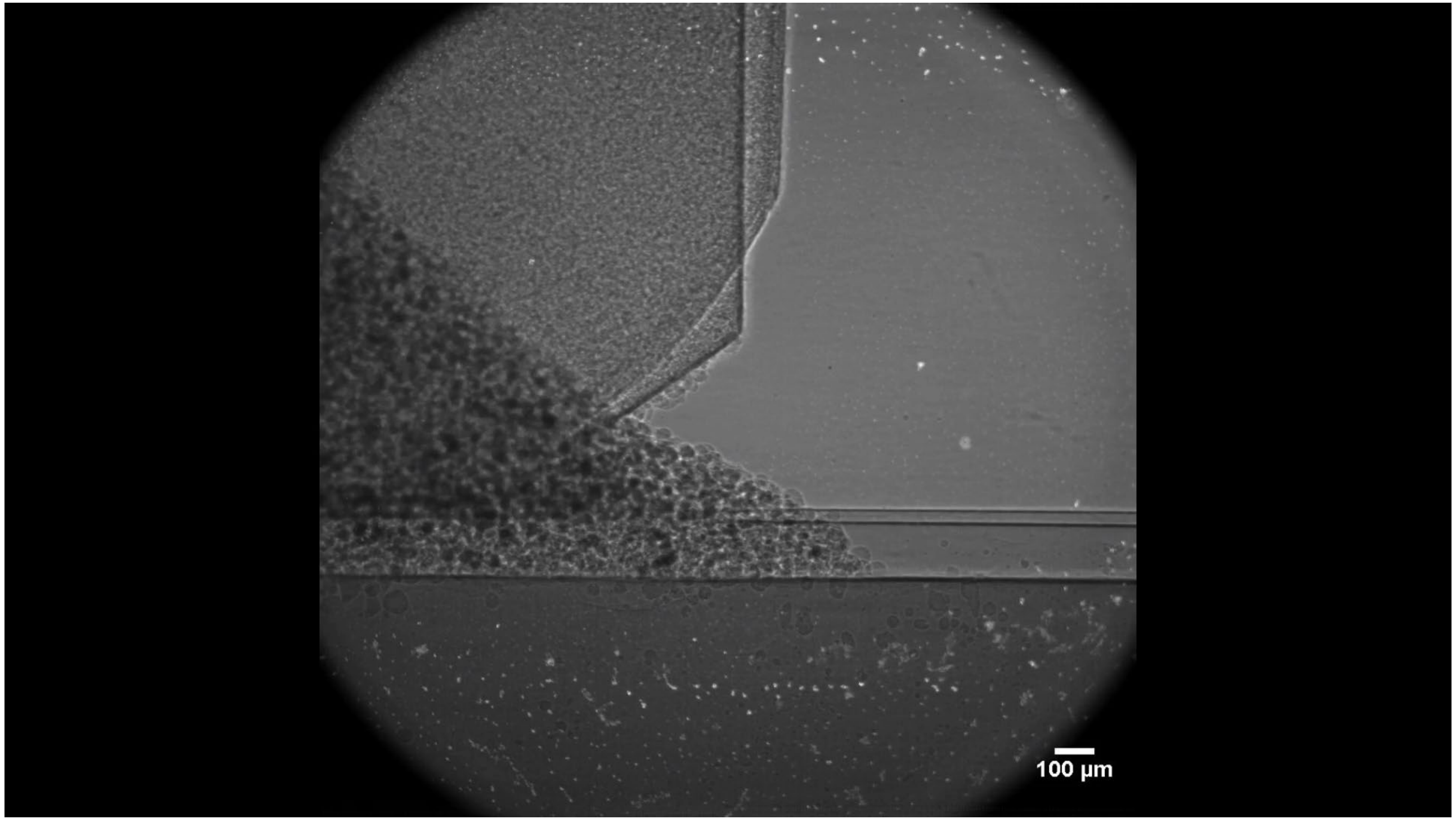

- Reveal powder spreading mechanisms
- Establish the correlation between powder bed quality and powder characteristics, recoater material and geometry, and spreading parameter

Luis I. Escano et al., *Scientific Reports*, 8, 15079 (2018); *Review of Scientific Instruments* 93, 043707 (2022)

Quantitatively reveal the dynamics and mechanisms of LPBF process

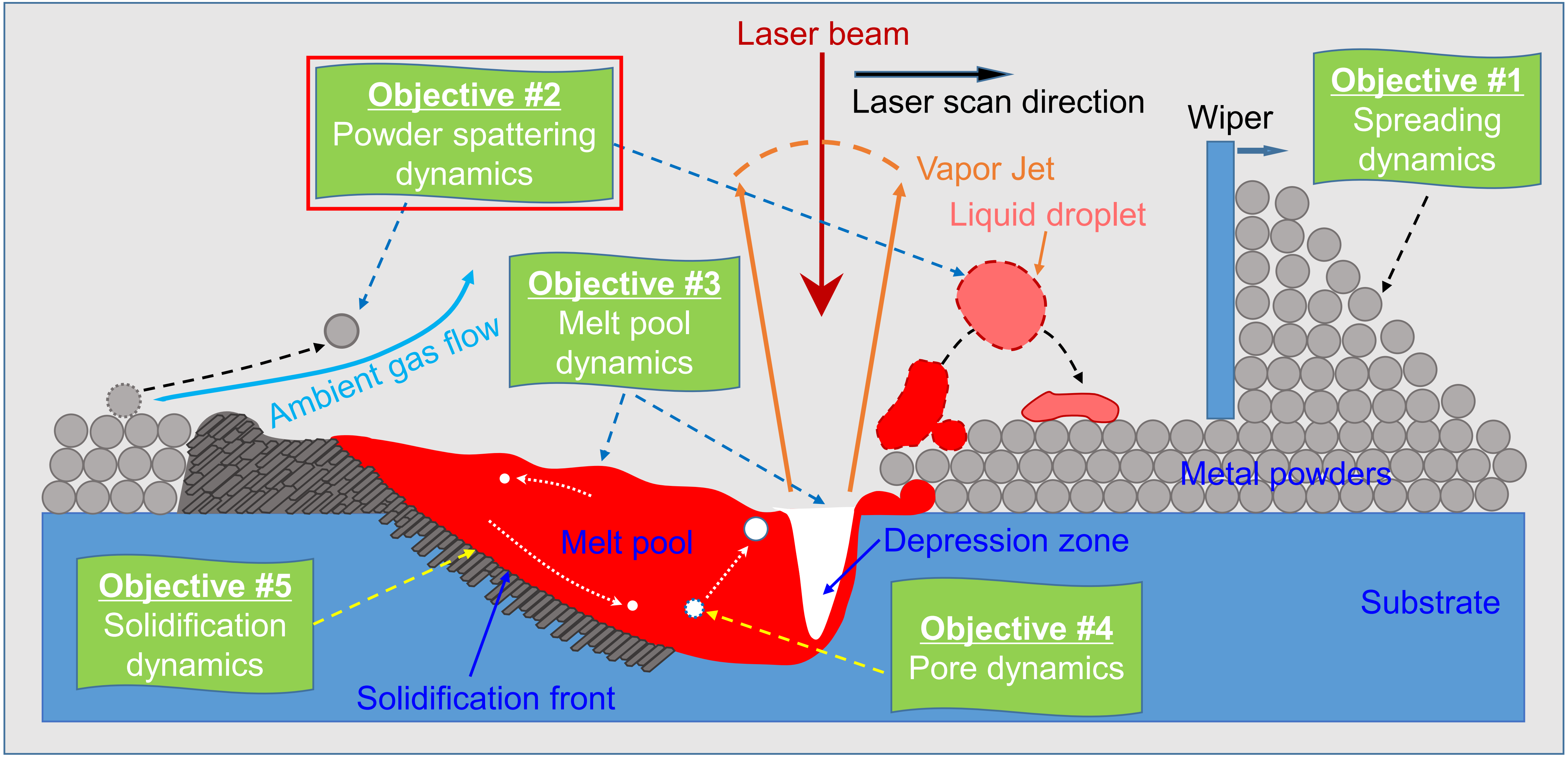

Laser scan speed: about m/s, wiper speed: 100s mm/s

Powder spattering dynamics during laser scan

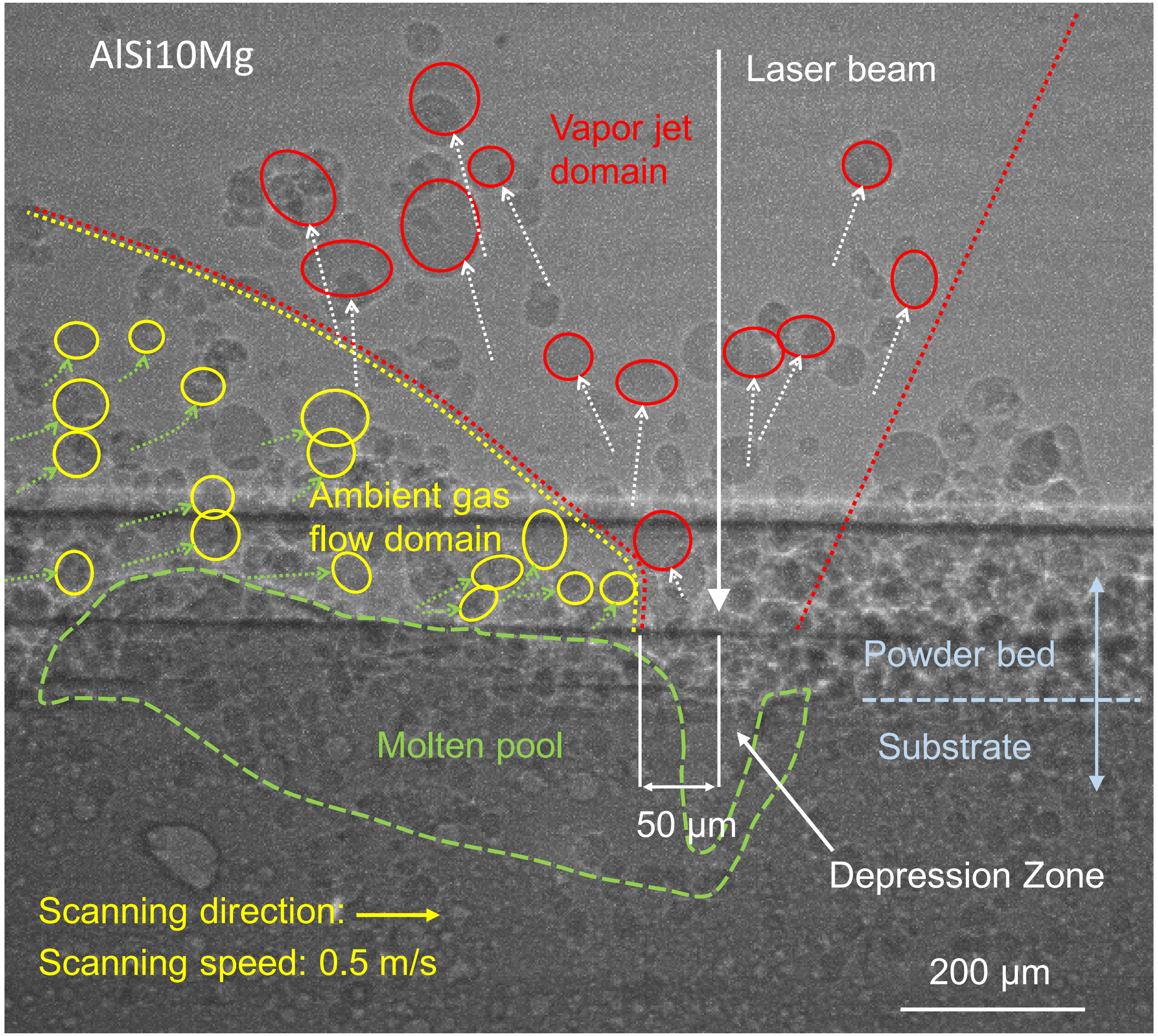

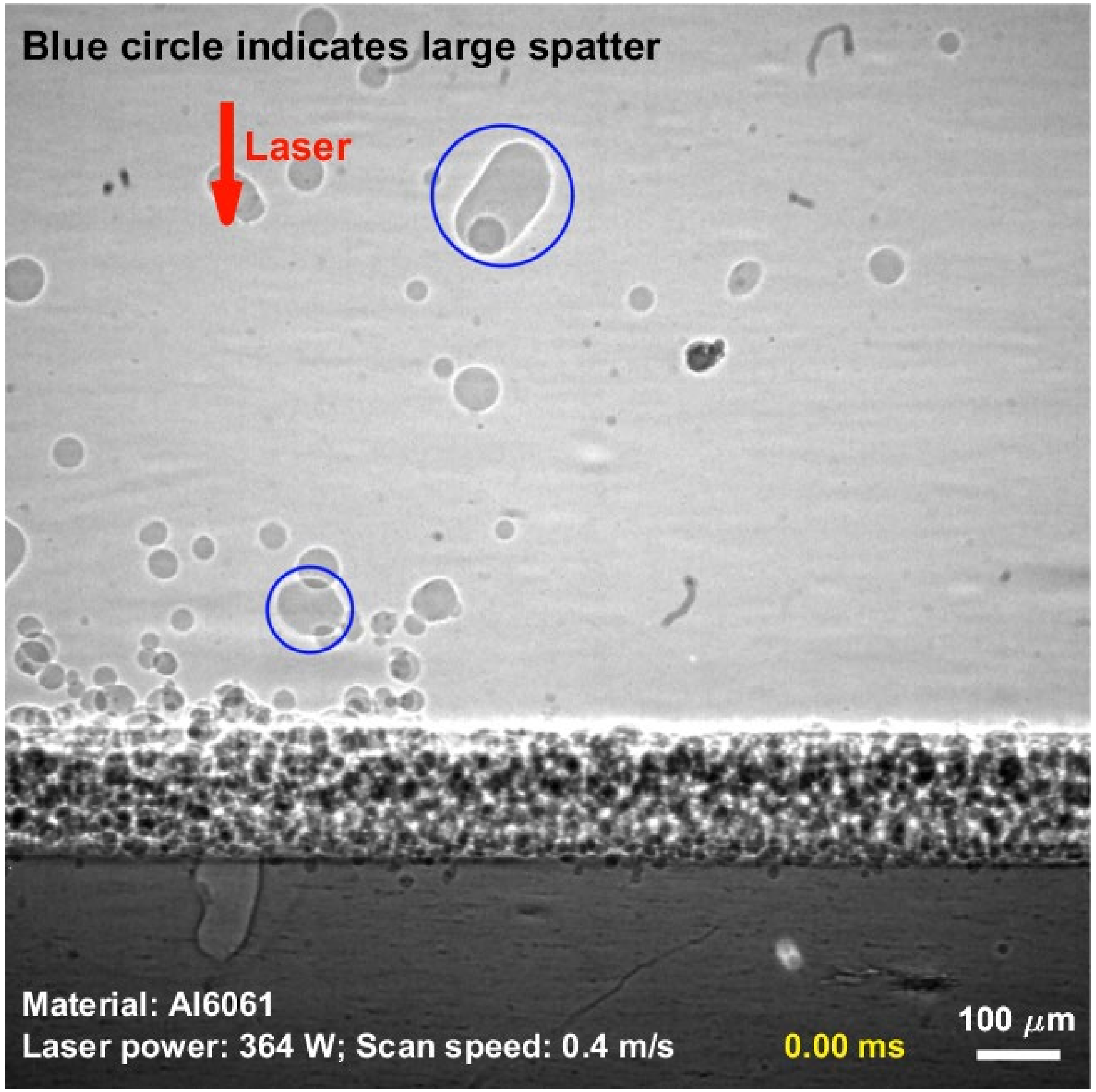

Spatter induced defects

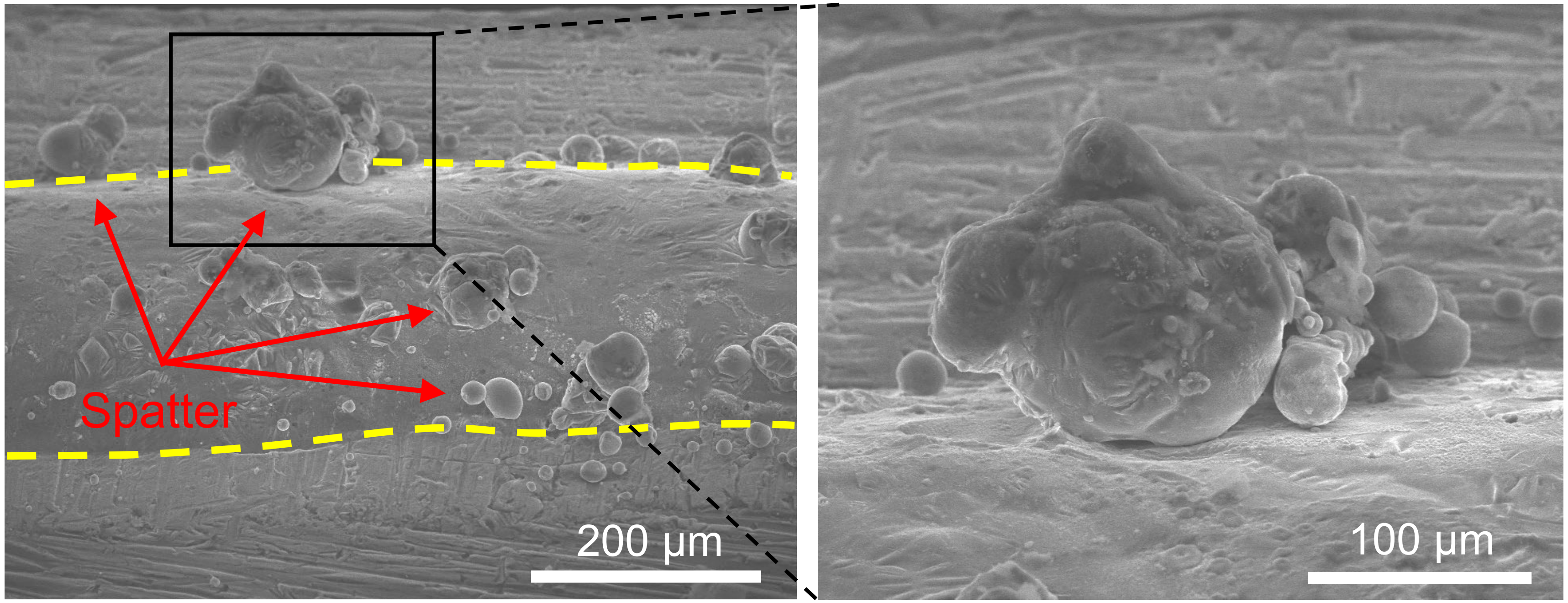

SEM images showing spatter-induced surface defects in an AlSi10Mg sample.

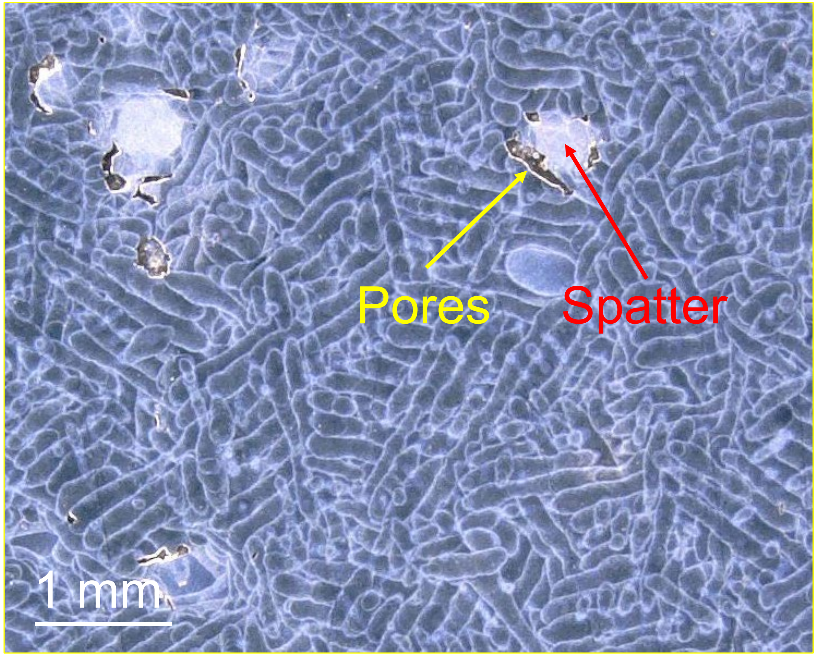

Optical image showing lack of fusion pore in an AM AlSi10Mg.

- **Zachary A. Young et al., Types of spatter and their features and formation mechanisms in laser powder bed fusion additive manufacturing process, *Additive Manufacturing*, 36, 101438 (2020).**
- **Qilin Guo et al., Transient dynamics of powder spattering in laser powder bed fusion additive manufacturing process revealed by in-situ high-speed high-energy x-ray imaging, *Acta Materialia*, 151, 169 (2018).**

Quantitatively reveal the dynamics and mechanisms of LPBF process

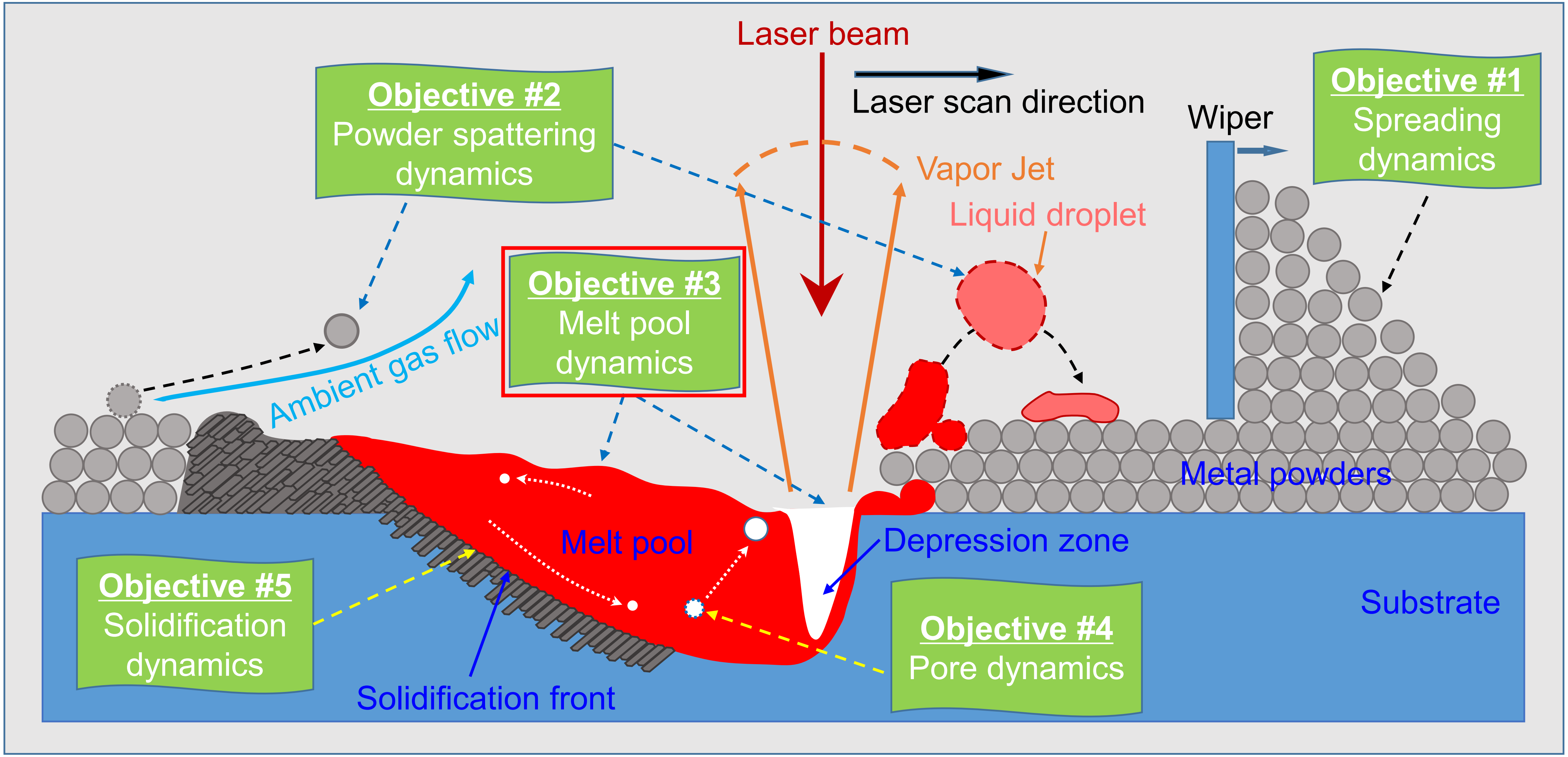

Laser scan speed: about m/s, wiper speed: 100s mm/s

Melt pool evolution

Processed

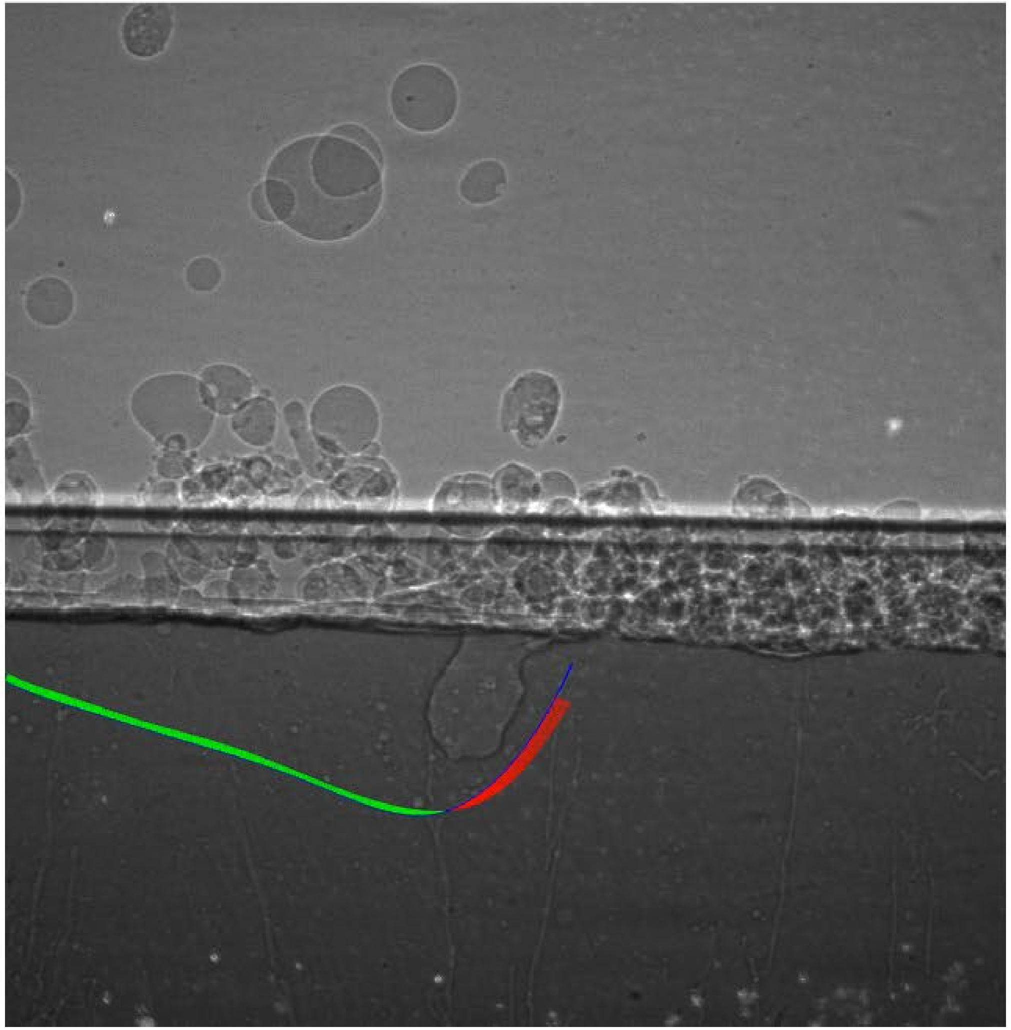

Original

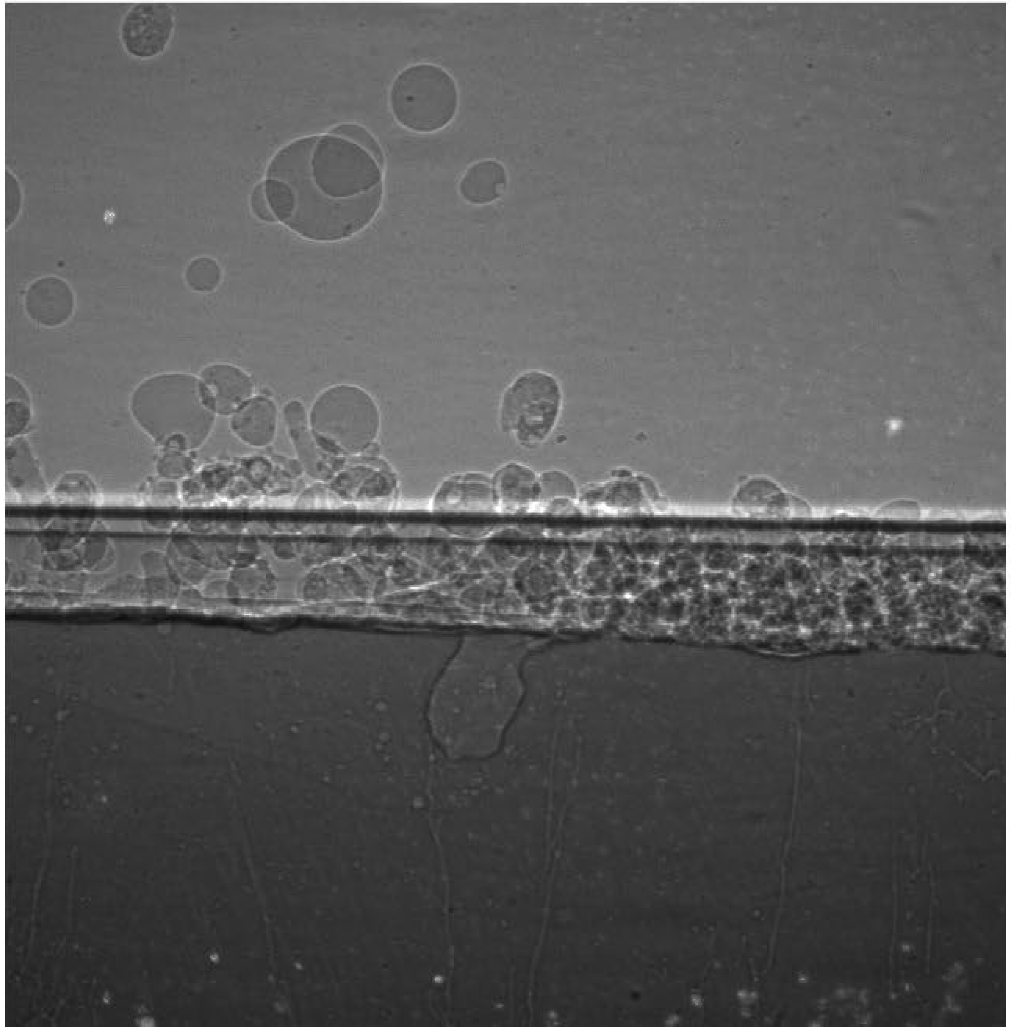

Melt pool variation under constant input energy density (IED)

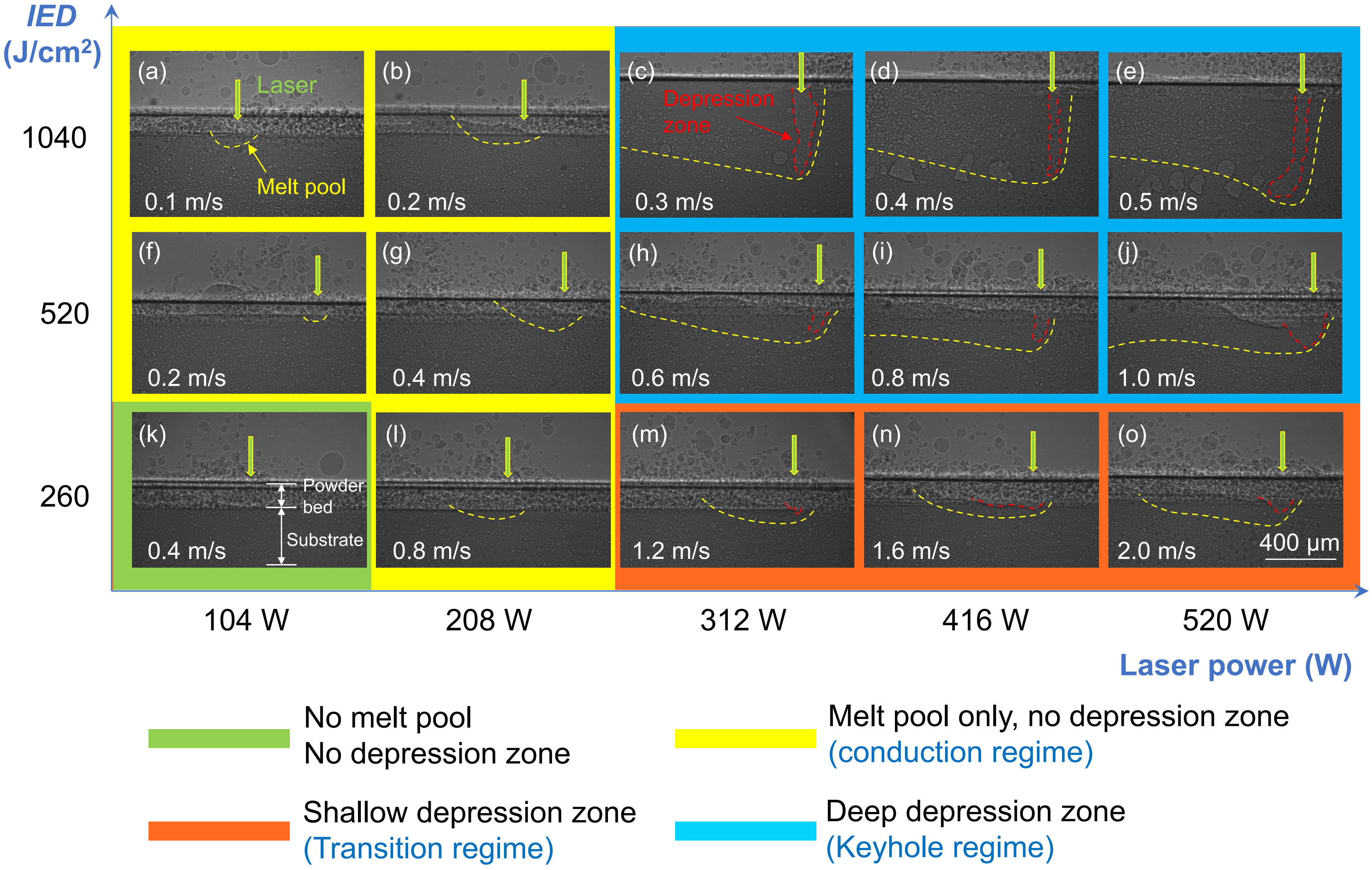

IED=p/(vd), p, laser power, v, scan speed, d, laser diameter

Up to two orders of magnitude change of melt pool volume

Qilin Guo et al., *Additive Manufacturing*, 28, 600-609 (2019).

Dynamics of melt flow

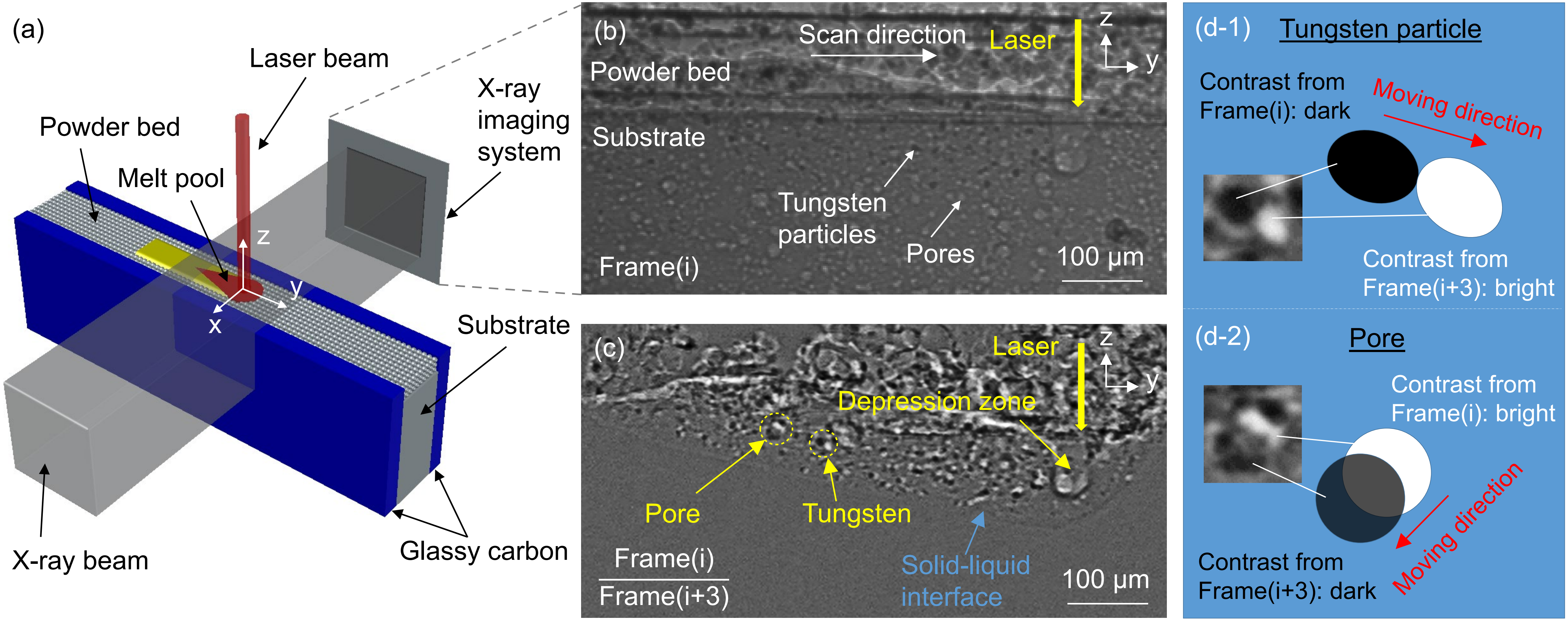

Full-field melt flow mapping approach to reveal the location-specific flow patterns in different regions of the melt pool, and to quantify the speeds of various types of flow.

Two-view observation to get 3D information

(a) Laser scan ⊥ x-ray

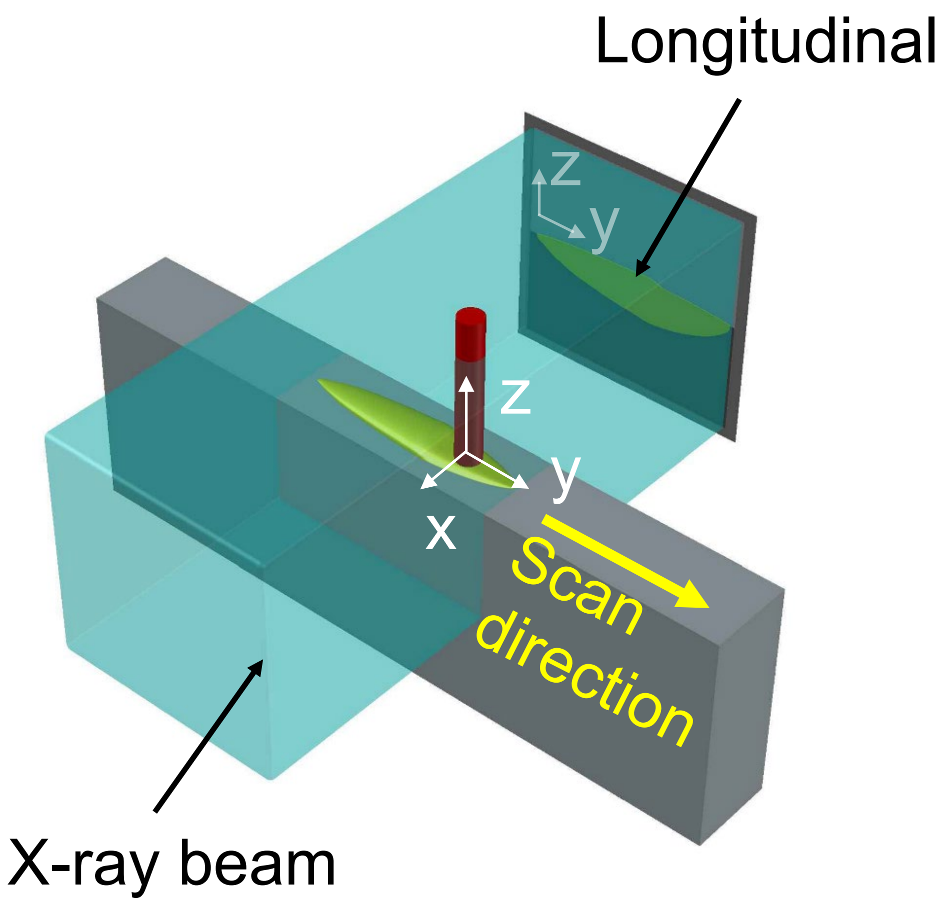

(b) Laser scan // x-ray

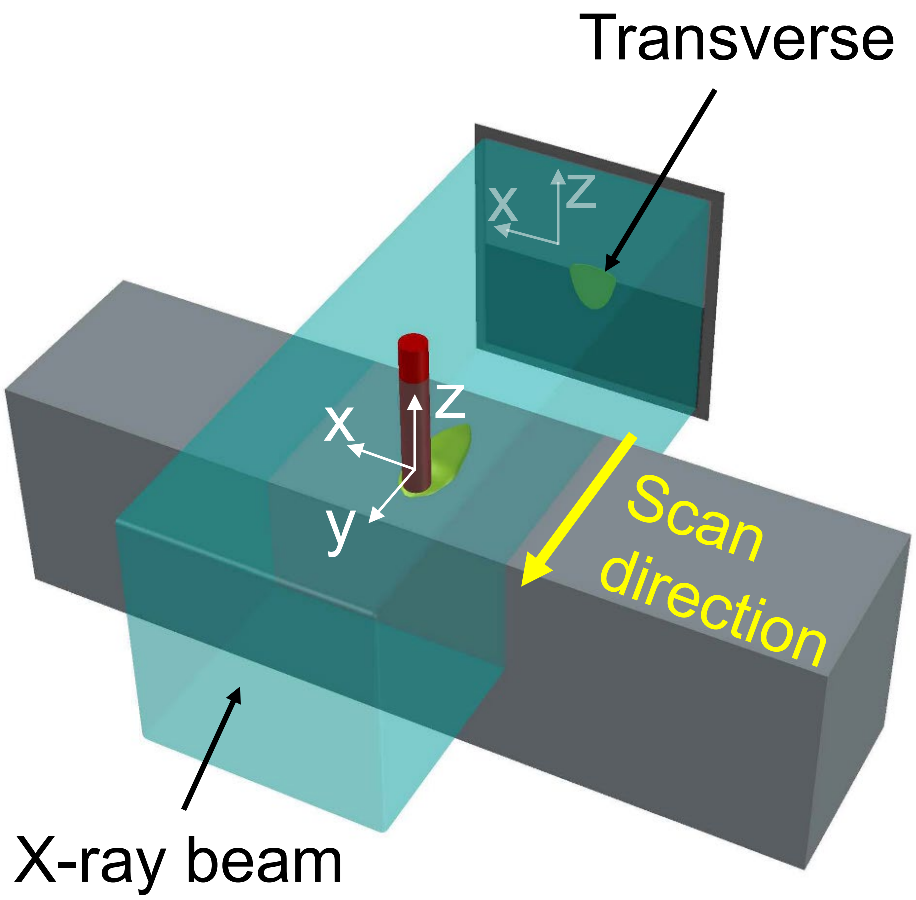

Melt flow in keyhole mode melting

- Longitudinal view

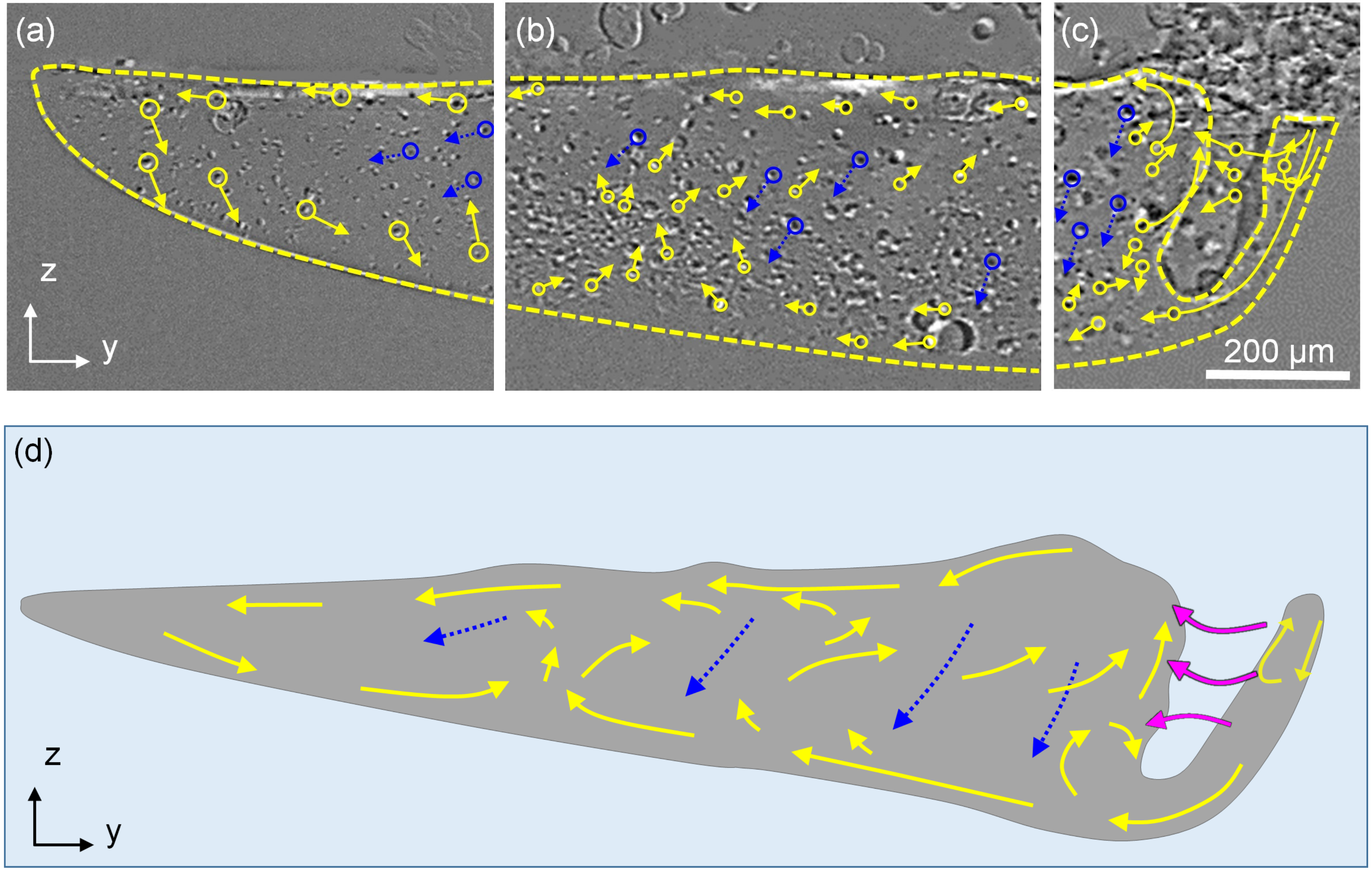

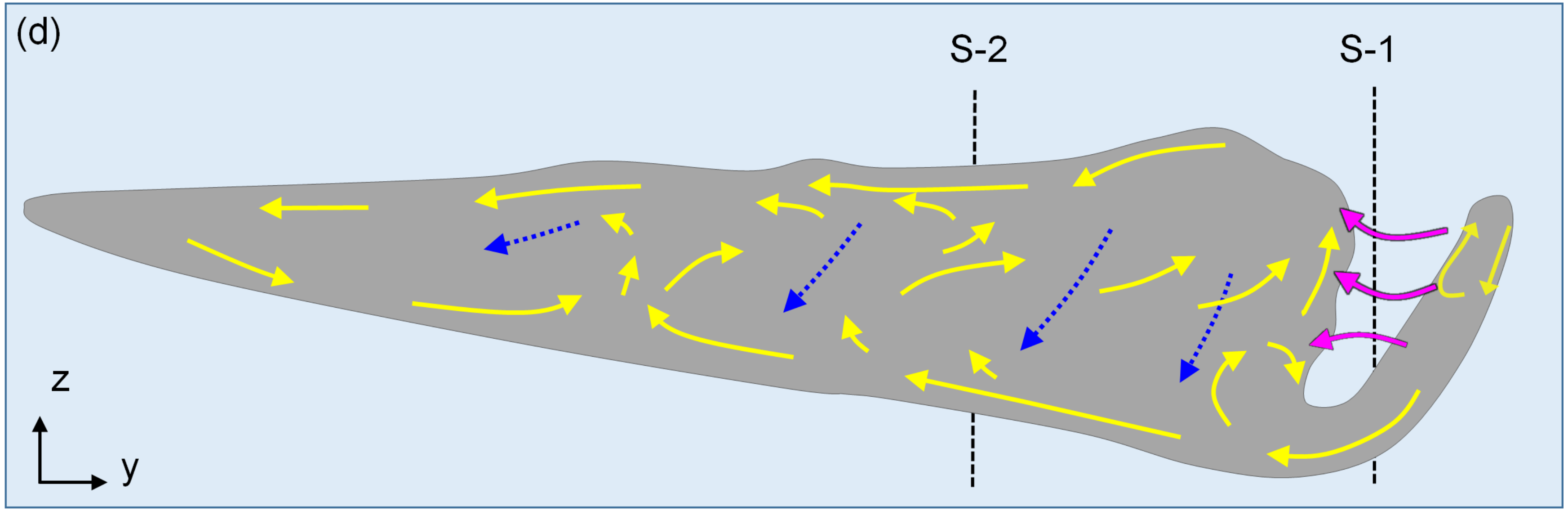

- Transverse view

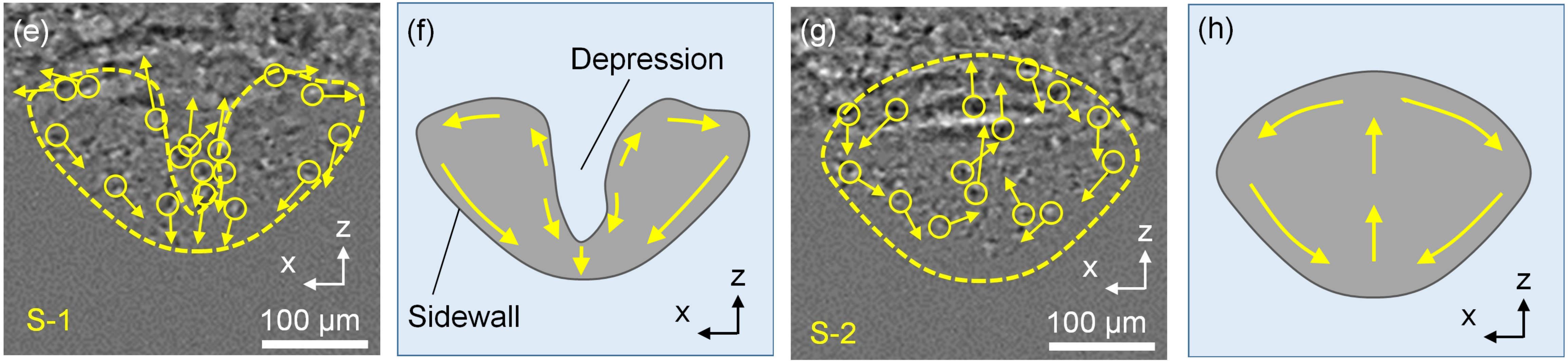

3D reconstruction

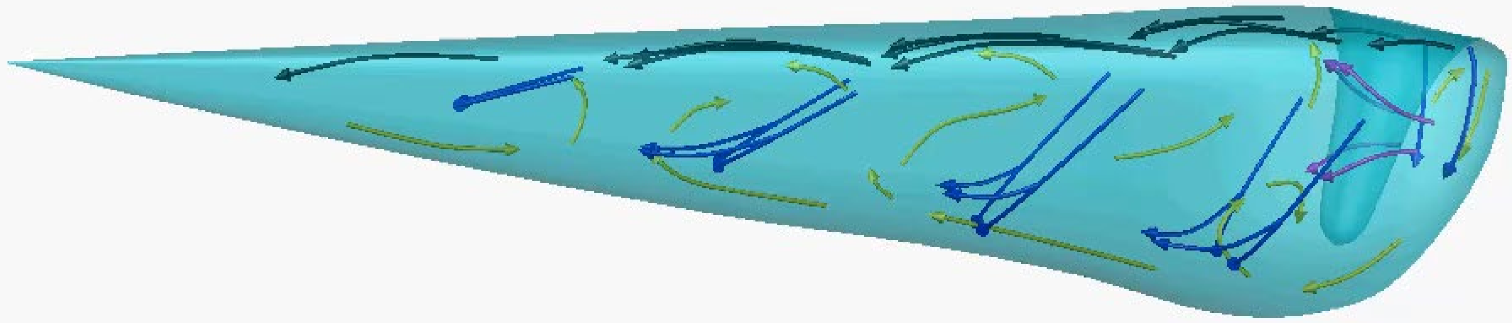

Qilin Guo et al., In-situ full-field mapping of melt flow dynamics in laser metal additive manufacturing, *Additive Manufacturing*, 31, 100939 (2020).

Melt flow instabilities

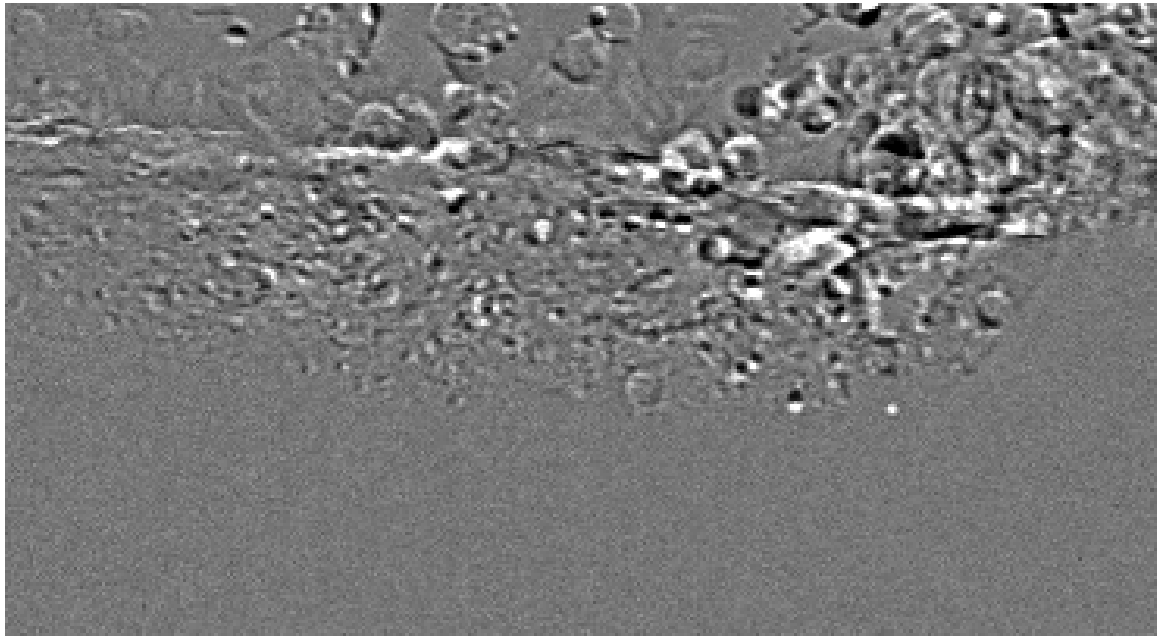

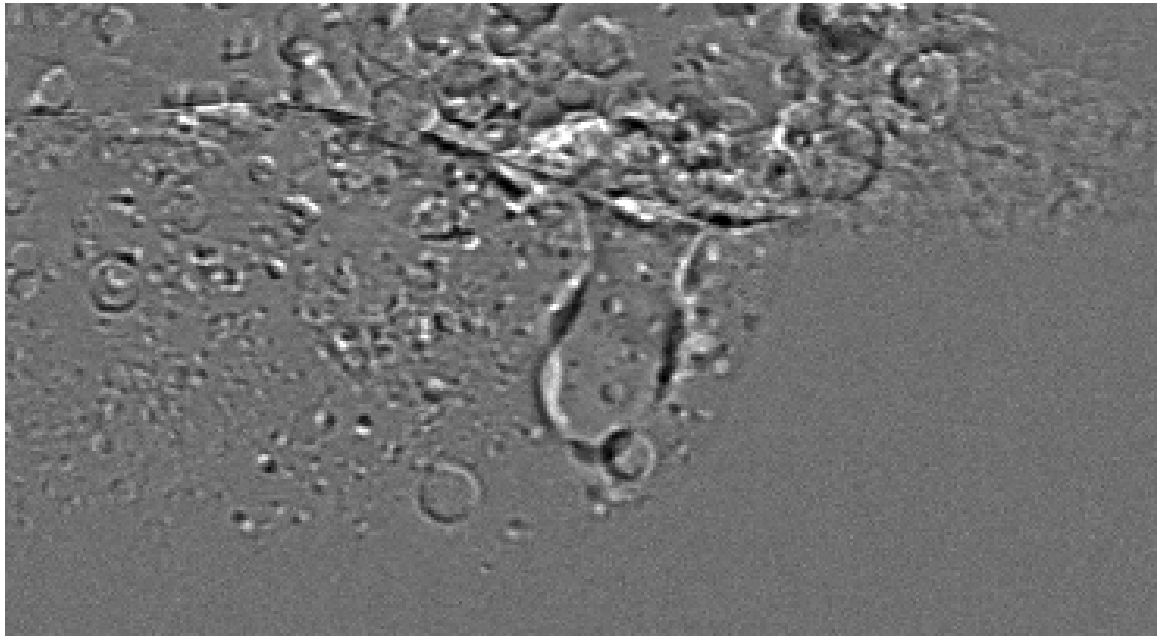

- Type I—Powder/droplet impact induced instability
- Type II—Significant keyhole oscillation induced instability
- Type III—Melting-mode switching induced instability

Qilin Guo et al., Revealing melt flow instabilities in laser powder bed fusion additive manufacturing of aluminum alloy via in-situ high-speed X-ray imaging, *International Journal of Machine Tools and Manufacture*, 175, 103861 (2022).

Quantitatively reveal the dynamics and mechanisms of LPBF process

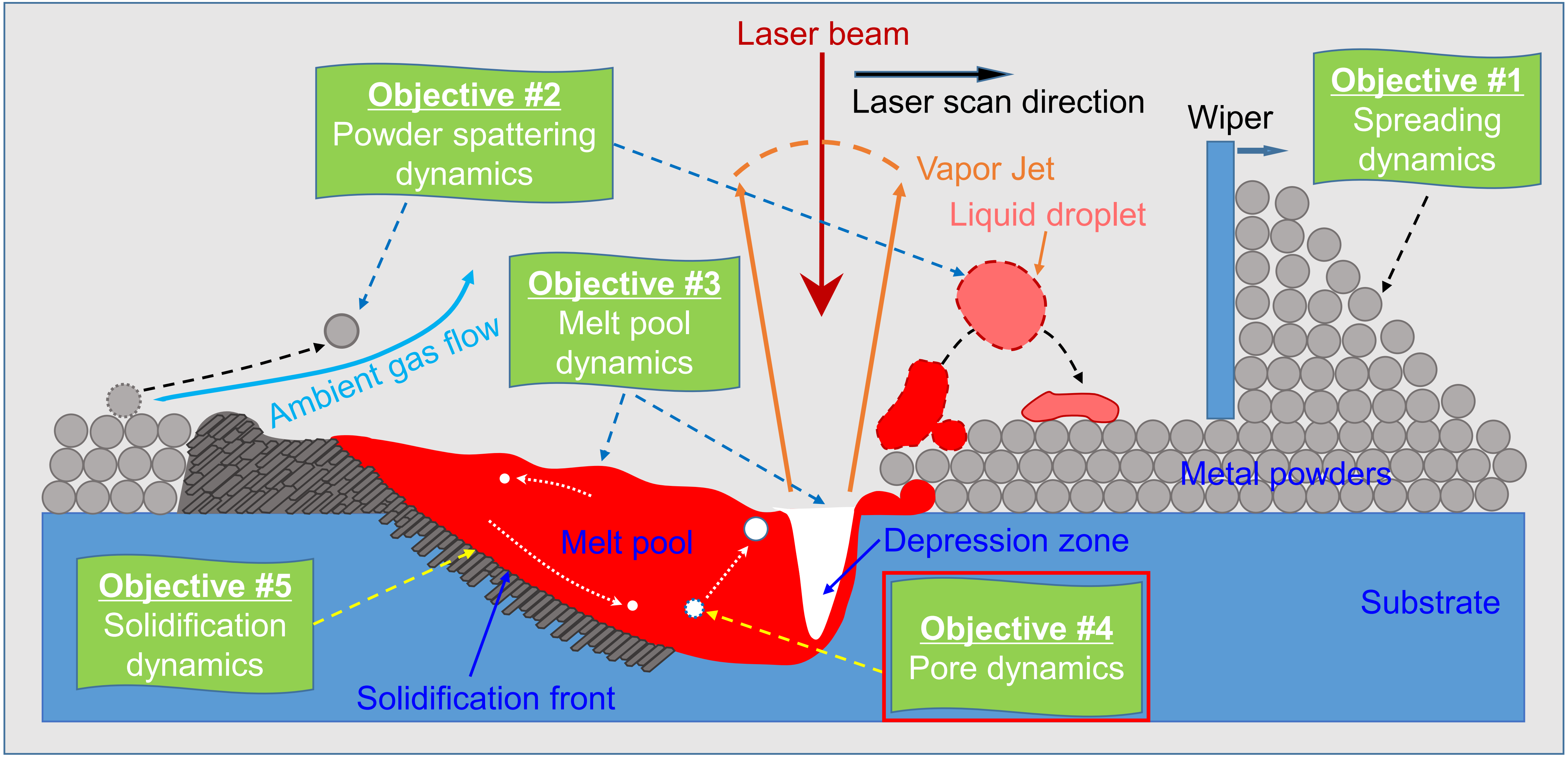

Laser scan speed: about m/s, wiper speed: 100s mm/s

Dynamics of pore formation

Transfer from feedstock powders

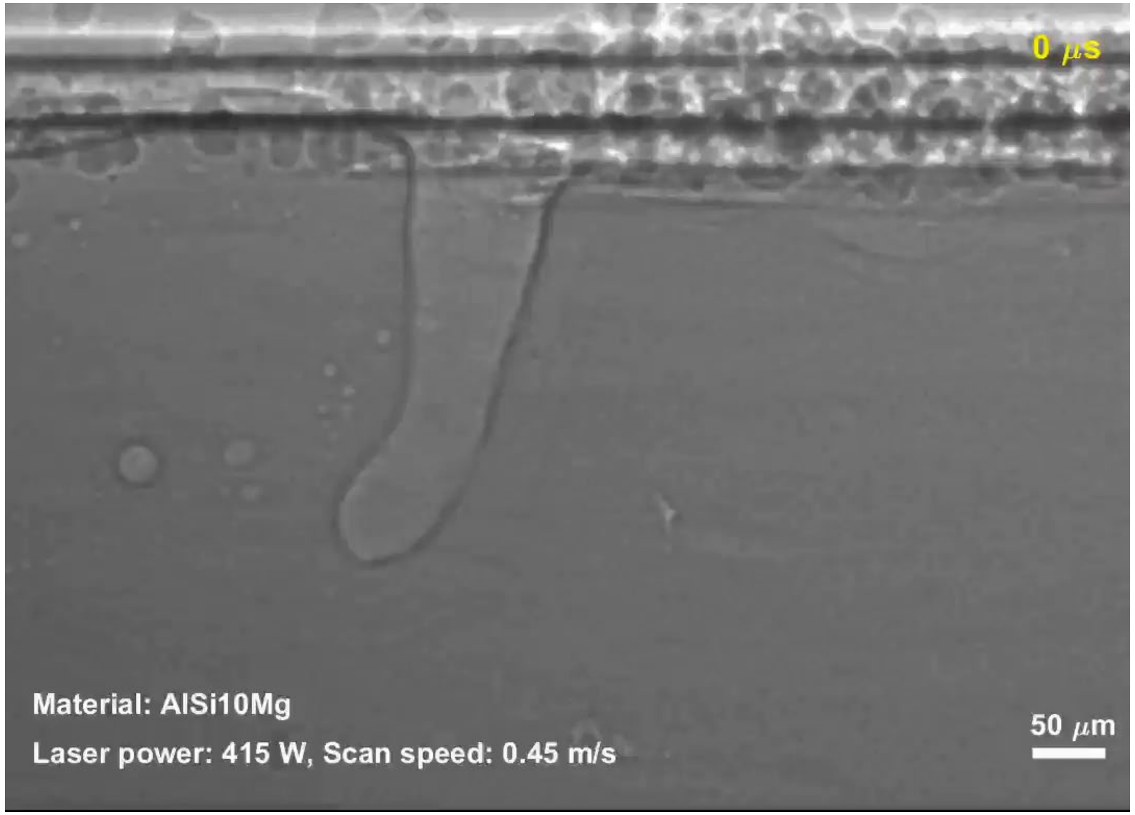

Depression zone instability

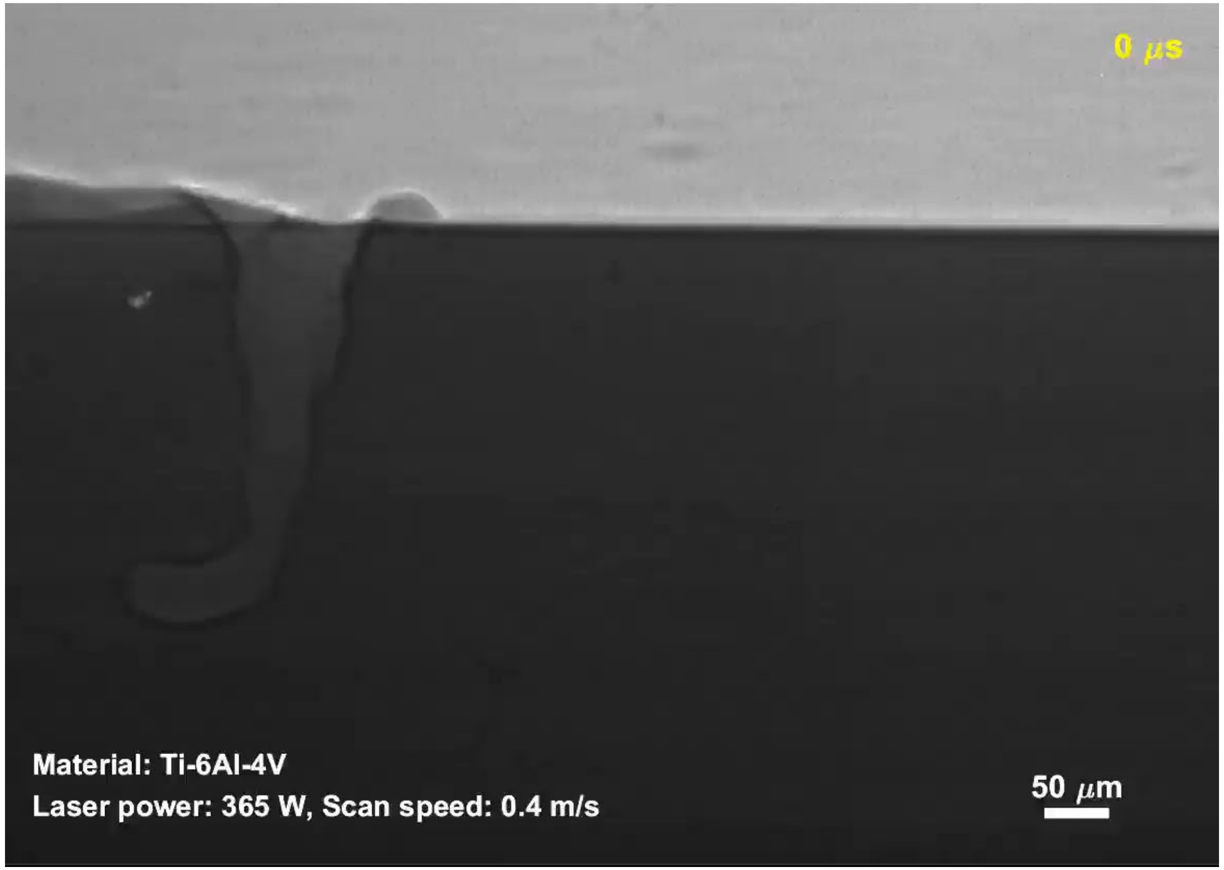

Surface fluctuation

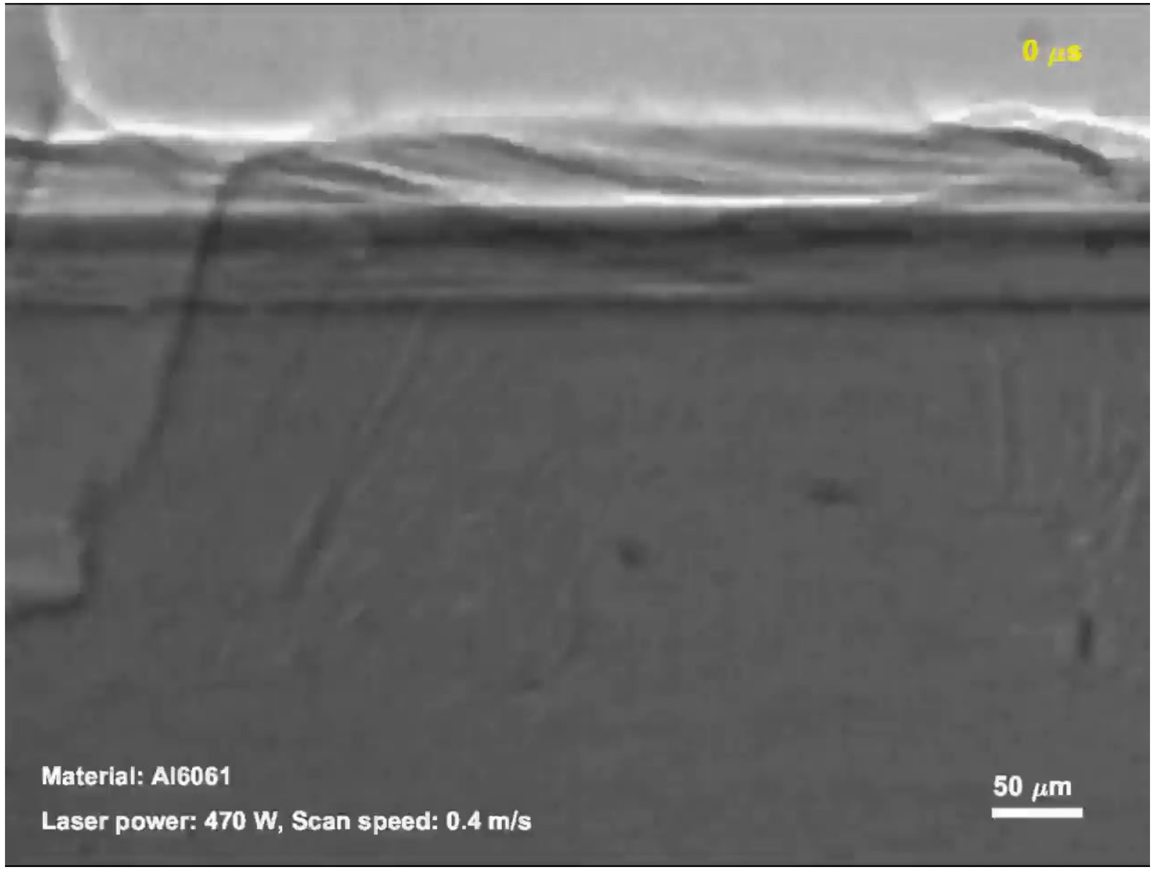

Crack induced pore

S. Mohammad. H. Hojjatzadeh et al., Direct observation of pore formation mechanisms during LPBF additive manufacturing process and high energy density laser welding, *International Journal of Machine Tools and Manufacture*, 153, 103555 (2020).

Dynamics of pore evolution

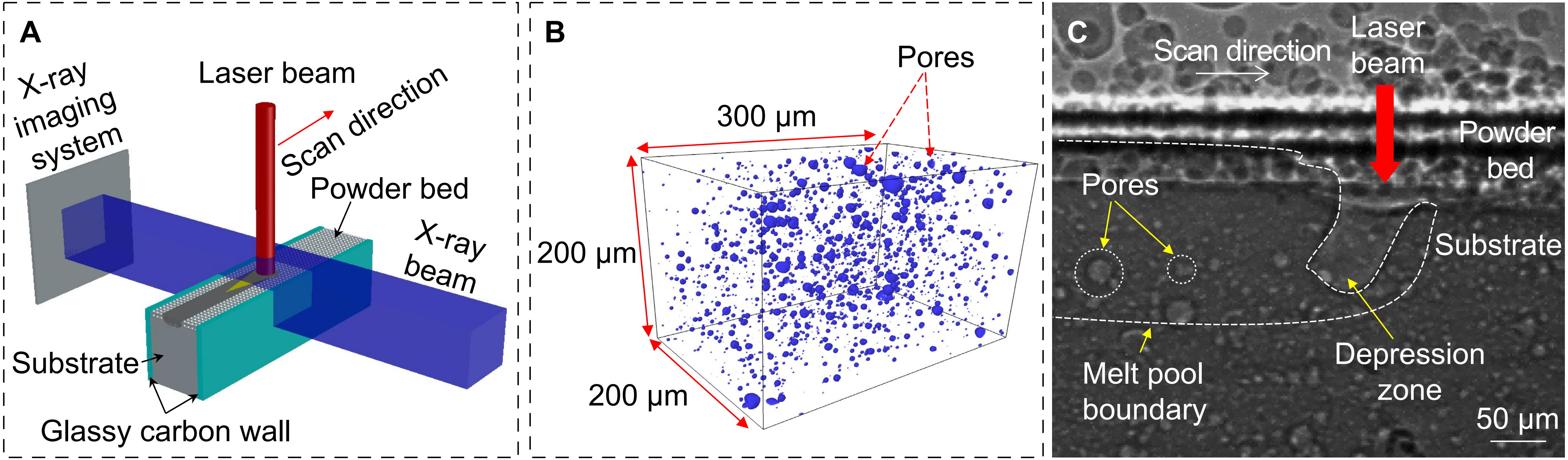

To probe pore motion in every location in the melt pool, AlSi10Mg plate samples, with uniformly dispersed pores (diameters of 10 to 60 μm), were used for this study.

Dynamics of pore evolution

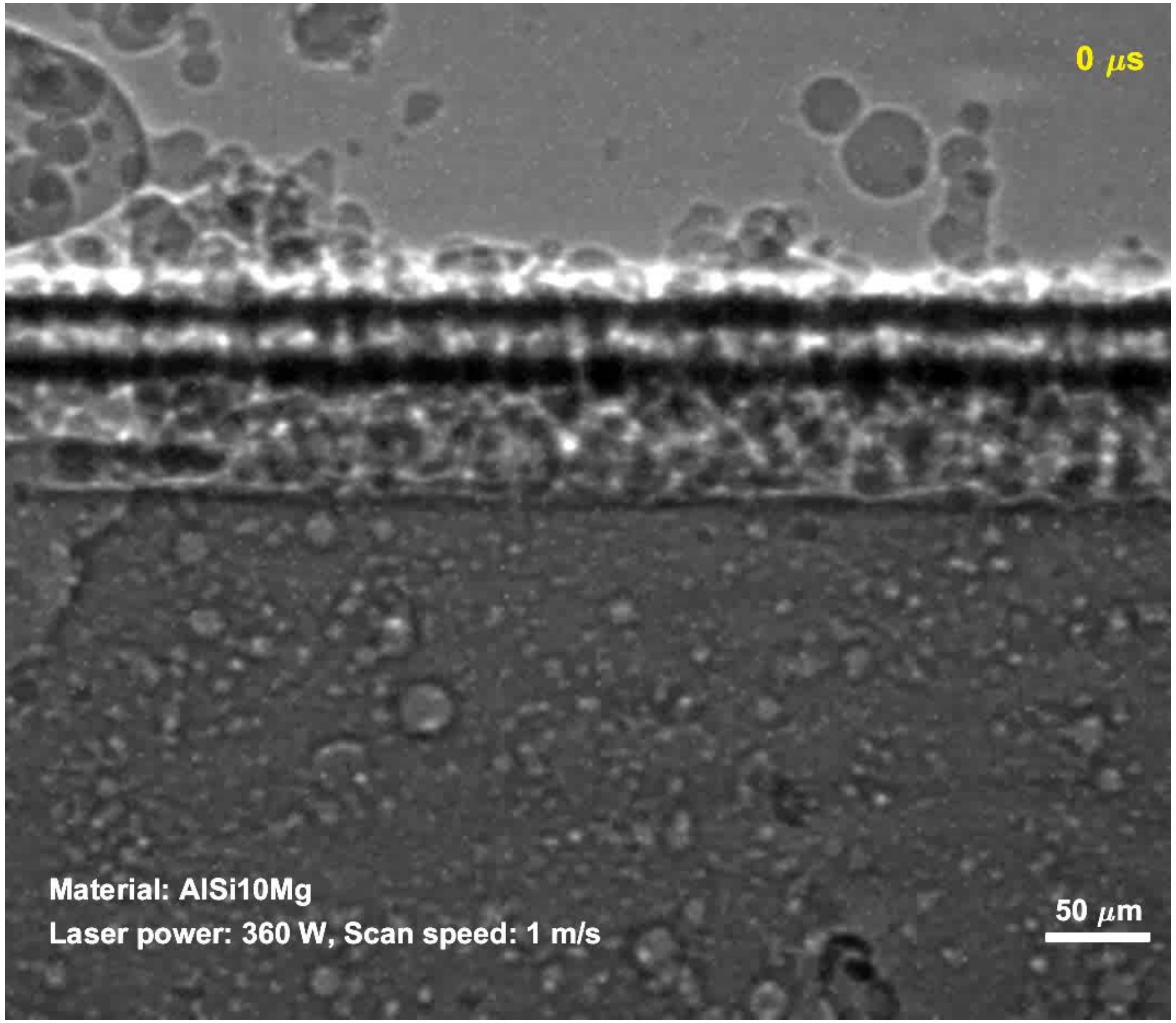

Pore motion patterns

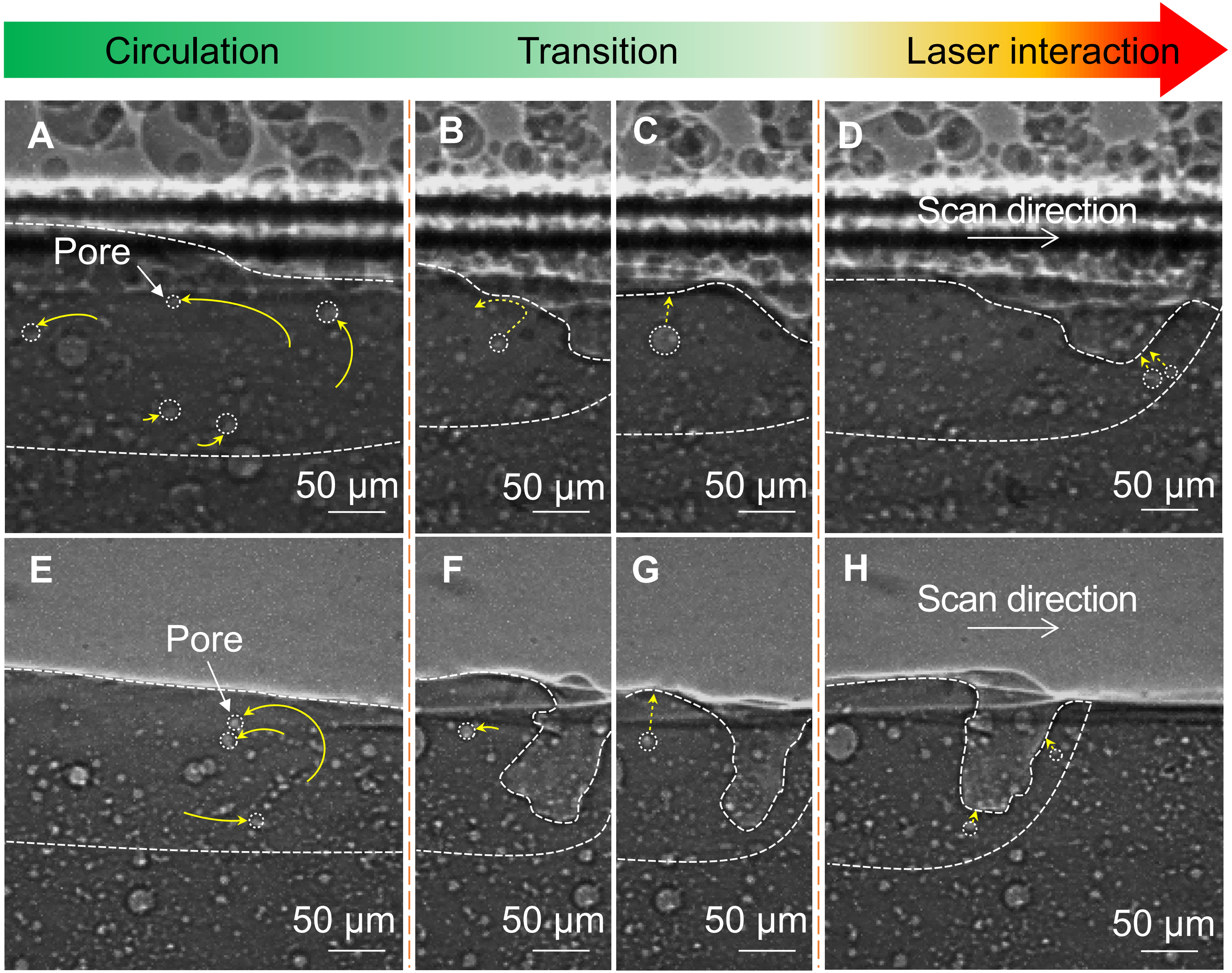

Driving forces for pore motion and elimination

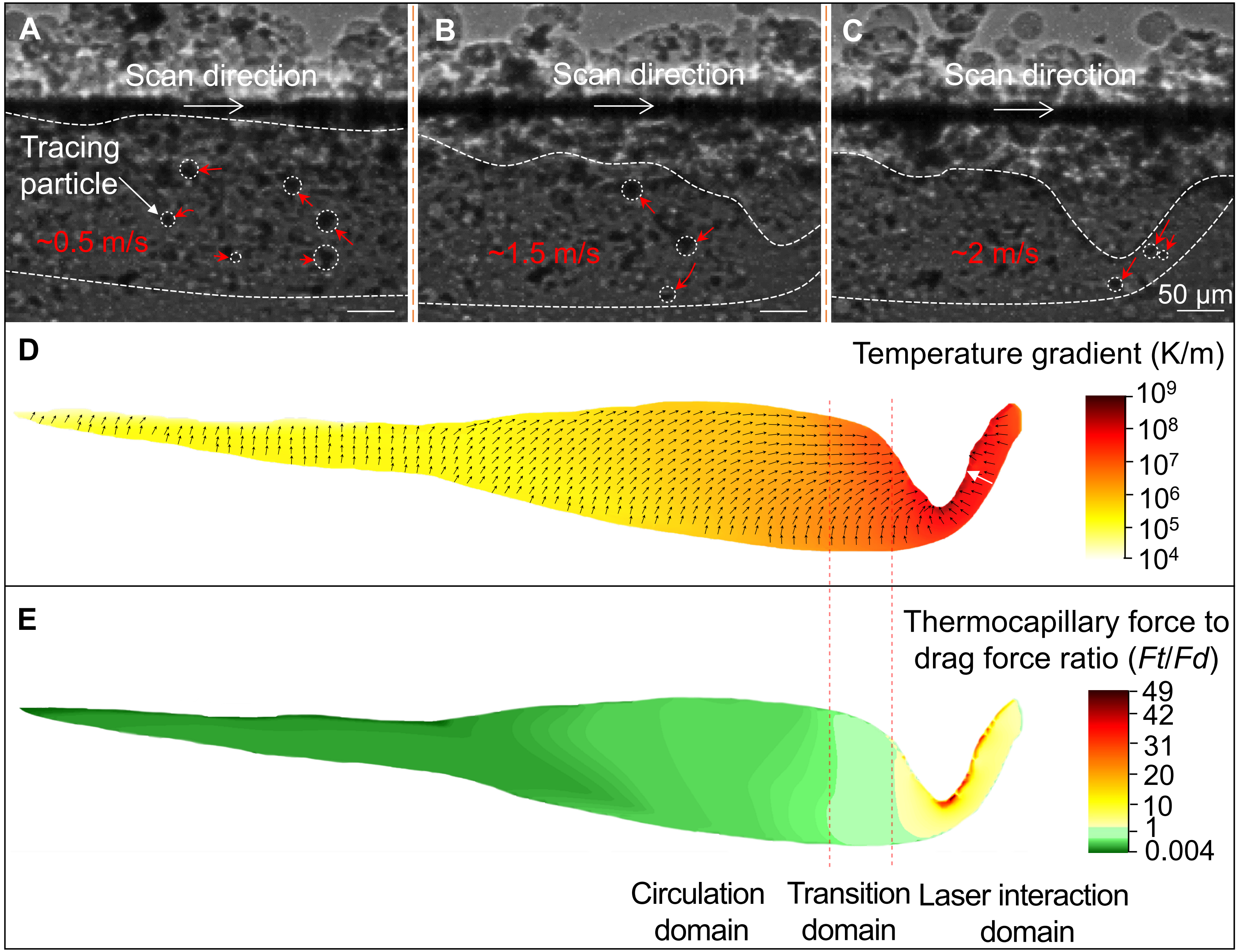

Mechanisms of pore motion and elimination

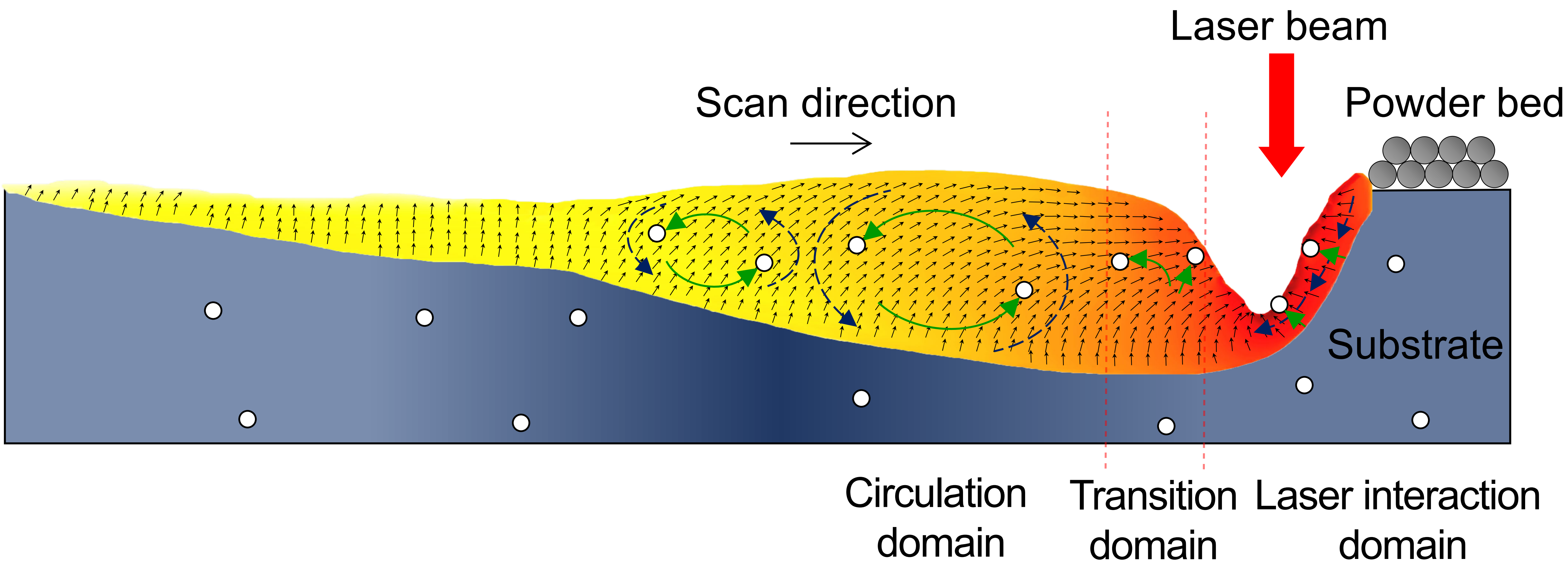

The competition between the melt flow induced drag force and the temperature gradient induced thermocapillary force determines pore moving behavior in the melt pool.

S. Mohammad. H. Hojjatzadeh et al., Pore elimination mechanisms during 3D printing of metals, *Nature Communications*, 10, 3088 (2019).

Quantitatively reveal the dynamics and mechanisms of LPBF process

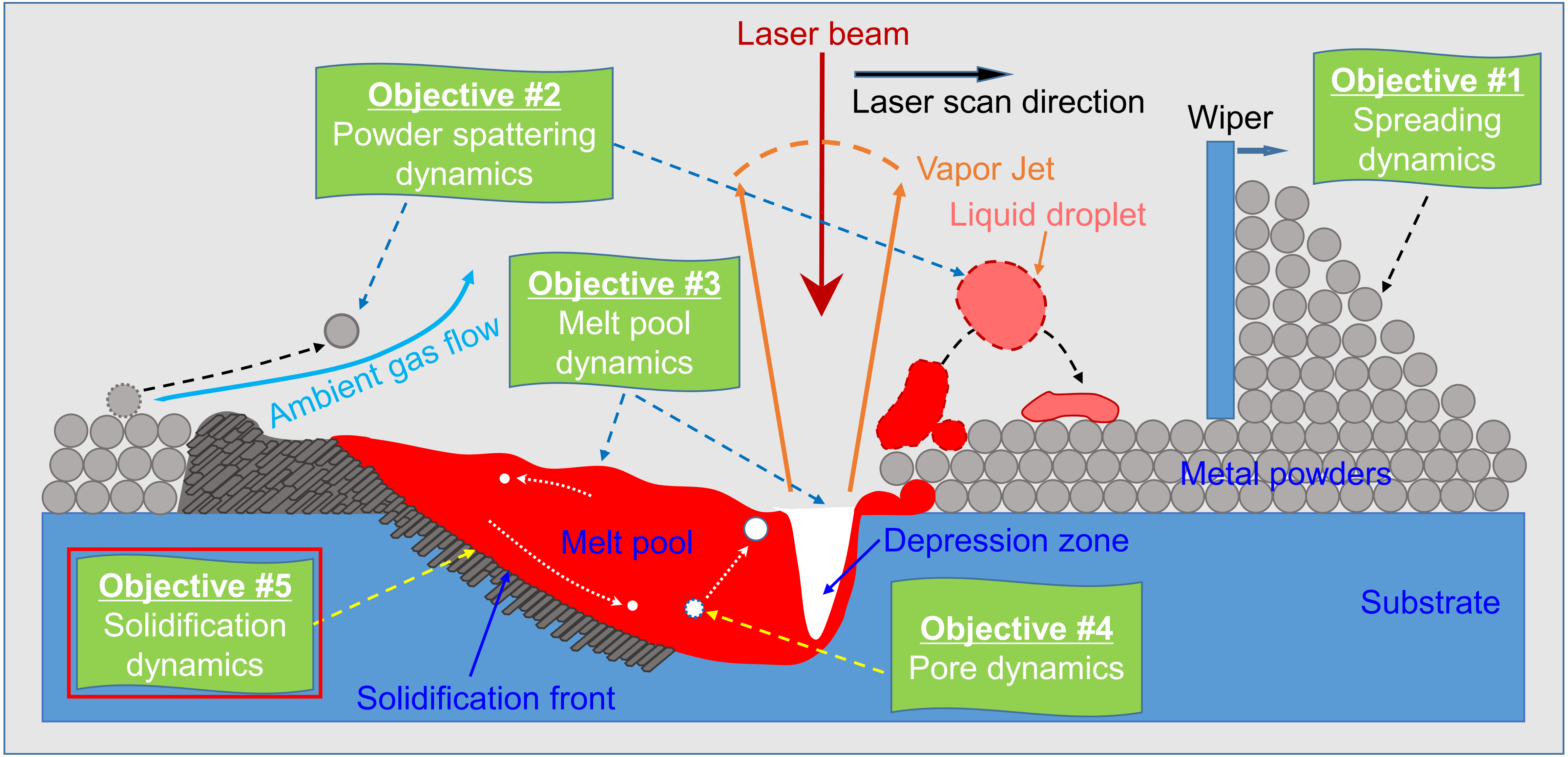

Laser scan speed: about m/s, wiper speed: 100s mm/s

Dynamics of solidification

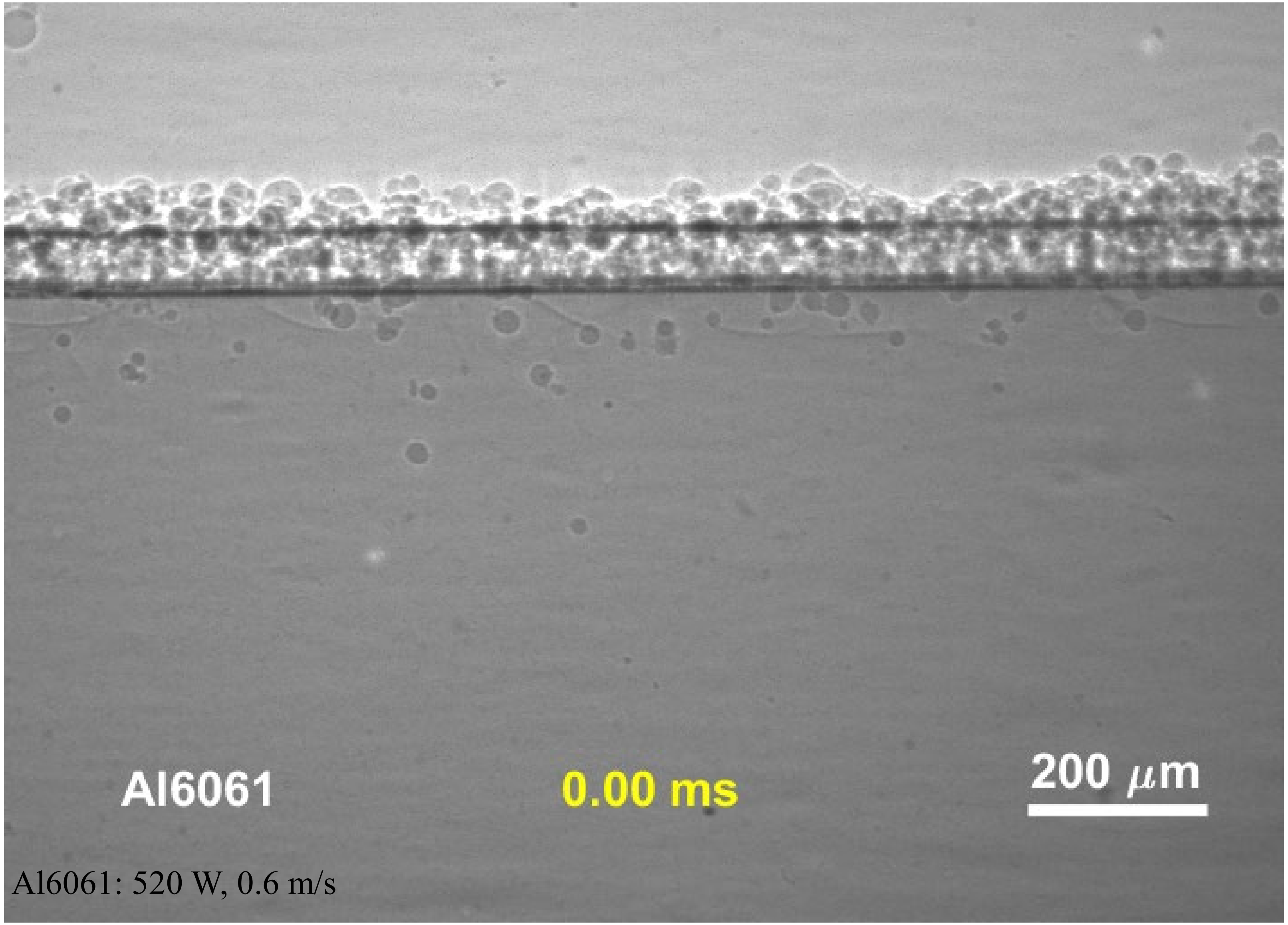

Cracks initiate and propagate during solidification

Calculation of solidification rate

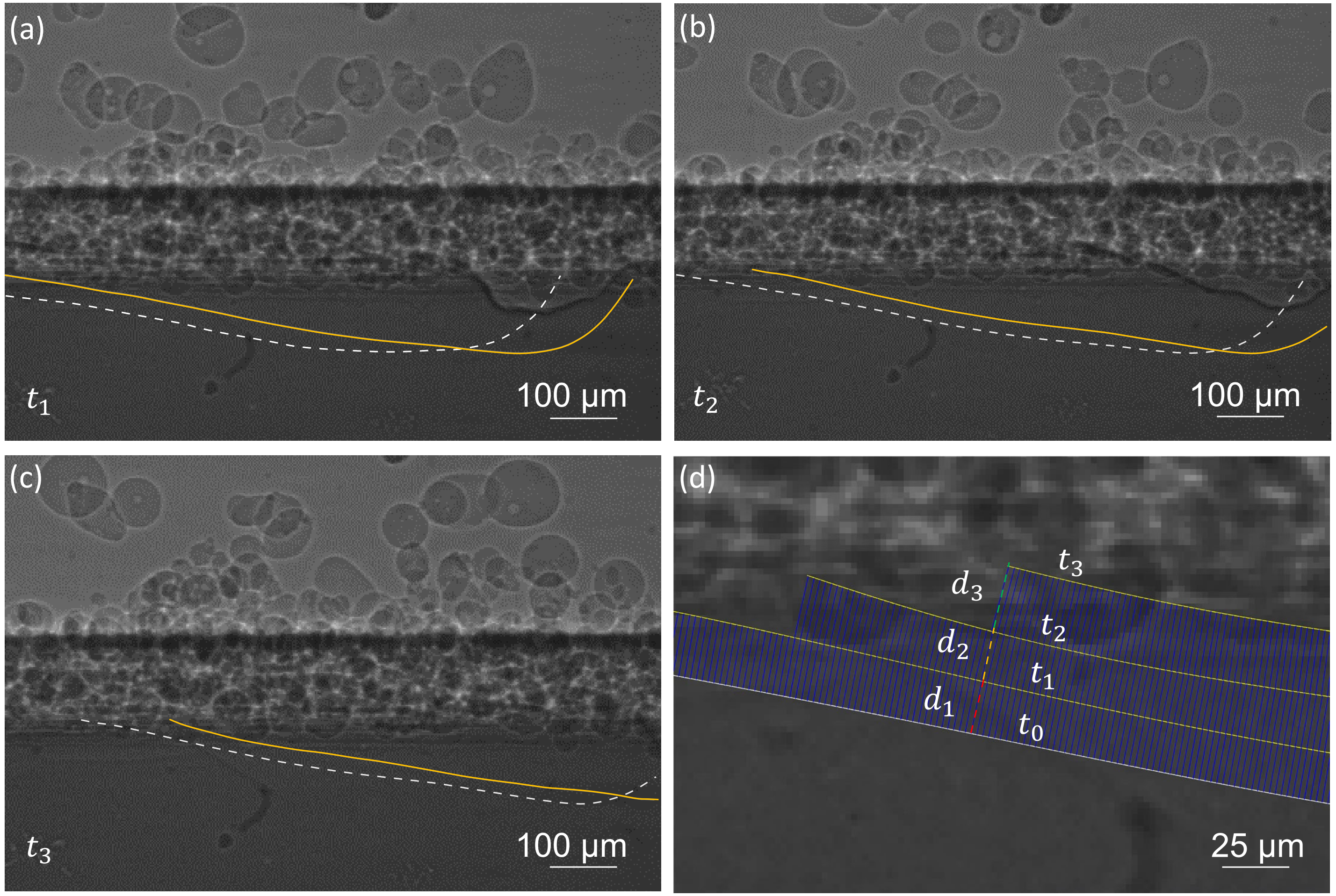

$$V_i = \frac{d_i}{(t_i - t_{i-1})}$$

V_i is the solidification rate of interface i, d_i is the distance the solidification front travels from time $t_{i\text{-}1}$ to time t_i. t_i and $t_{i\text{-}1}$ are times corresponding to interface i and interface i-1, respectively.

Solidification rate evolution

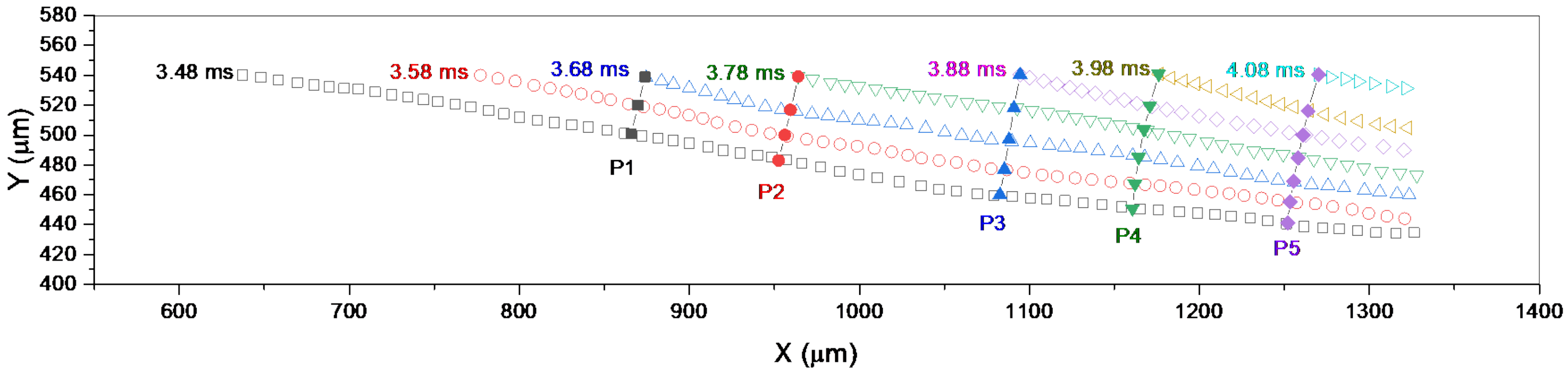

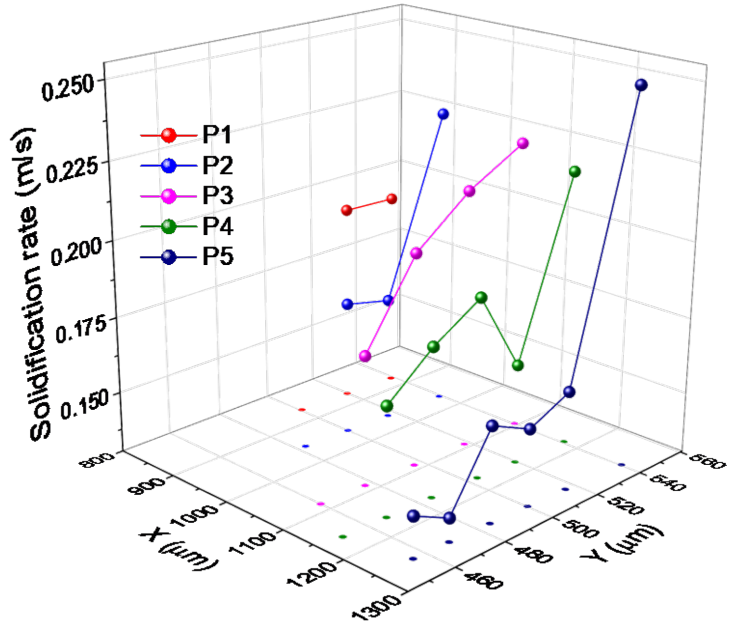

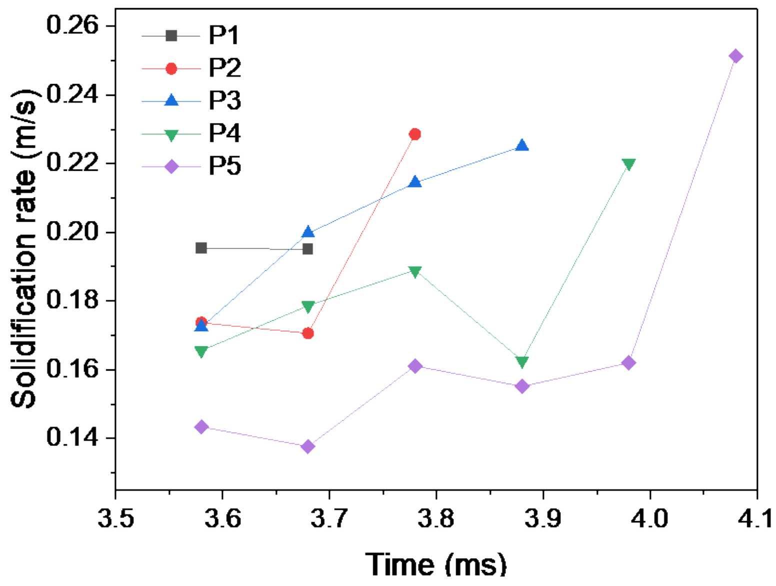

M. Michael Coday et al., Undercooling in laser powder bed fusion metal additive manufacturing, submitted to *Acta Materialia*.

Transient phase transformation

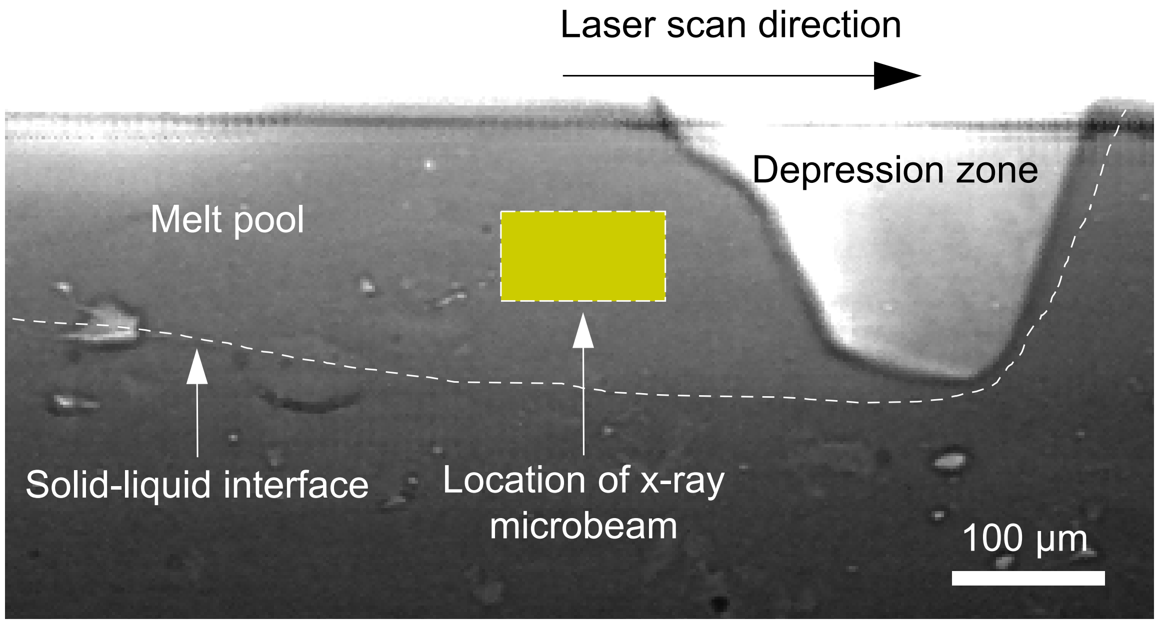

304L stainless steel, 312 W, 0.4 m/s

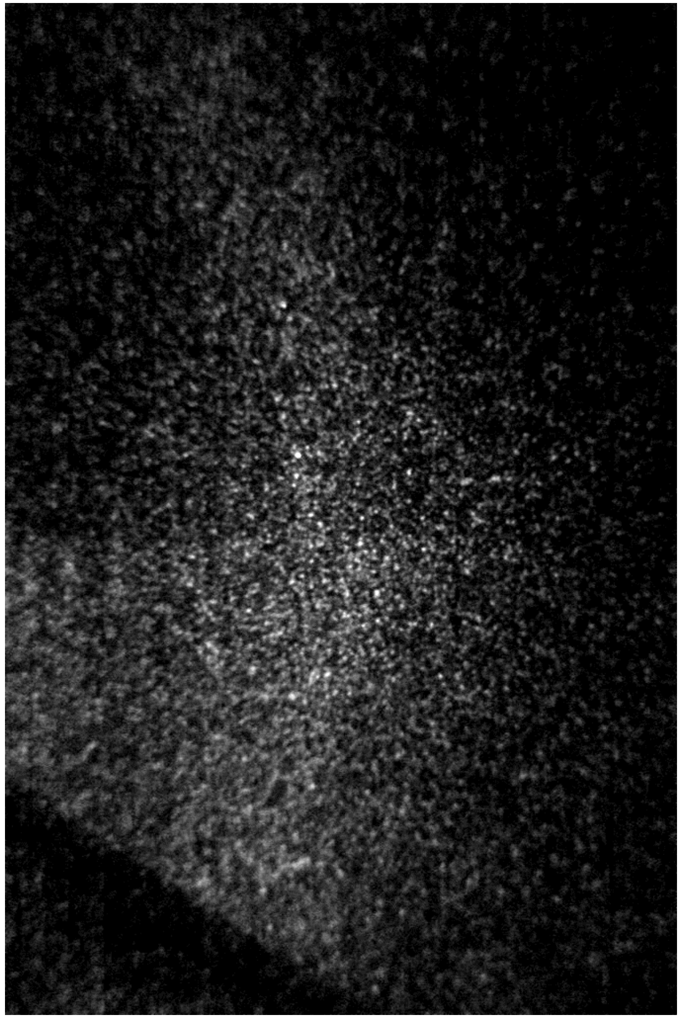

Quantitative phase evolution dynamics

In-situ high-energy high-resolution X-ray diffraction

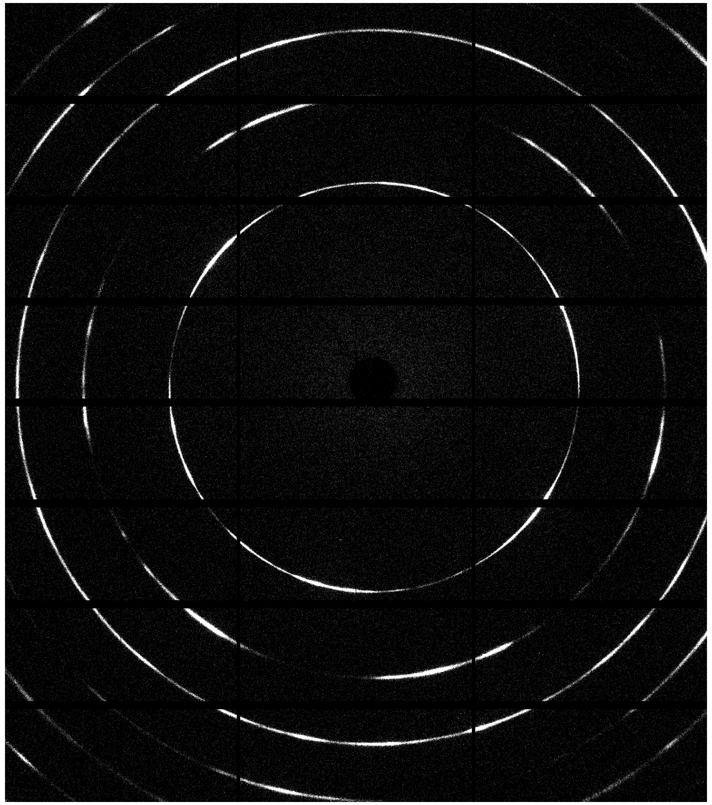

Frame rate: 250 Hz

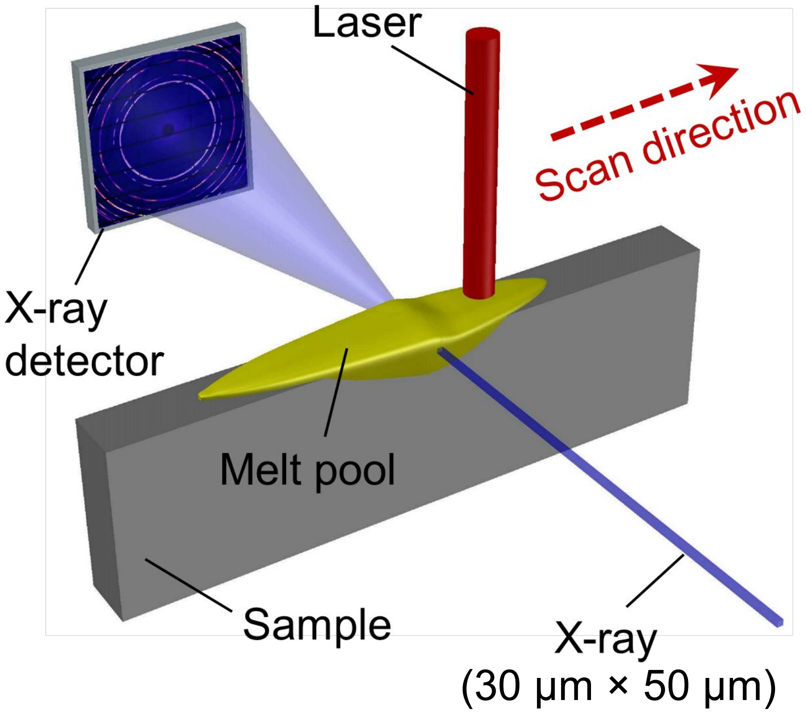

X-ray energy: 61.332 keV

Beamline 1-ID-E, Advanced Photon Source

Types of phases, relative amount, lattice parameter change (to estimate stress, temperature)

Phase evolution in 17-4 PH stainless steel

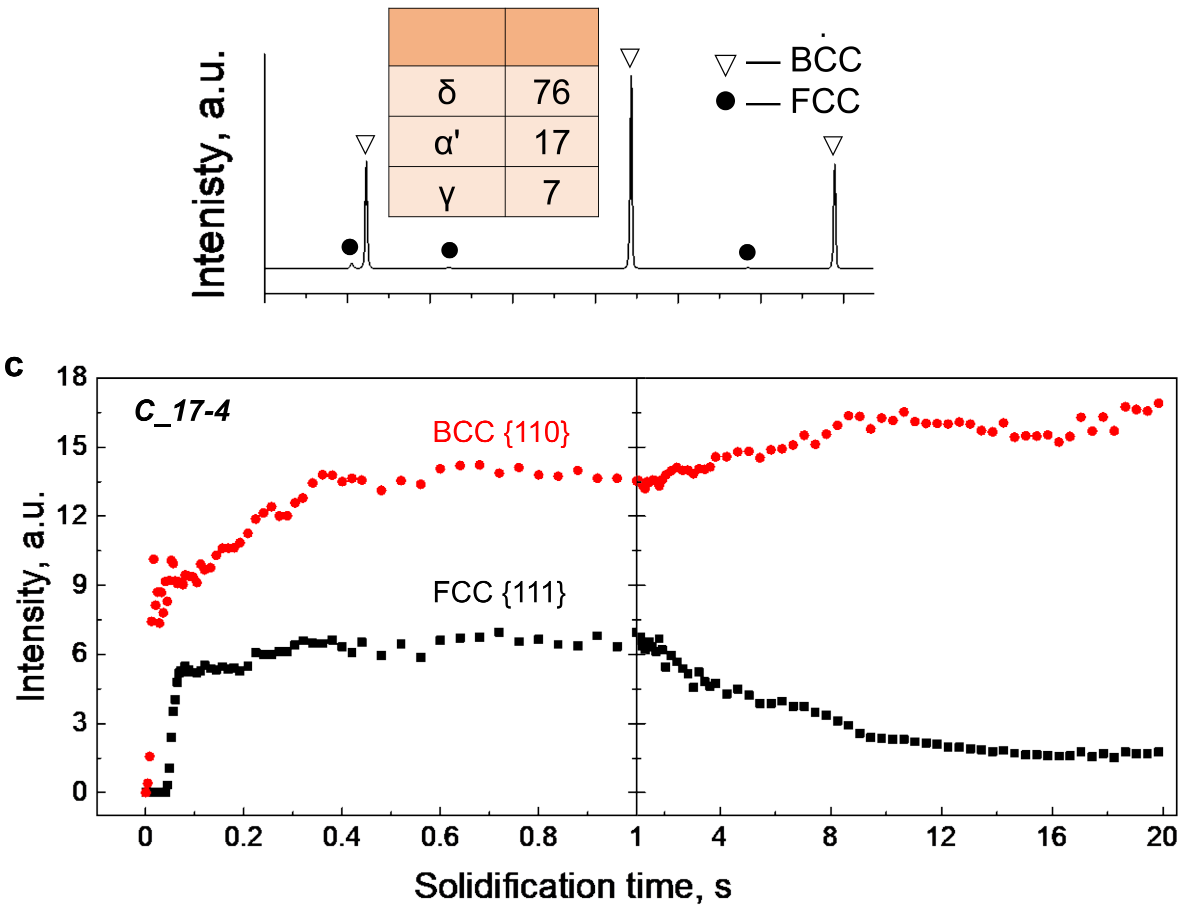

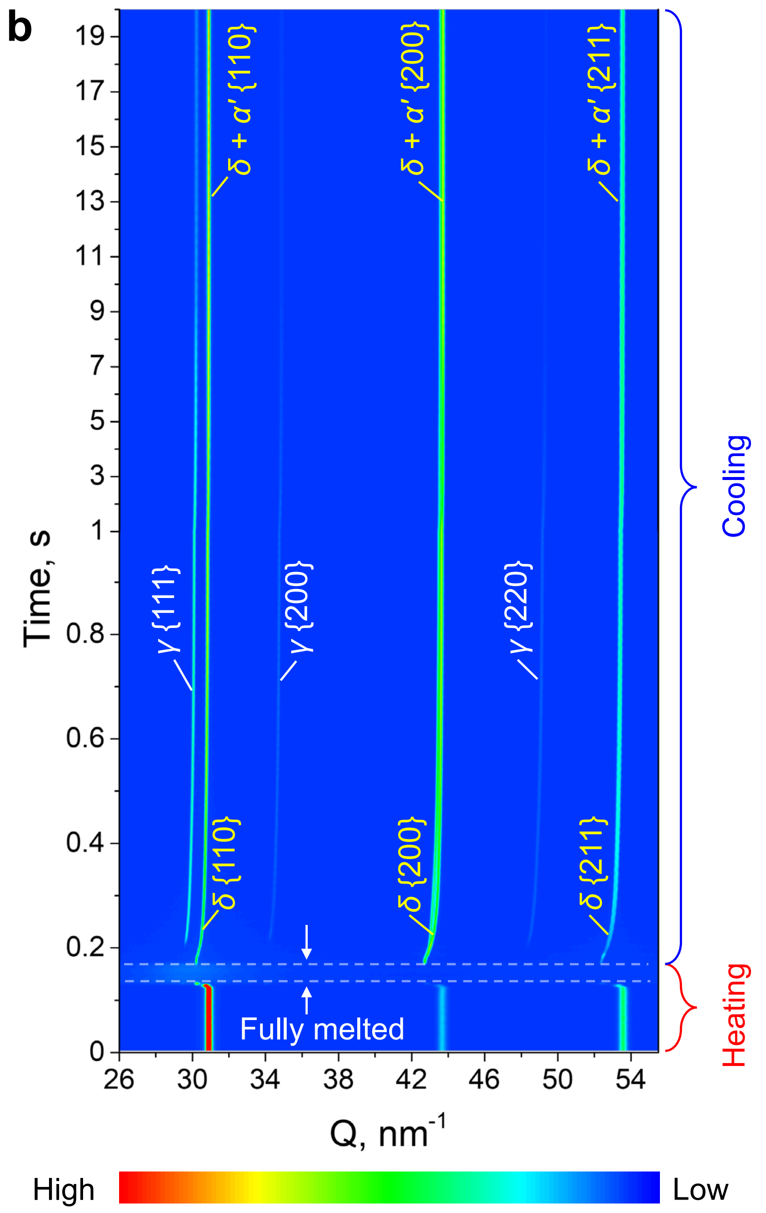

17-4 PH	Cr	Ni	Cu	Mn	Nb	C
Specification	15.0-17.5	3.0-5.0	3.0-5.0	1.0 max.	0.15-0.45	0.07 max
AMed with Ar atomized powder	16.7	4.3	4.0	0.22	0.3	0.02

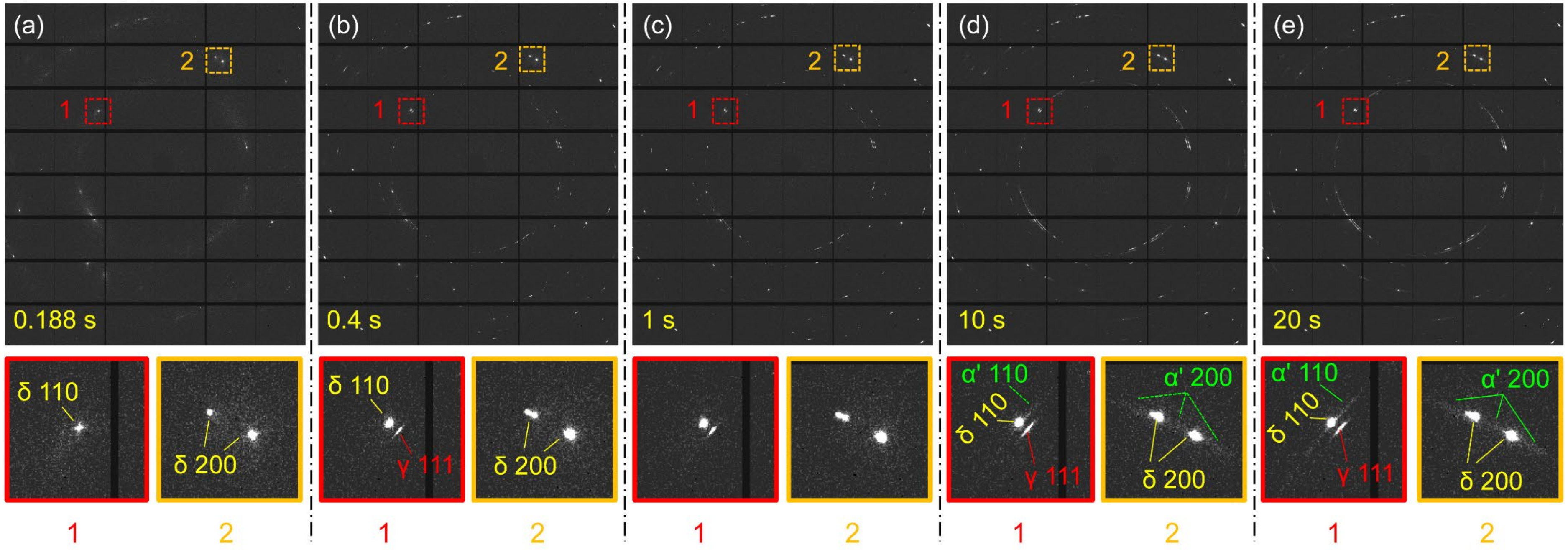

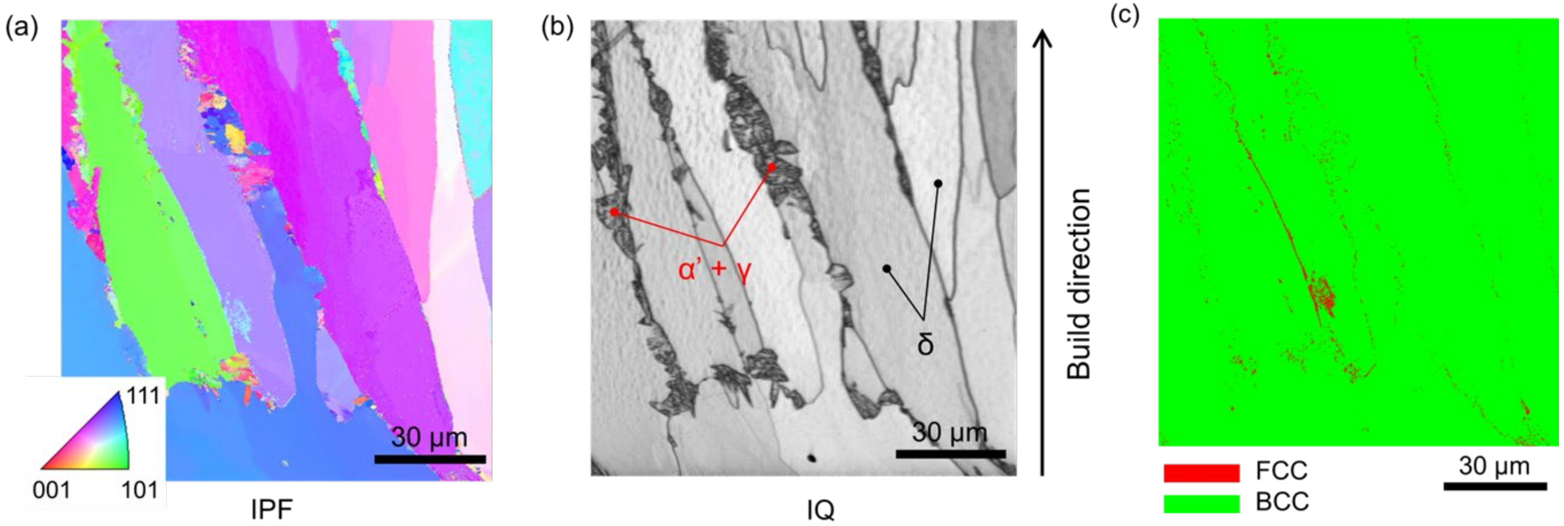

Qilin Guo et al., Phase transformation dynamics guided alloy development for additive manufacturing, *Additive Manufacturing*, in press, 103068 (2022).

Outline

- Introduction to fast X-ray imaging and diffraction
- Fast X-ray imaging system
- Fast X-ray diffraction system
- Revealing dynamics of additive manufacturing process by fast X-ray imaging and diffraction
- **Approaches to mitigate/eliminate defects in additive manufacturing**

Mitigate spatter induced defects

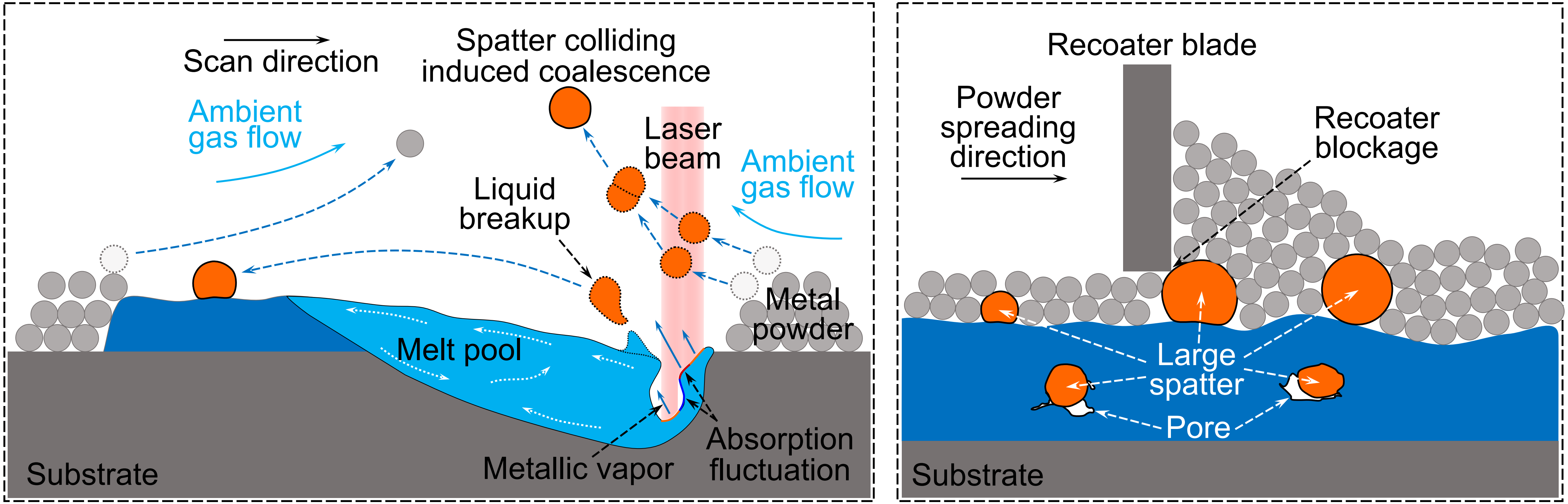

The stochastic formation of large spatter (spatter larger than layer thickness) is a major cause of unpredictable defect formation in LPBF process and a big challenge for quality control.

Elimination of large spatter by using nanoparticles

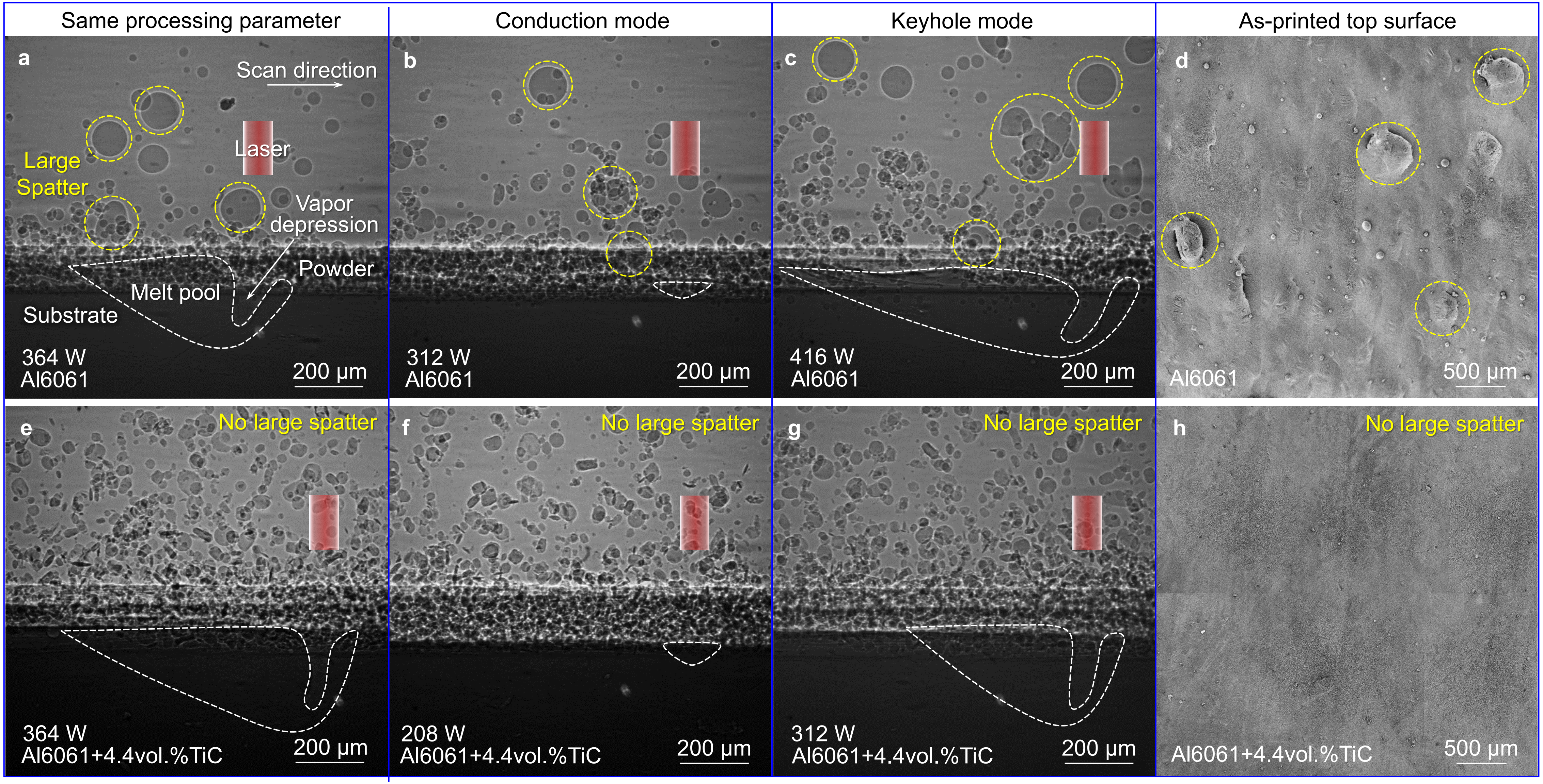

Defect lean sample

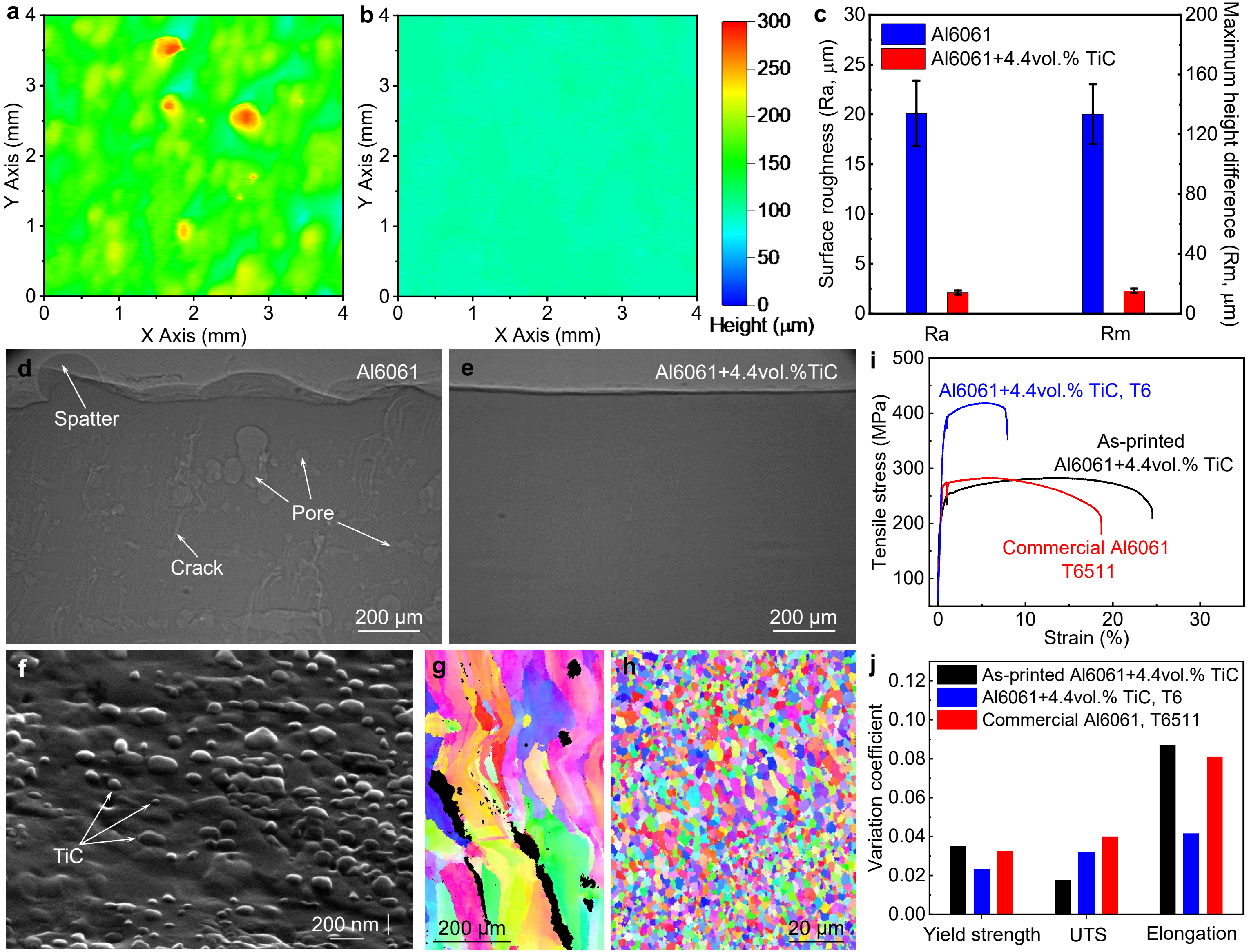

Nanoparticle-enabled control of molten pool fluctuation

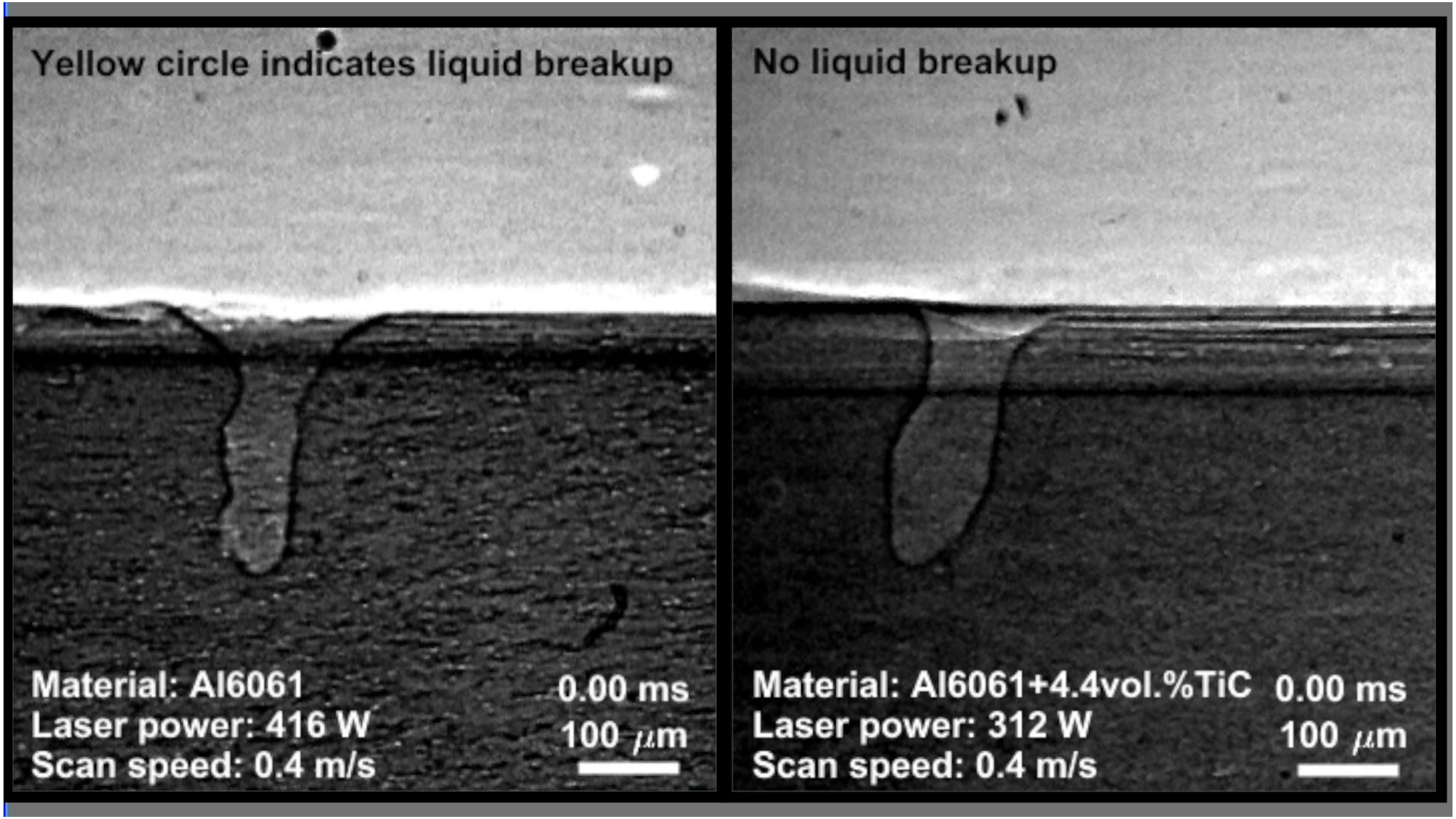

Eliminate liquid breakup induced large spatters

Nanoparticle-enabled control of liquid droplet coalescence

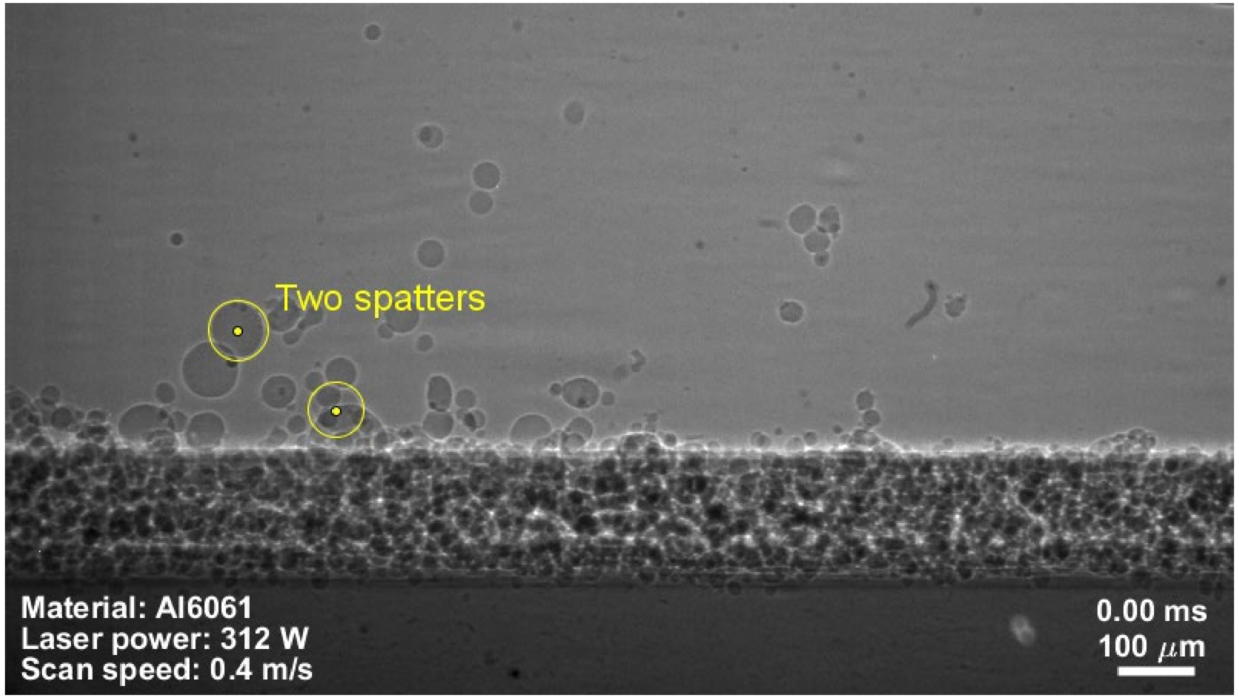

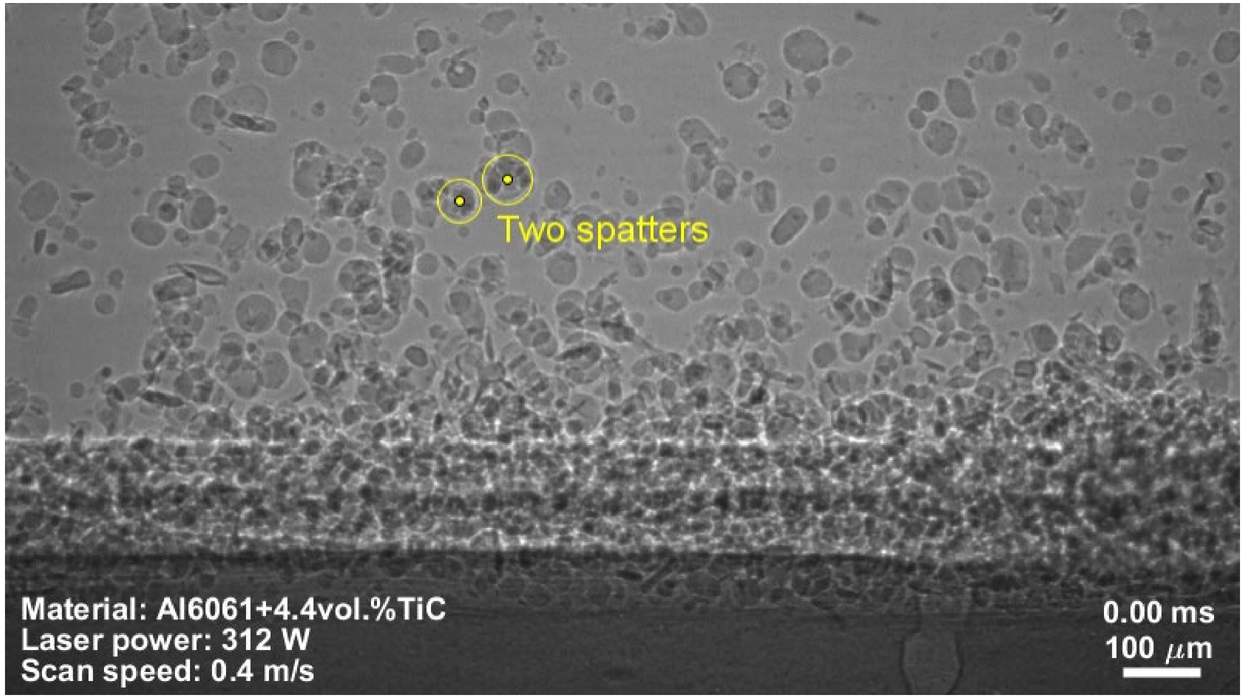

Eliminate liquid droplet colliding induced large spatters

Minglei Qu et al., Controlling process instability for defect lean metal additive manufacturing, *Nature Communications*, 13, 1079 (2022).

Minglei Qu et al., Mitigating keyhole pore formation by nanoparticles during laser powder bed fusion additive manufacturing, *Additive Manufacturing Letters*, 3, 100068 (2022).

Minglei Qu et al., Controlling melt flow by nanoparticles to eliminate surface wave induced surface fluctuation, *Additive Manufacturing*, in press, 103081 (2022).

Pore elimination by thermocapillary force

Eliminate pore in feedstock powders

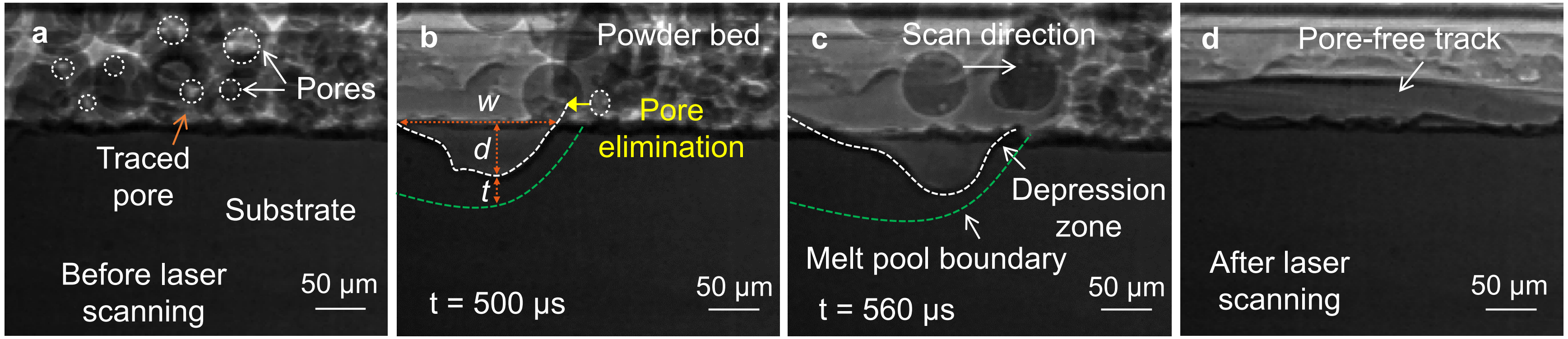

Eliminate pore in previous built layers

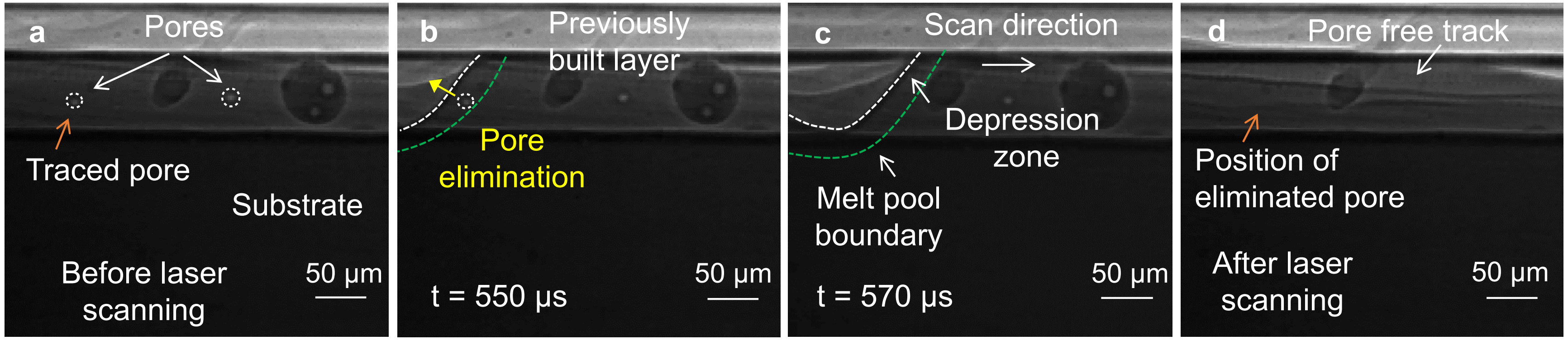

Pores can be eliminated by thermocapillary force under proper processing conditions (large high temperature gradient region).

Development of alloy for AM

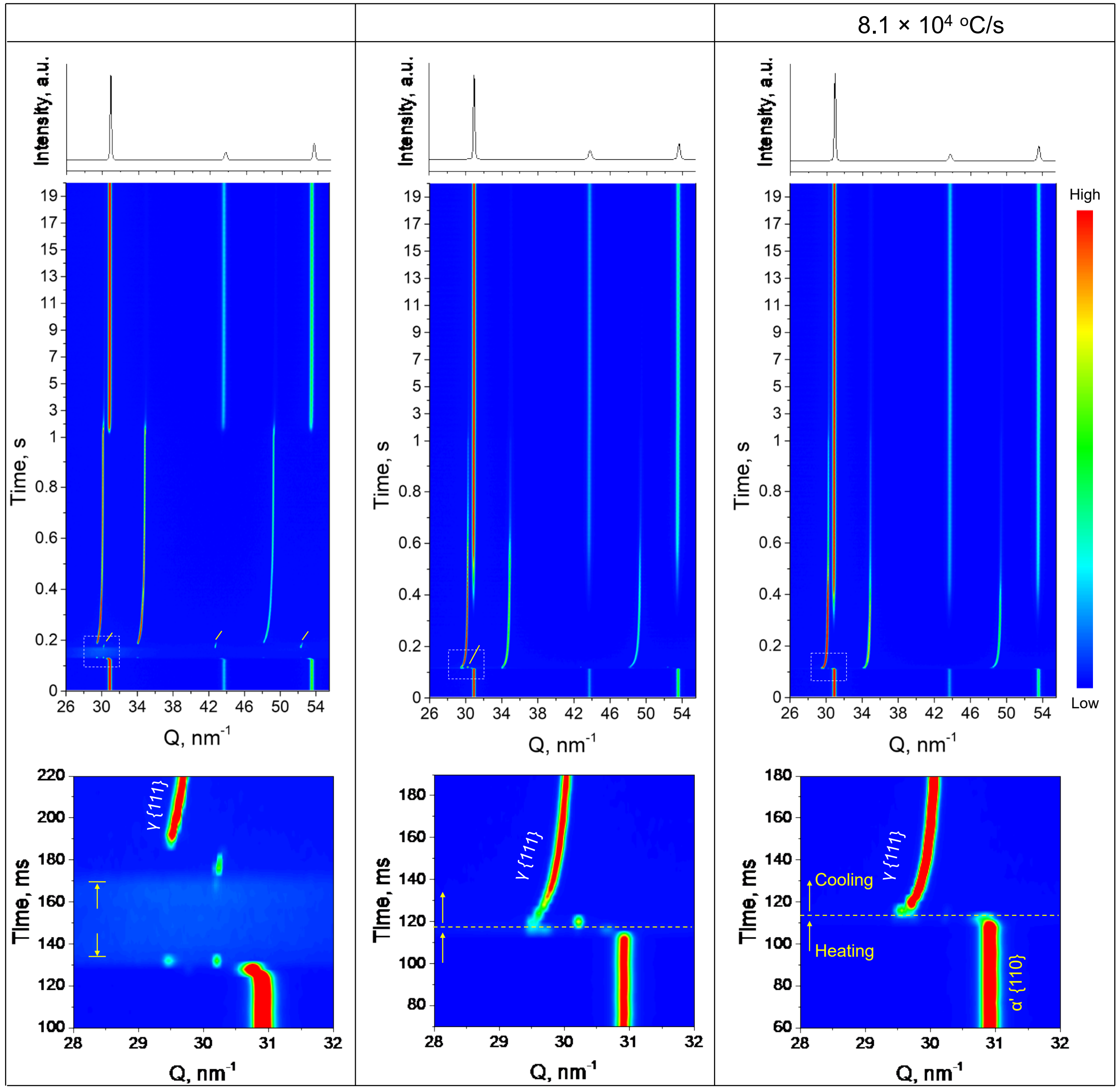

17-4 with full martensite phase

Consistent phase in a wide range of cooling rate

10^2 °C/s

10^4 °C/s

10^7 °C/s

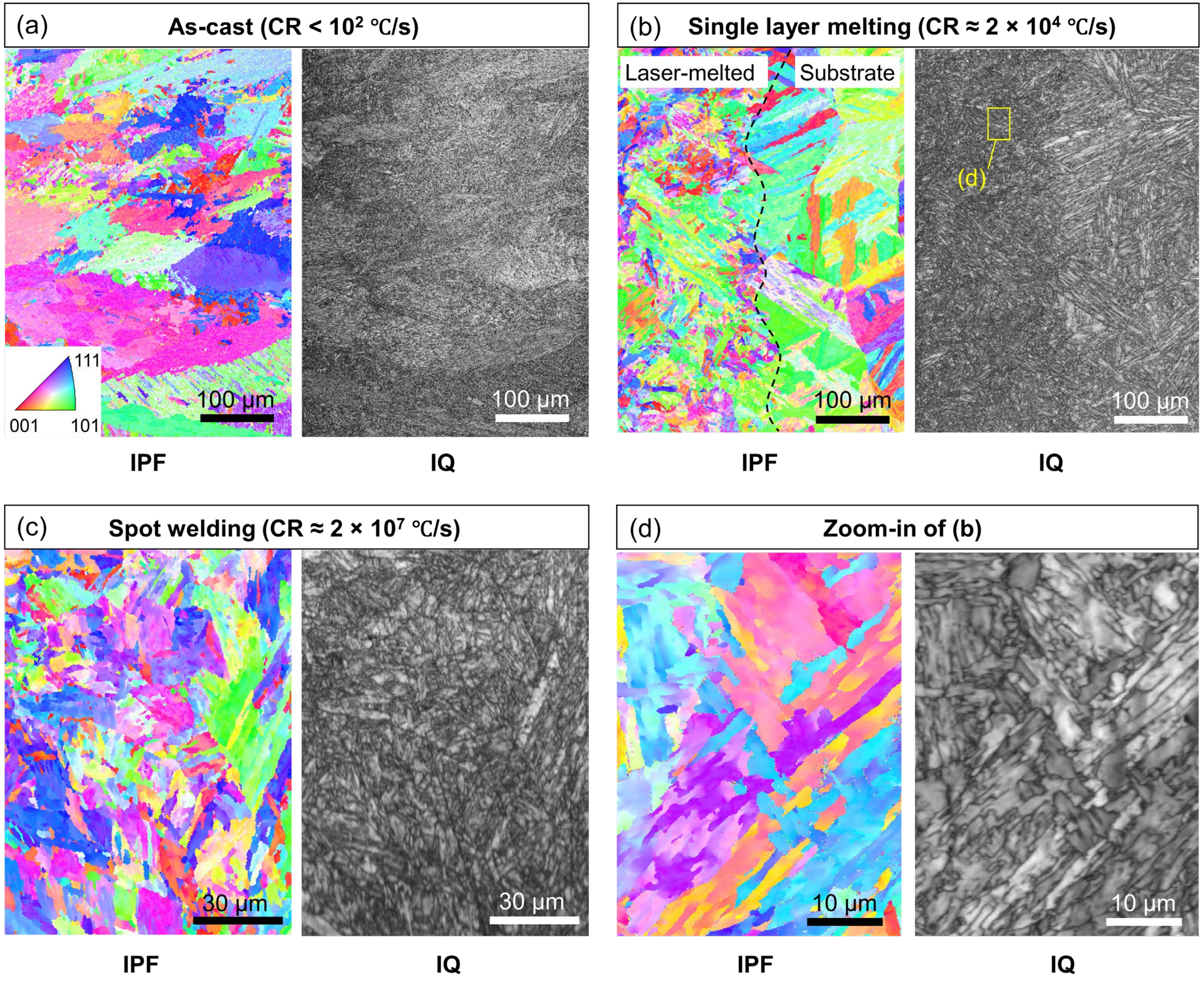

Microstructure and property of printed sample

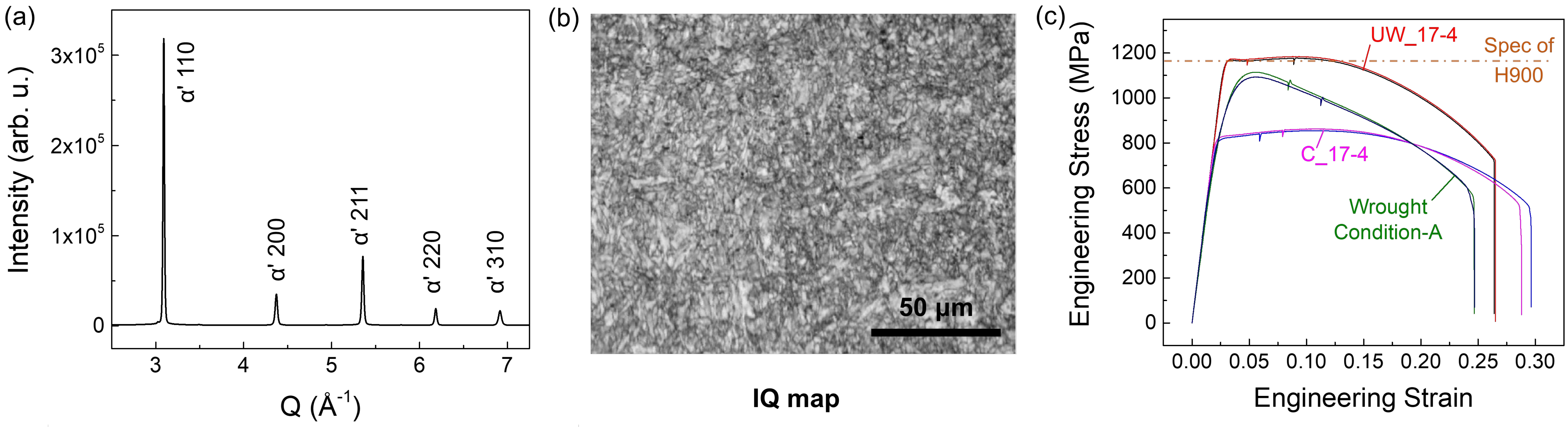

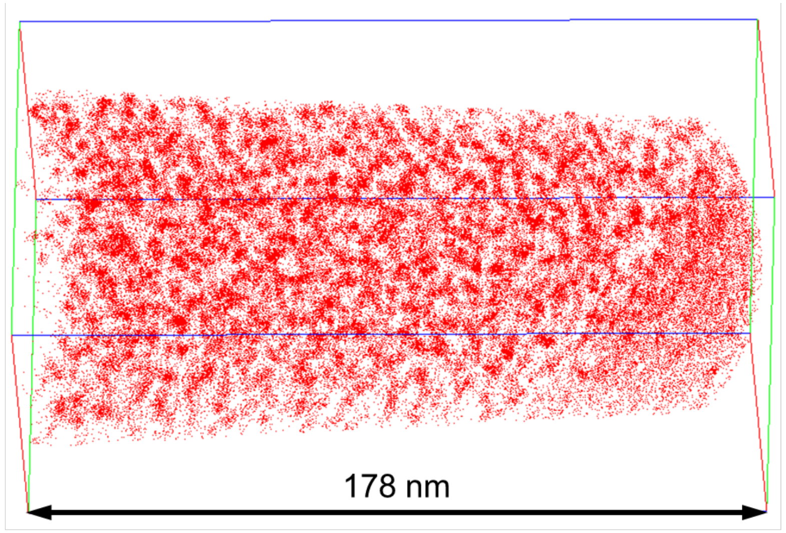

- **Fully martensitic structure in as-printed part**
- **High yield strength, comparable to H900 17-4 (precipitation-hardened)**

Qilin Guo et al., Phase transformation dynamics guided alloy development for additive manufacturing, *Additive Manufacturing*, in press, 103068 (2022).

Acknowledgements

Students/collaborators:

UW-Madison/Missouri S&T: Qilin Guo, Lianghua Xiong, Luis I. Escano, Zachary Young, S. Mohammad H. Hojjatzadeh, Minglei Qu, Meelap M. Coday, Joseph Louis Volpe, Raghavender Reddy Jakka, Khalid Solangi, Ali Nabaa, Junye Huang, Jiandong Yuan, William Dong, Xinhang Zhang

Argonne National Laboratory: Tao Sun, Andrew Chuang, Samuel J Clark, Kamel Fezzaa, Peter Kenesei

National Institute of Standards and Technology: Fan Zhang

University of Virginia: Tao Sun

Honeywell Federal Manufacturing & Technologies: Wes Everhart, Ben Brown

National University of Singapore: Wentao Yan

University of Michigan: Wenda Tan

Sponsors:

National Science Foundation

Honeywell Federal Manufacturing & Technologies

The Boeing Company

Department of Energy

Department of Commerce

Wisconsin Alumni Research Foundation

Thank you!

Contact information: Lianyi Chen
University of Wisconsin-Madison
Email: lianyi.chen@wisc.edu
Phone: 608-890-0664

Feedback

NXS Lecture - Fast X-ray imaging and diffraction - Lianyi Chen

https://forms.office.com/g/9RK5XQhEKK